HIGH-SPEED MACHINING OF INCONEL WITH CERAMIC TOOLS:

A MACHINABILITY STUDY

HIGH-SPEED MACHINING OF INCONEL WITH CERAMIC TOOLS: A MACHINABILITY STUDY

By FARHAD MOLAIEKIYA, B.Sc., M.Sc.

A Thesis

Submitted to the School of Graduate Studies

in Partial Fulfilment of the Requirements

for the Degree

Doctor of Philosophy

DOCTOR OF PHILOSOPHY (2020) McMaster University

(Mechanical Engineering) Hamilton, Ontario

TITLE:	High-speed machining of inconel with ceramic tools: A Machinability study
AUTHOR	Farhad Molaiekiya, B.Sc., M.Sc.
SUPERVISOR	Dr. Stephen C. Veldhuis Department of Mechanical Engineering
SUPERVISORY COMMITTEE	Dr. Phillip Koshy Department of Mechanical Engineering
	Dr. Nabil Bassim Department of Materials Science and Engineering
PAGE COUNT	xvi, 119

TO MY PARENTS

ACKNOWLEDGEMENTS

I would like to extend my utmost gratitude to my supervisor, Professor Stephen Veldhuis, for his guidance and support throughout my studies at McMaster University. I also need to thank my Ph.D. committee members Dr. Philip Koshy and Dr. Nabil Bassim for their valuable advice and inputs during this research.

My sincerest appreciation to Dr. Maryam Aramesh, Dr. Abul Fazal Arif, Dr. Bipasha Bose, and Dr. German Fox-Rabinovich and all of my colleagues and friends at McMaster Manufacturing Research Institute (MMRI) for their continuous help and support along the way. Also, special thanks to my fantastic lab mates and dear friends at Material Property Assessment Laboratory (MPAL), Ali Khoei and Dr. Shahereen Chowdhury for their kind support and encouragement.

Finally, my heartfelt appreciation to my mother, Nasrin, and my father, Mehdi. I am forever grateful for your love and patience. Thank you.

I acknowledge the Natural Sciences and Engineering Research Council of Canada (NSERC) and the Canadian Network for Research and Innovation in Machining Technology (CANRIMT) for the financial support of this research.

LAY ABSTRACT

Recent studies on the machining of advanced industrial components show that improving the process productivity by increasing the material removal rate has the most significant contribution to reducing the cost of manufacturing. Hence, high-speed machining has been an important topic for researchers in academia and industry for the past few decades. Recent advancements in the mechanical properties of exotic tool materials like structural ceramics have remarkably contributed to the successful implementation of high-speed machining concepts for difficult-to-cut alloys. The present research attempts to investigate and understand the prevailing phenomena governing the machinability of inconel 718 in a high-performance dry milling process using advanced SiAlON ceramic tools.

ABSTRACT

Inconel 718 (IN718) is a widely-used nickel-based superalloy in the aerospace industry, which is known for its superior mechanical properties and microstructural reliability at elevated temperatures. However, the poor machinability of this heat resistant alloy has always been a challenge for the manufacturing industry. The high shear strength, low thermal conductivity and intensive work hardening properties of IN718 induce high thermo-mechanical stresses on the tool's cutting edge which leads to rapid tool wear even at extremely low cutting speeds. Hence, limited scientific data is available around high-speed machining of IN718, especially on more demanding applications such as interrupted cutting during milling. This research is focused on IN718 machinability studies at extreme conditions, using a dry high-speed face milling process with exotic tool materials like advanced SiAlON ceramics. Comprehensive material characterization techniques and machinability studies have been performed using tool wear studies, micro and nanomechanical indentations, optical 3D imaging, SEM/EDS studies and finite element modelling to identify the dominant tool wear mechanisms over a wide range of cutting parameters. Also, further investigations have been done on the mechanisms of chip formation, shear deformation at extreme conditions and tribological aspects of tool-chip-workpiece interactions such as the formation of built-up layers and tribofilms. Results suggest that there is a narrow operational window (around 1000 m/min cutting speed) in which high-speed machining of IN718 superalloy can be performed using a carefully selected ceramic tool material. Experimental results under this cutting speed show a drastic transformation in the machinability of inconel 718 when surpassing a high level of temperature and strain rate. Following further surface integrity studies on the machined workpiece, it can be concluded that such a process is suitable for rough or semi-finishing of IN718 parts at a four times higher material removal rate as compared with conventional practices currently used in industry.

TABLE OF CONTENTS

LIST of FIGURES

LIST Of TABLES

Chapter 1. Introduction

1.1 Background

1.1.1 Inconel machinability

Since the introduction of heat resistant superalloys (HRSAs) in the 1940s and the subsequent improvements in their high-temperature mechanical and microstructural properties in the following decades, poor machinability of these materials has always been a costly challenge for the manufacturing sector (Schirra and Viens 1994; Choudhury and El-Baradie 1998; Zhu, et al. 2013). The workpiece material used in this study is a hardened IN718 nickel-based superalloy. The microstructure of IN718 consists of a background gamma FCC austenitic phase which is a randomly distributed Ni-Cr-Fe solid solution matrix. The main strengthening mechanism of the microstructure is the precipitation of nickel aluminum titanium (γ') and nickel niobium (γ''). Also, the presence of hard carbides (mostly TiC and NbC) at the grain boundaries provides additional strengthening mechanisms in the microstructure (Schirra and Viens 1994).

Due to the ever-growing demand in the manufacturing industry, considerable research has been performed to study the machinability of nickel-based alloys. Several attempts can be found in the literature to improve the tool life and the machining performance of superalloys (Ezugwu 2005; Sharman, et al. 2001; Kadirgama, et al. 2011; Nalbant, et al. 2007). Main areas of approach in this regard are:

(1) Tooling design - There are a few categories of materials that can be employed as cutting tools under the aggressive cutting conditions that arise during the machining of nickel-based alloys. The tool material should have superior mechanical properties such as high hardness and wear resistance, high mechanical strength and toughness, and thermal stability. One of the main areas of research on this topic is the deposition of coating layers on conventional carbide tools. In coated tools, while the substrate material is aimed to sustain its strength and toughness to bear the load, the coating is designed to enhance the resistance to wear, oxidation and thermal load which influences the tribological characteristics and friction response (Montazeri, et al. 2019; Bhatt, et al. 2010; Fox-Rabinovich, et al. 2010). In addition, some investigations have been carried out to develop advanced CBN or ceramic-based materials with excellent high-temperature properties which have become very popular with machinists (Zheng, et al. 2012; Hao, et al. 2017; Costes, et al. 2007; Dudzinski, et al. 2004).

(2) Non-conventional machining techniques - Laser-assisted machining is one example of such a technique. In this strategy, an external heat source, i.e., Laser, is used to decrease the mechanical strength of the workpiece material through thermal softening. Implementing this concept is expensive, power-consuming, and requires the installation of extra components in the machine's workspace. Experimental results show that laser-assisted machining does not have a significant effect on the tool life or the productivity of the process but instead creates a better surface finish and lower cutting forces (Pan, et al. 2017; Chryssolouris, et al. 1997; Attia, et al. 2010; Tadavani, et al. 2017).

(3) Coolant delivery - Several attempts have been made in the literature to minimize the cutting edge temperature using cryogenic cooling, minimum quantity lubrication (MQL), and high-pressure cooling techniques. It has been shown that implementing these methods has a positive effect on tool life and surface roughness, but they fail to increase the material removal rate of the process (Kaynak 2014; Obikawa, et al. 2008; Aramcharoen and Chuan 2014; Lima, et al. 2017). Table 1.1 summarizes some selected publications on the machinability of nickel-based superalloys.

Table 1.1- Some recent academic publications on machinability studies of nickel-based superalloys

Workpiece	Cutting Tool	Process	Speed (m/min)	Implemented Technique	Ref.
IN718	Coated WC-Co	Turning (Wet)	80	Nano-structured TiAlN Coating	(Devillez, et al. 2007)
IN718	PVD coated PCBN	Turning (Wet)	200	PCBN tool & TiSiN coating	(Soo, et al. 2016)
IN718	Coated WC-Co	Milling (Dry)	20-40	Nano-structured TiAlSiN/TiSiN/TiAl N Coating	(Kursuncu, et al. 2018)
IN718	Coated WC-Co	Milling (Wet)	75	TiCN/Al2O3/TiN multilayered coating MQL cooling	(Park, et al. 2015)
Incoloy 825	Coated WC-Co	Turning (Dry)	51	Nano-structured TiN/TiAlN	(Thakur and Gangopadhyay 2016)
IN718	WC-Co	Turning (Wet)	30-120	MQL cooling	(Kaynak 2014)
IN718	WC-Co	Turning (Wet)	100	CO_2 cryogenic cooling	(Bagherzadeh and Budak 2018)
Hastelloy C276	Whisker reinforced ceramic	Milling (Wet)	24-120	Ceramic tool	(Al-Falahi, et al. 2016)
IN718	SiAlON ceramic	Milling (Dry)	585	Ceramic tool	(Çelik, et al. 2017)

IN718	SiAlON ceramic	Milling (Dry)	50-200, 350, 500	Ceramic tool	(Hao, et al. 2017)
IN718	Whisker reinforced ceramic	Milling (Dry)	660	Ceramic tool & air jet cooling	(Obikawa and Yamaguchi 2015)
IN718	Whisker reinforced ceramic	Turning (Dry)	200, 300, 400	Ceramic tool	(Rinaldi, et al. 2020)
IN718	Alumina based	Turning (Dry)	300, 350, 400	Ceramic tool	(Zhao, et al. 2019)

1.1.2 Metal Cutting and Tool Wear

Metal cutting is a manufacturing process in which a sharp wedge-shaped tool shears and removes thin layers from a bulk material through relative motion between the tool and workpiece. Numerous parameters and factors are involved in this complex process namely, cutting parameters (cutting speed, feed rate, depth of cut), workpiece material, tool material, tool geometry, edge preparation and use of coatings, machine dynamics, and environmental conditions like coolant (Figure 1.1).

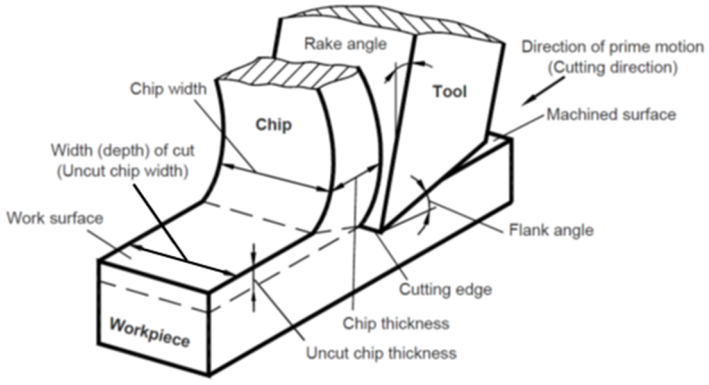

Figure 1.1- Basic terminologies in metal cutting - adapted with permission (Astakhov and Davim 2008)

Tool life is considered to be the most important criterion used for the selection of cutting conditions. In a cutting process, the tool is subjected to extreme tribological conditions and gradually degrades over time. Flank wear, crater wear, notch wear, plastic deformation, built-up edge (BUE) formation, chipping and fracture are the main types of tool wear which are caused by physical or chemical phenomena (Figure 1.2). These wear modes evolve on the rake face or the flank face of the tool mainly as a consequence of adhesion, abrasion, oxidation, and diffusion mechanisms (Astakhov and Davim 2008). According to ISO 3685:1993, Flank wear land width is the most common tool life criteria. Figure 1.3 illustrates the definition of flank wear in metal cutting.

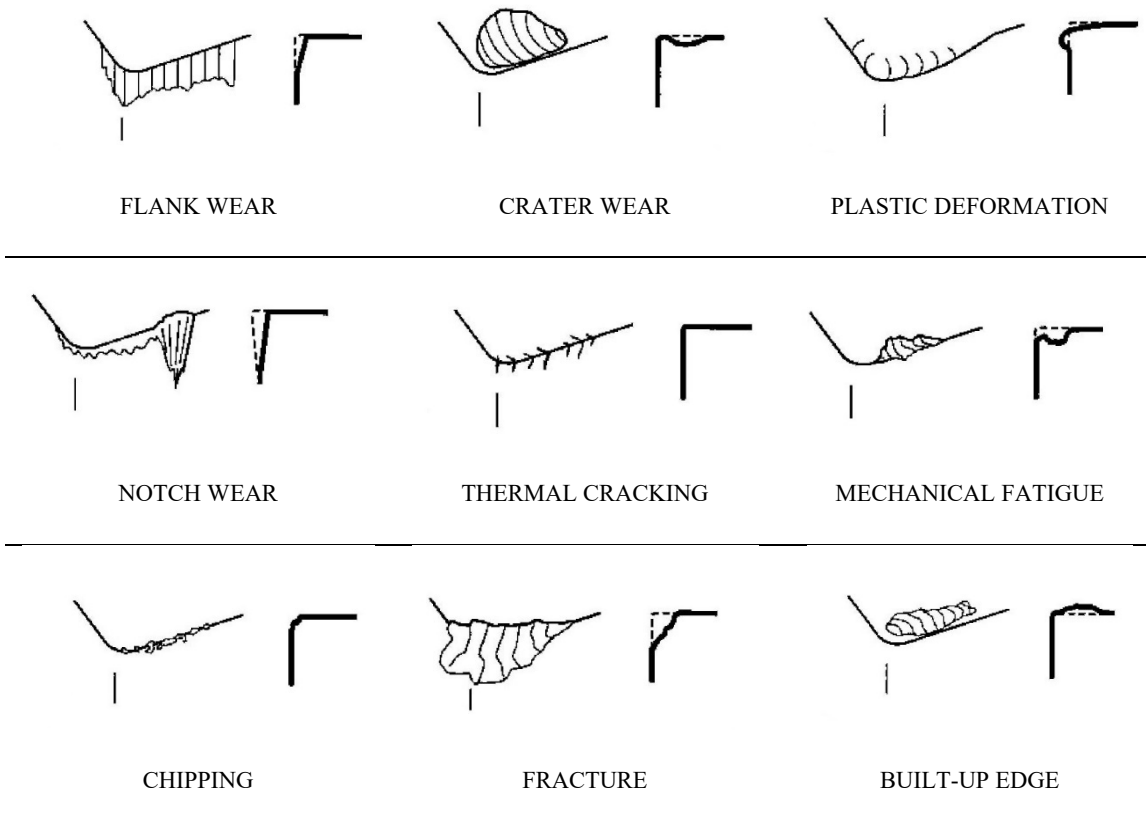

Figure 1.2- Various tool wear types – adapted with permission (Astakhov and Davim 2008)

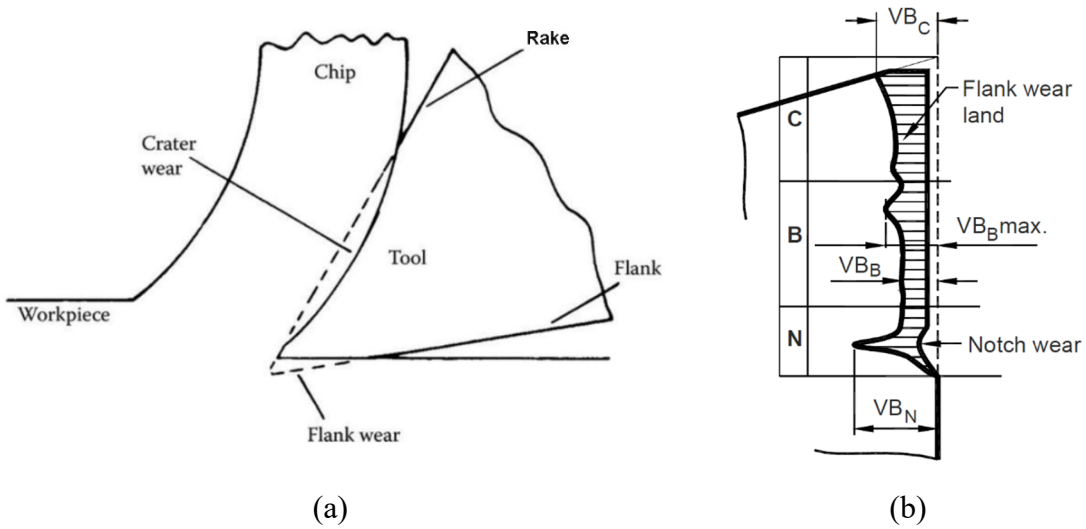

*Figure 1.3- **(a)** Schematic of a worn tool;*
***(b)** Flank wear definition – adapted with permission (Klocke and Kuchle 2011)*

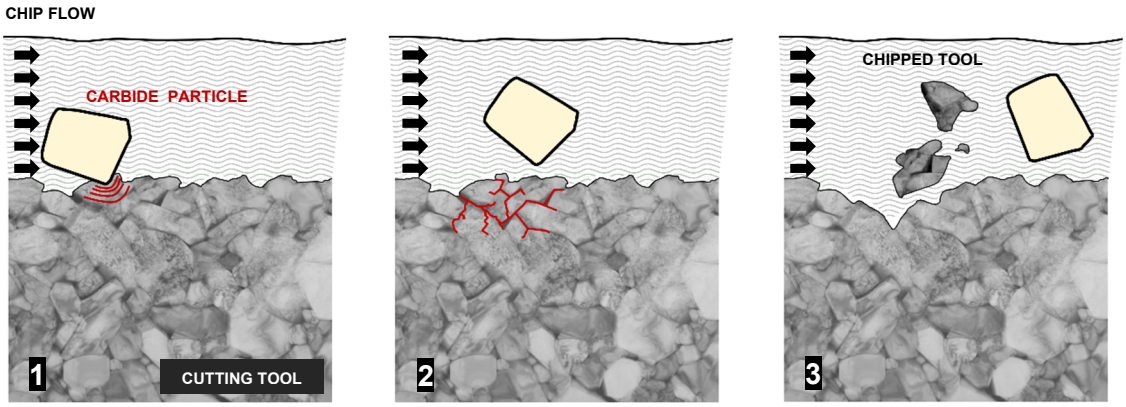

Figure 1.4 – Schematic of chipping wear in metal cutting

High weldability and high shear strength of IN718 at elevated temperatures together with the presence of hard carbide particles in the workpiece microstructure are some of the main factors that contribute to two main types of wear on the cutting edge: chipping and built-up (BUE) formation. Chipping is caused by concentrated contact stress similar to the

mechanism that was exploited by primitive man to create stone tools (Chai and Lawn 2007). Figure 1.4 shows a schematic of the chipping wear mechanism in which the impact of hard precipitation particles in the chip like niobium carbides can cause high local mechanical stresses on the tool and produce micro-cracks that can lead to chipping. Likewise, the formation of unstable BUE leads to the initiation of small cracks that propagate through the tool-BUL interface and promote attrition tool wear as illustrated in Figure 1.5.

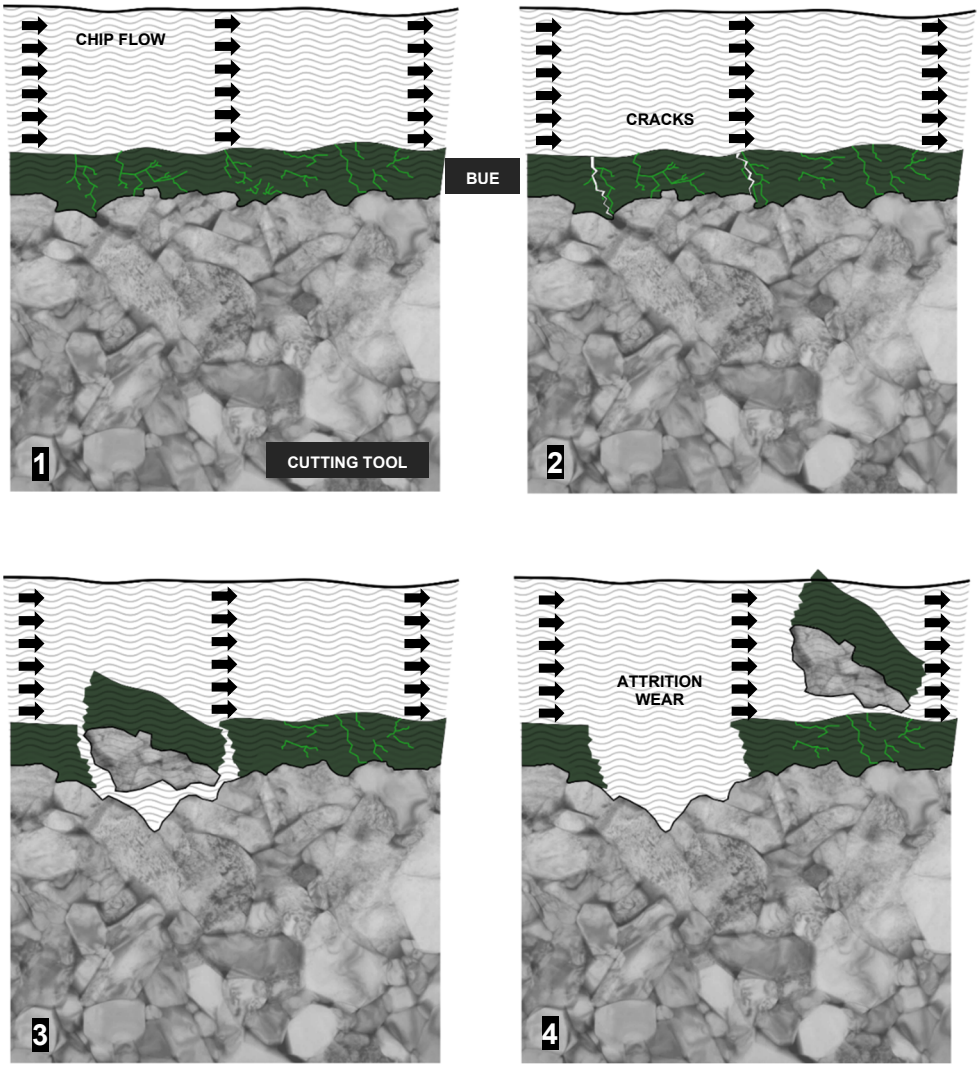

Figure 1.5- Schematic of BUE attrition wear mechanism in metal cutting

1.1.3 Ceramic Tools

Recently, some investigations have been carried out to develop new advanced ceramic materials with excellent high-temperature physical and mechanical properties (Bitterlich, et al. 2008; Izhevskiy, et al. 2000). Using a correctly chosen ceramic material with carefully selected cutting parameters, high-speed dry cutting of hardened superalloys at much higher speeds has now become possible. Currently, using uncoated and coated conventional WC-Co tools, it is only feasible to perform machining on IN718 at a maximum speed of 50 m/min resulting in a low material removal rate (MRR) and limited tool life (Kaynak 2014; Kursuncu, et al. 2018; Park, et al. 2015; Thakur and Gangopadhyay 2016; Bagherzadeh and Budak 2018). In contrast, by utilizing ceramic tools, higher cutting speeds approaching 1000 m/min can be achievable, which leads to much higher MRR and productivity and could mitigate the time and cost of machining substantially.

Different variations of advanced structural ceramics such as oxide ceramics, silicate ceramics, carbide ceramics, and Nitride ceramics have been implemented in industry with applications in metal cutting:

Oxide ceramic: Aluminum oxide based (Al_2O_3), with added zirconia (ZrO_2) for crack inhibition. This generates a material that is chemically very stable but lacks thermal shock resistance.

Mixed (Black) ceramic: Particle reinforced through the addition of cubic carbides or carbonitrides (TiC, Ti(C, N)). This improves toughness and thermal conductivity.

Whisker-reinforced ceramic: Uses Silicon carbide whiskers (SiCw) to increase toughness dramatically and enables the use of coolant. Whisker-reinforced ceramics are used for machining nickel-based alloys (Al-Falahi, et al. 2016; Çelik, et al. 2017; Obikawa and Yamaguchi 2015).

SiAlON ceramic: Silicon aluminum oxynitride combines the strength of a self-reinforced Silicon nitride network with enhanced chemical stability, thus making SiAlON grades ideal candidates for machining heat-resistant superalloys (Hao, et al. 2017; Çelik, et al. 2017).

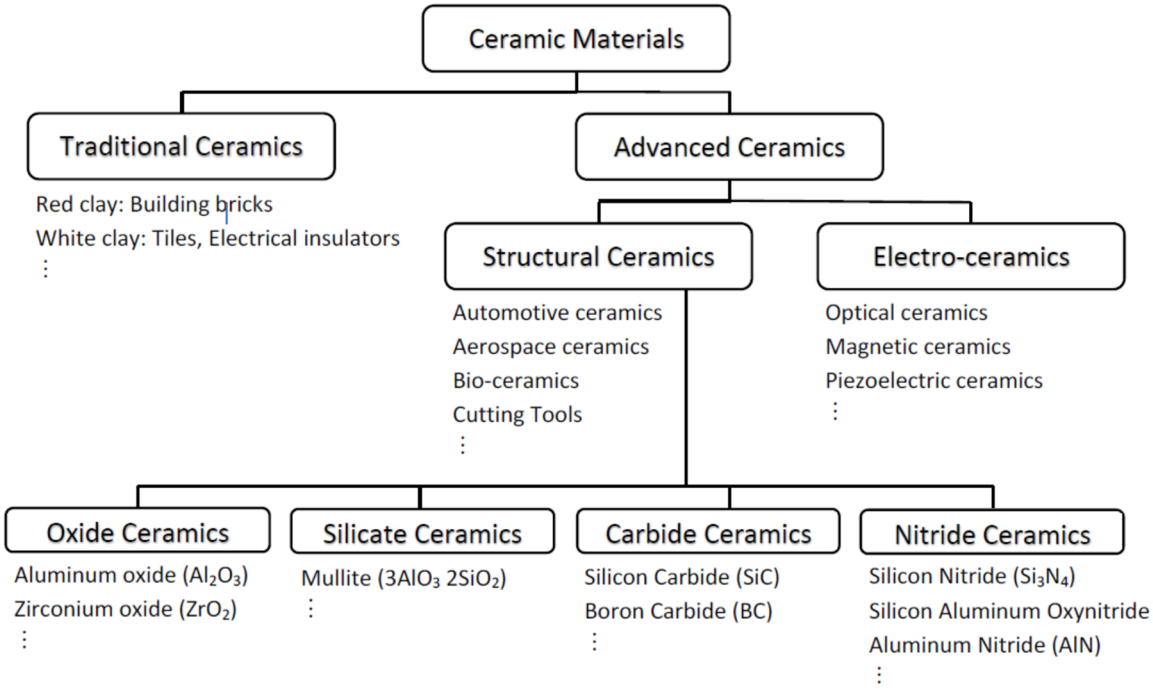

Figure 1.6- Different categories of traditional and advanced ceramics

1.2 Research Gaps

Prior studies on machining hard-to-cut materials with ceramic tools were mostly focused on turning applications, which is a less demanding process in terms of tool toughness and impact resistance. However, instead, limited research has been conducted to explore the behavior of ceramic tools in the face milling of nickel-based superalloys in which the tool is exposed to intermittent cutting forces and thermal fatigue cycles (Devillez, et al. 2011; Marques, et al. 2016). By choosing the face milling process for the machinability experiments, higher cutting speeds can be achieved with lower spindle RPM and consequently limited vibrations and chatter. Little research can be found in the current literature achieving the cutting speeds discussed in this thesis. Furthermore, no comprehensive investigations are available on the proper selection of the ceramic compound for the demanded application which is supported in this research with the results of micro and nano-characterization techniques.

This research discusses fundamental and dominant phenomena at different shear deformation zones in the cutting area around which there is a significant lack of data in the current literature. Topics such as chip formation mechanisms, the formation of lubricious and thermal barrier tribofilms at extreme frictional interactions, metallurgical studies of built-up edge and transferred layers, and carbide phase transformations at chip cross-sections are among the subjects covered in this thesis and make up the novel contributions of this research to the literature.

1.3 Motivation and Research Objectives

Recent surveys reveal that the top motivations behind industry's investments in machine tools are an increase in productivity, an increase in capacity, or cost reduction (Rüßmann, et al. 2015). In a machining process, productivity is defined by the volume of the workpiece material being removed per unit of time (MRR). Hence, the demand for high throughput machining processes is increasing more than ever before.

High-performance machining has also become an attractive topic for manufacturing researchers in academia. Nevertheless, successful implementation of such a process requires a deep understanding of the phenomena governing the tool wear, chip formation and tribological response of the tool-chip-workpiece tribosystem. Besides, physical and metallurgical characteristics of tool and workpiece material are among the principal factors influencing the performance of a high-speed machining setup. In this regard, one of the most difficult-to-cut materials that have always been a target of machinability studies in the academic community is IN718.

During this research, by using a carefully chosen ceramic material for tooling, unprecedented cutting speeds have been achieved in dry milling of a hardened inconel superalloy. This research attempts to provide in-depth reasoning behind the drastic transformation in the machinability of the workpiece material at elevated cutting speeds. Various numerical and experimental results have been used in this study to form a comprehensive understanding of different aspects of this manufacturing process.

With respect to the outlined motivations and research gaps, the main objectives of this project have been defined as follows:

1. Material characterization and performance assessment of ceramic cutting tools in high-speed machining of IN718.
2. Investigating the effect of process parameters in high-speed milling of IN718 using a ceramic tool and identifying its main tool wear mechanisms.
3. Investigating tool-chip-workpiece tribosystem in high-speed machining of IN718 with ceramic tools.
4. Investigating deformation characteristics, chip formation mechanisms and IN718 material behavior under extreme conditions using machinability studies.
5. Surface integrity studies of IN718 after high-speed machining with ceramic tools and its comparison with conventional carbide tools.

1.4 Thesis Outline

This research is organized into three major phases. Each of the following three chapters contains the manuscript of journal articles prepared by the author, covering different phases and objectives of the project. A general overview of the thesis contents is as follows:

Chapter 1 presents an introduction to the research, along with the research gaps, motivations, and research objectives. Relevant background and literature review around the thesis topic are also provided in this chapter.

Chapter 2 provides results and discussion on the characterization and selection of ceramic tools via micro and nanoindentation methods, numerical modelling of the machining process, tool life studies, investigation of dominant wear mechanisms, and optimization of the process parameters.

This chapter covers the first two objectives of the research as the first phase of the project. Chapter 2 script is published in *The International Journal of Advanced Manufacturing Technology 105.1-4 (2019): 1083-1098,* titled *"Influence of process parameters on the cutting performance of SiAlON ceramic tools during high-speed dry face milling of hardened Inconel 718."*

Chapter 3 presents phenomena-based studies of chip formation and tribological behavior of the process, aiming to investigate the mechanism of shear deformation under extreme conditions, frictional interactions of the tool-chip-workpiece tribosystem, and formation of built-up edges and transferred layers during the high-speed milling.

This chapter covers the third and fourth objectives of the research as the second phase of the project. Chapter 3 script is published in *Wear 446 (2020): 203191.,* titled *"Chip formation and tribological behavior in high-speed milling of IN718 with ceramic tools."*

Chapter 4 provides results and discussions regarding the surface integrity of the machined surfaces using various characterization methods and near-surface metallography observations alongside with 3D surface scanning. This chapter also presents a comparison between the surface finish of conventional PVD coated WC-Co tools and SiAlON ceramics.

This chapter covers the final objective of the research and the third phase of the project. A manuscript from the content of chapter 4 has been submitted to *The International Journal of Advanced Manufacturing Technology,* titled *"Surface integrity of inconel 718 in high-speed dry milling using SiAlON"* and is currently under peer review by the journal.

Chapter 5 summarizes the main observations and fundamental conclusions of the study and discusses the contribution and overall implication of the research as well as suggestions for future work.

1.5 Note to Reader

Since the contents of this thesis are a series of individual peer-reviewed journal articles, some repetition or overlap in content may be found, especially in the introduction of different chapters and research methodologies. Nevertheless, the reader is highly

encouraged to read the full material as each introduction section is focused on the specific investigations discussed in the respective chapter.

1.6 References

Al-Falahi, Muath, et al. 2016. "Surface Defects in Groove Milling of Hastelloy-C276 under Fluid Coolant." *Materials and Manufacturing Processes* 31, no. 13: 1724-1732. https://dx.doi.org/10.1080/10426914.2015.1103854.

Aramcharoen, Ampara, et al. 2014. "An Experimental Investigation on Cryogenic Milling of Inconel 718 and Its Sustainability Assessment." *Procedia Cirp* 14, no. 1: 529-534.

Astakhov, Viktor P., et al. 2008. "Tools (Geometry and Material) and Tool Wear." 29-57. London: Springer London.

Attia, H., et al. 2010. "Laser-Assisted High-Speed Finish Turning of Superalloy Inconel 718 under Dry Conditions." *CIRP Annals - Manufacturing Technology* 59, no. 1: 83-88. https://dx.doi.org/10.1016/j.cirp.2010.03.093.

Bagherzadeh, Amin, et al. 2018. "Investigation of Machinability in Turning of Difficult-to-Cut Materials Using a New Cryogenic Cooling Approach." *Tribology International* 119, no. December 2017: 510-520. https://dx.doi.org/10.1016/j.triboint.2017.11.033.

Bhatt, Abhay, et al. 2010. "Wear Mechanisms of Wc Coated and Uncoated Tools in Finish Turning of Inconel 718." *Tribology International* 43, no. 5-6: 1113-1121. https://dx.doi.org/10.1016/j.triboint.2009.12.053.

Bitterlich, Bernd, et al. 2008. "Sialon Based Ceramic Cutting Tools." *Journal of the European Ceramic Society* 28, no. 5: 989-994. https://dx.doi.org/10.1016/j.jeurceramsoc.2007.09.003.

Çelik, Ali, et al. 2017. "Wear Behavior of Solid Sialon Milling Tools During High Speed Milling of Inconel 718." *Wear* 378-379: 58-67. https://dx.doi.org/10.1016/j.wear.2017.02.025.

Chai, Herzl, et al. 2007. "A Universal Relation for Edge Chipping from Sharp Contacts in Brittle Materials: A Simple Means of Toughness Evaluation." *Acta Materialia* 55, no. 7: 2555-2561.

Choudhury, IA, et al. 1998. "Machinability of Nickel-Base Super Alloys: A General Review." *Journal of Materials Processing Technology* 77, no. 1-3: 278-284.

Chryssolouris, G., et al. 1997. "Laser Assisted Machining: An Overview." *Journal of Manufacturing Science and Engineering* 119, no. 4B: 766-766. https://dx.doi.org/10.1115/1.2836822.

Costes, Jean-Philippe, et al. 2007. "Tool-Life and Wear Mechanisms of Cbn Tools in Machining of Inconel 718." *International Journal of Machine Tools and Manufacture* 47, no. 7-8: 1081-1087.

Devillez, A., et al. 2011. "Dry Machining of Inconel 718, Workpiece Surface Integrity." *Journal of Materials Processing Technology* 211, no. 10: 1590-1598. https://dx.doi.org/10.1016/j.jmatprotec.2011.04.011.

Devillez, A., et al. 2007. "Cutting Forces and Wear in Dry Machining of Inconel 718 with Coated Carbide Tools." *Wear* 262, no. 7-8: 931-942. https://dx.doi.org/10.1016/j.wear.2006.10.009.

Dudzinski, D., et al. 2004. "A Review of Developments Towards Dry and High Speed Machining of Inconel 718 Alloy." *International Journal of Machine Tools and Manufacture* 44, no. 4: 439-456. https://dx.doi.org/10.1016/S0890-6955(03)00159-7.

Ezugwu, E. O. 2005. "Key Improvements in the Machining of Difficult-to-Cut Aerospace Superalloys." *International Journal of Machine Tools and Manufacture* 45, no. 12-13: 1353-1367. https://dx.doi.org/10.1016/j.ijmachtools.2005.02.003.

Fox-Rabinovich, GS, et al. 2010. "Multi-Functional Nano-Multilayered Altin/Cu Pvd Coating for Machining of Inconel 718 Superalloy." *Surface and Coatings Technology* 204, no. 15: 2465-2471.

Hao, Zhao Peng, et al. 2017. "New Observations on Wear Mechanism of Self-Reinforced Sialon Ceramic Tool in Milling of Inconel 718." *Archives of Civil and Mechanical Engineering* 17, no. 3: 467-474. https://dx.doi.org/10.1016/j.acme.2016.12.011.

Izhevskiy, V. A., et al. 2000. "Progress in Sialon Ceramics." *Journal of the European Ceramic Society* 20, no. 13: 2275-2295. https://dx.doi.org/10.1016/S0955-2219(00)00039-X.

Kadirgama, K., et al. 2011. "Tool Life and Wear Mechanism When Machining Hastelloy C-22hs." *Wear* 270, no. 3-4: 258-268. https://dx.doi.org/10.1016/j.wear.2010.10.067.

Kaynak, Yusuf. 2014. "Evaluation of Machining Performance in Cryogenic Machining of Inconel 718 and Comparison with Dry and Mql Machining." *International Journal of Advanced Manufacturing Technology* 72, no. 5-8: 919-933. https://dx.doi.org/10.1007/s00170-014-5683-0.

Klocke, F., et al. 2011. "Manufacturing Processes 1: Cutting." *Springer*. https://scholar.google.ca/scholar?hl=en&as_sdt=0,5&q=Manufacturing+Processes+1-Cutting+Fritz+Klocke.

Kursuncu, Bilal, et al. 2018. "Improvement of Cutting Performance of Carbide Cutting Tools in Milling of the Inconel 718 Superalloy Using Multilayer Nanocomposite Hard Coating and Cryogenic Heat Treatment." *International Journal of Advanced Manufacturing Technology*: 1-13. https://dx.doi.org/10.1007/s00170-018-1931-z.

Lima, Fabio F., et al. 2017. "Wear of Ceramic Tools When Machining Inconel 751 Using Argon and Oxygen as Lubri-Cooling Atmospheres." *Ceramics International* 43, no. 1: 677-685. https://dx.doi.org/10.1016/j.ceramint.2016.09.214.

Marques, Armando, et al. 2016. "Surface Integrity Analysis of Inconel 718 after Turning with Different Solid Lubricants Dispersed in Neat Oil Delivered by Mql." *Procedia Manufacturing* 5: 609-620. https://dx.doi.org/10.1016/j.promfg.2016.08.050.

Montazeri, Saharnaz, et al. 2019. "An Investigation of the Effect of a New Tool Treatment Technique on the Machinability of Inconel 718 During the Turning Process." *International Journal of Advanced Manufacturing Technology* 100, no. 1-4: 37-54. https://dx.doi.org/10.1007/s00170-018-2669-3.

Nalbant, Muammer, et al. 2007. "The Effect of Cutting Speed and Cutting Tool Geometry on Machinability Properties of Nickel-Base Inconel 718 Super Alloys." *Materials & design* 28, no. 4: 1334-1338.

Obikawa, Toshiyuki, et al. 2008. "Micro-Liter Lubrication Machining of Inconel 718." *International Journal of Machine Tools and Manufacture* 48, no. 15: 1605-1612.

Obikawa, Toshiyuki, et al. 2015. "Suppression of Notch Wear of a Whisker Reinforced Ceramic Tool in Air-Jet-Assisted High-Speed Machining of Inconel 718." *Precision Engineering* 39: 143-151. https://dx.doi.org/10.1016/j.precisioneng.2014.08.002.

Pan, Zhipeng, et al. 2017. "Heat Affected Zone in the Laser-Assisted Milling of Inconel 718." *Journal of Manufacturing Processes* 30, no. October: 141-147. https://dx.doi.org/10.1016/j.jmapro.2017.09.021.

Park, Kyung-Hee, et al. 2015. "Tool Wear Analysis on Coated and Uncoated Carbide Tools in Inconel Machining." *International Journal of Precision Engineering and Manufacturing* 16, no. 7: 1639-1645. https://dx.doi.org/10.1007/s12541-015-0215-x.

Rinaldi, Sergio, et al. "A Physically Based Model to Predict Microstructural Modifications in Inconel 718 High Speed Machining." *Procedia Manufacturing* 47 (2020): 487-492. https://doi.org/10.1016/j.promfg.2020.04.344

Rüßmann, Michael, et al. 2015. "Industry 4.0: The Future of Productivity and Growth in Manufacturing Industries." *Boston Consulting Group* 9, no. 1: 54-89.

Schirra, J. J., et al. 1994. "Metallurgical Factors Affecting the Machinability of Inconel 718." *Superalloys 1994*: 827-838.

Sharman, Adrian, et al. 2001. "Tool Life When High Speed Ball Nose End Milling Inconel 718(Tm)." *Journal of Materials Processing Technology* 118, no. 1-3: 29-29. http://www.sciencedirect.com/science/article/B6TGJ-44NM96N-6/2/d6569714f8f8f391d7481d3401571621.

Soo, Sein Leung, et al. 2016. "High Speed Turning of Inconel 718 Using Pvd-Coated Pcbn Tools." *CIRP Annals - Manufacturing Technology* 65, no. 1: 89-92. https://dx.doi.org/10.1016/j.cirp.2016.04.044.

Tadavani, Soheila Azhdari, et al. 2017. "Pulsed Laser-Assisted Machining of Inconel 718 Superalloy." *Optics & Laser Technology* 87: 72-78.

Thakur, A., et al. 2016. "Dry Machining of Nickel-Based Super Alloy as a Sustainable Alternative Using Tin/Tialn Coated Tool." *Journal of Cleaner Production* 129: 256-268. https://dx.doi.org/10.1016/j.jclepro.2016.04.074.

Zhao, Bin, et al. "Cutting performance and crack self-healing mechanism of a novel ceramic cutting tool in dry and high-speed machining of Inconel 718." *The International Journal of Advanced Manufacturing Technology* 102.9-12 (2019): 3431-3438. https://doi.org/10.1007/s00170-019-03386-x

Zheng, Guangming, et al. 2012. "Cutting Performance and Wear Mechanisms of Sialon-Si 3n 4 Graded Nano-Composite Ceramic Cutting Tools." *International Journal of Advanced Manufacturing Technology* 58, no. 1-4: 19-28. https://dx.doi.org/10.1007/s00170-011-3379-2.

Zhu, Dahu, et al. 2013. "Tool Wear Characteristics in Machining of Nickel-Based Superalloys." *International Journal of Machine Tools and Manufacture* 64: 60-77. https://dx.doi.org/10.1016/j.ijmachtools.2012.08.001.

Chapter 2. Process Parameters Optimization and Identifying Wear Mechanisms

F.Molaiekiya, P. Stolf, J. M. Paiva, B. Bose, G. Fox-Rabinovich, S. C. Veldhuis "*Influence of process parameters on the cutting performance of SiAlON ceramic tools during high-speed dry face milling of hardened Inconel 718*" *The International Journal of Advanced Manufacturing Technology* 105.1-4 (2019): 1083-1098.

Authors' Contributions

F. Molaiekiya	Designed and performed the experiments Analyzed and interpret the results Wrote and prepared the manuscript
P. Stolf	Assisted with the finite element modeling
J. M. Paiva	Assisted with writing/editing the manuscript
B. Bose	Assisted with the tests performed at MPAL
G. Fox-Rabinovich	Assisted with the interpretation of data Edited the manuscript
S. C. Veldhuis	Supervised the project

Abstract

Heat resistant superalloys (HRSAs) exhibit excellent mechanical strength and structural stability at elevated temperatures. Hence, aerospace and power industries have consistently chosen Nickel-based superalloys over the years for manufacturing hot-section components. However, poor machinability of these alloys has always been a challenge. This paper investigates the cutting performance of new-generation SiAlON ceramics under extreme conditions of dry high-speed face milling of hardened Inconel 718. Comprehensive characterization of the ceramic tool and its milling performance were conducted using instrumented micro/nano-mechanical indentations, tool life studies, optical 3D imaging, and SEM/EDS investigation of wear patterns. Also, experimental results were linked to the finite element analysis (FEA) of temperature and stress profiles. It is demonstrated that a few major factors govern the ceramic tool life under the outlined cutting conditions: (1) High temperature at the cutting edge exceeding 1250 °C. This temperature is close to the melting point of Inconel 718, and moreover, it is highly localized around the cutting edge-chip interface. (2) High resultant mechanical stress on the tool of around 5.8 GPa. (3) Thermal and mechanical fatigue loading due to the discontinuity of the milling process, combined with (4) intensive built-up edge formation caused by severe weldability of the softened workpiece to the tool. Combination of these phenomena results in a significant change in the machinability of the workpiece material after surpassing a certain limit of cutting speed. The cutting forces, tool wear, and chipping show a significant decline with increasing the speed high enough, which is attributed to the change in the material properties of the workpiece and dissolution of the hard particles within the Inconel microstructure.

Keywords

High-speed milling; Cutting parameters; SiAlON ceramic; Inconel 718; Tool wear; Material characterization

2.1 Introduction

Previous studies have shown that in manufacturing processes, neither tool life improvement nor the reduction of tooling costs can meaningfully reduce the final product cost. On the other hand, an increase in process productivity can significantly reduce manufacturing costs. In machining, the productivity of the process can be quantified by the material removal rate (MRR) which is the volume of material being removed per minute (mm^3/min). In this regard, achieving higher MRR via the implementation of high-speed machining concepts has been one of the key manufacturing research areas since the early 1980s. Aerospace and automotive industries now greatly benefit from the advancement of metal cutting technologies, which enables reaching cutting speeds as high as 3000 m/min and MRR values above 4500 mm^3/min in Aluminum machining (2016; Schulz and Moriwaki 1992; King 1985). Advances in rigid machine tool designs, tool holder stiffness, cutting tool material, and machining programming are crucial supporting elements of a successful high-speed machining process. Yet, physical and mechanical properties of the workpiece material also play a vital role in this matter. Not all metals and alloys can be effectively machined at high cutting speeds. For instance, in contrast to aluminum alloys, cutting speeds in the machining of heat resistant superalloys (HRSAs) are strictly limited due to their poor machinability (M'Saoubi, et al. 2015).

From the category of HRSAs, Nickel-based superalloys are widely employed in the manufacturing of aeronautical hot-section components due to their favorable high-temperature strength, structural reliability, as well as high corrosion, creep, and fatigue resistance (Schirra and Viens 1994). However, these beneficial mechanical

properties are also the source of their poor machinability. Some fundamental reasons behind low machinability of Nickel-based alloys are: (1) high shear strength, (2) occurrence of intensive work-hardened layer, (3) presence of hard and abrasive particles in the microstructure such as carbide precipitations, (4) generation of extremely high temperatures at the tool-chip interface, (5) low thermal conductivity impairing proper heat dissipation from the cutting zone, and (6) high weldability of the workpiece material to the cutting tool, and thus extensive formation of built-up edges (BUEs) (Rahman, et al. 1997; Li, et al. 2002; Ezugwu 2005). Consequently, only a few categories of materials can be employed as cutting tools at the aggressive cutting conditions prevalent in the machining of Nickel-based alloys, namely Inconel 718. Recently, development of advanced structural ceramics with excellent high-temperature properties enabled cutting parameters of IN718 to reach much higher speeds, owing to the fact that advanced ceramic tools can better sustain extreme tribological conditions in high-speed dry machining of hard-to-cut alloys. SiAlON ceramic is one good example of such materials.

Silicon Aluminum Oxynitride or SiAlON was first introduced in the 1970s. This class of engineered ceramics has gone through multiple microstructural modifications during the past few decades, promoting outstanding thermal and mechanical properties for commercial and industrial applications with severe working conditions (Hoffmann and Petzow 1994). In cutting tool applications, SiAlON compounds are distributed in an M-Si-Al-O-N matrix in which M stands for metal, e.g., Yttrium (Metselaar 1998). The microstructure of these ceramic tools consists of two different SiAlON phases, α-SiAlON with a global structure, characterized by its high hardness, and β-SiAlON with a rod-like

structure, which in contrast, is rather tough. By adjusting the α/β ratio in the microstructure, a combination of excellent hardness and high fracture toughness could be achieved for different purposes (Wacinski 2016; Izhevskiy, et al. 2000). It has been shown that during high-speed turning of Inconel 718, SiAlON ceramic cutting tools exhibit a relatively high fracture toughness, low thermal conductivity, high wear resistance, and a robust chemical/mechanical stability at elevated temperatures (Liu, et al. 2016; Bitterlich, et al. 2008). These properties prescribe SiAlON ceramics as a promising cutting tool material for high-performance face milling of hard-to-cut Nickel-based superalloys.

Prior studies around this topic are mostly focused on the continuous turning of materials with ceramic tools (Devillez, et al. 2011; Marques, et al. 2016), but limited research was performed to explore the behavior of SiAlON ceramic tools during the milling operation of nickel-based superalloys. Selection of milling as the cutting operation in this study, enabled us to reach very high speeds and investigate the material behavior at extreme conditions, for which there is a significant lack of scientific data. Moreover, chipping and fracture of ceramic tools, especially during intermittent cutting operations like milling, is still considered as an important drawback of these tools; but, not enough studies have been performed to understand the dominant failure mechanisms, how to choose the best ceramic tool for a specific cutting application, and the performance of these tools in extreme conditions. Hence, a comprehensive study is performed to investigate the material properties of SiAlON ceramic cutting tools and their wear behavior during high-performance dry face milling of hardened IN718. This paper strives to uncover the main wear and failure mechanisms of the SiAlON ceramic tools based on a set of milling

experiments at different cutting parameters, alongside comprehensive micro/nano-mechanical material characterization techniques. Additionally, finite element modeling has been performed to estimate the thermal and mechanical stresses on the cutting edge, the results of which were correlated to the experimental observations with a very good agreement.

The results of this study reveal that a unique phenomenon happens in the machining of IN718 at very high speeds, leading to a 400% improvement in the productivity of the cutting process compared to the common practices in the industry, while restraining chipping and rapid tool wear of ceramic inserts. It has been found that by sufficiently increasing the cutting speed, dissolution of hard carbide particles in the workpiece microstructure would result in a significant reduction of cutting forces and a consequent improvement in tool life.

2.2 Methods and Procedures

2.2.1 Experimental Setup

The workpiece used for this study was an Inconel 718 block, hardened up to 45±2 HRC. The chemical composition and mechanical properties of the workpiece material are presented in Table 2.1. The microstructure of the IN718, captured by a high resolution optical microscope (Keyence VH-ZST), is illustrated in Figure 2.1 The partially recrystallized IN718 austenite grains are distributed in a necklace-type structure. The material was etched by swabbing a cotton ball rinsed in a solution consisting of 15 ml

Hydrochloric acid, 10 ml Nitric acid, 10 ml Acetic acid, and less than a drop of Glycerin for 10 seconds.

Table 2.1- Chemical composition and mechanical properties of IN718

Chemical Composition							
Element	Ni	Cr	Fe	Nb	Al	Ti	Si
Weight (%)	53.70	18.43	18.30	6.37	1.20	1.03	0.97

Mechanical Properties (Room Temperature)				
Hardness (HRC)	Yield Strength $\sigma_{0.2}$ (MPa)	Tensile Strength σ_b (MPa)	Elongation δ_5 (%)	Toughness a_k (J/cm^2)
45	1230	1490	21	43

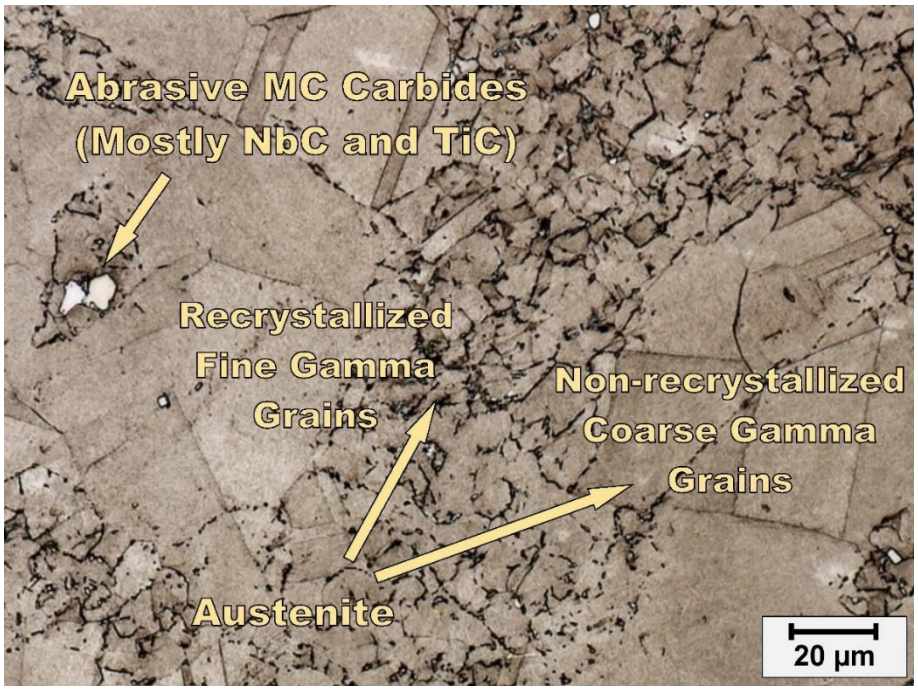

Figure 2.1- Optical microscope image of the IN718 microstructure (partially recrystallized)

A set of six RNGN120400T01020 round milling inserts were used as cutting tools, made of KYS30 SiAlON ceramic grade, manufactured by Kennametal. The ceramic phase composition was analyzed using Bruker D8 Discover X-ray powder diffraction (XRD) with Co anode source and Vantec-500 detector. Furthermore, Micro/nano-mechanical evaluations were done using Micro Materials Nano Test Platform 3, and Anton Paar Revetest Scratch Tester (RST^3). The Oliver-Pharr nonlinear curve fit method was used to calculate the nano-hardness of the samples. For the machinability test, these inserts were clamped on an indexable KCRA250RN4306S075L175 face mill holder featuring complex through-spindle air coolant channels, aimed at the rake face of each insert. The clearance, axial and radial rake angles were 10°, -10°, and -5°, respectively.

Machining was carried out on a robust CNC horizontal machining center (Makino MC56-5XA) with a spindle power of 30 kW, and a maximum spindle speed of 15000 RPM. This machine is capable of providing through-spindle air coolant with three bar pressure for better evacuation of chips and achieving a longer tool life. The face milling setup is illustrated in Figure 2.2. To observe the effect of cutting parameter variations on the tool performance, five different cutting speeds from 500 to 1300 m/min were investigated and then under the best cutting speed, three different feed rates (from 20 to 60 μm per tooth) were tested. Each test has been performed twice, and all six inserts have been assessed, and average results are presented. Table 2.2 shows the cutting parameters and the strategy used for the cutting path.

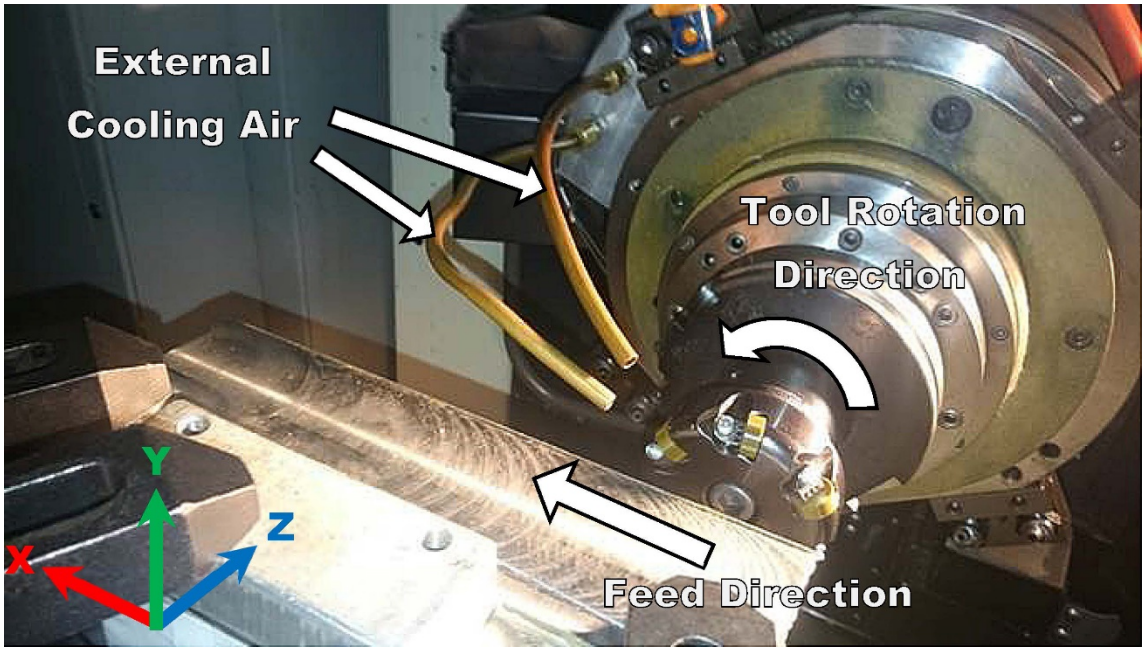

Figure 2.2- Experiment setup

Table 2.2- Face milling process parameters

Application	**Tool path**	**Coolant**	
Horizontal face milling	Roll-in technique	Through-spindle air (3 bar)	(2x) 4 mm air nozzles (7 bar)

Cutter Diameter	**Number of Teeth**	**Radial Depth of Cut**	**Axial Depth of Cut**
63.5 mm	6	34.5 mm	1 mm

Feed per Tooth (mm)	0.02, 0.04, 0.06				
Cutting Speed (m/min)	500	700	900	1100	1300
Spindle RPM	2768	3875	4982	6089	7197
Table speed (mm/min)*	664	930	1196	1461	1727

* For 0.04 mm/tooth feed rate

During the experiment, the 3D volumetric tool wear was measured periodically using a white light high-precision 3D measurement system (Alicona Infinite Focus XL200 G5) with ±2 microns scanning resolution. The maximum flank wear land width was also evaluated using a Keyence VHX-5000 optical microscope. Maximum flank wear of 1.0 mm was determined to be the tool life criterion for the category of ceramic tools, based on industrial practices.

The resultant cutting forces were measured using Kistler 9255B, a 3-component piezoelectric dynamometer with 10 kHz sampling rate. The dynamometer was connected to a Kistler type 5001 charge amplifier, National Instruments USB-9162 DAQ system, and LabVIEW data acquisition software. Additionally, an InfraTec VarioCAM HD 1024 thermal infrared camera with 1024×768 pixels resolution and a 60 Hz frame frequency was used to monitor the resultant cutting temperature at the cutting zone.

The worn SiAlON cutting inserts were then imaged and analyzed by a Tescan Vega II LSU scanning electron microscope (SEM), equipped with an Oxford X-Max 80 energy-dispersive X-ray spectroscopy (EDX) detector and Inca software version 4.14. The spatial resolution of the EDS data was set to 1-5 μm^3 for low and 0.2-1 μm^3 for high atomic numbers using 10 kV accelerating voltage. To understand the wear mechanism and built-up edge formation, the accumulated IN718 BUE on the top of the worn edges was chemically etched out to reveal the worn ceramic surface underneath. For this purpose, the ceramics were heat-treated at 750 °C for 1 to 1.5 hours and air cooled. Then, the treated samples were dipped in a solution of 4 ml Hydrochloric acid, 2 ml Nitric acid and 2 ml Hydrofluoric acid with 50 ml distilled water at 50 - 60 °C for a few hours. This procedure

removed the BUE from the cutting edges by dramatically increasing the rate of oxidation and corrosion of sticky IN718, while causing negligible harm to SiAlON.

2.2.2 Finite Element Analysis (FEA)

Finite element modeling and analysis are widely approved tools for the evaluation of resultant cutting conditions, such as temperature and stress profiles near the cutting zone. In order to obtain such informative data, FEM analysis is further performed in this study.

The current model was developed by "Third Wave Systems AdvantEdge" CAE software. It employs a Lagrangian approach combined with adaptive remeshing capabilities. This model addresses the non-linearities caused by high plastic deformation, strain rates, and inherent resolution issues that emerge from the milling process. As a constitutive model, the power law is utilized to describe strain hardening and rate sensitivity. Moreover, a fifth-order polynomial function is used to calculate the thermal softening (Man, et al. 2012):

$$g(\alpha) = \sigma_0 \left(1 + \frac{\alpha}{\alpha_0}\right)^{\frac{1}{N}} \tag{1}$$

$$\Gamma(\dot{\alpha}) = \left(1 + \frac{\dot{\alpha}}{\dot{\alpha}_0}\right)^{\frac{1}{M}} \tag{2}$$

$$\Theta(T) = c_0 + c_1 T + \cdots + c_5 T^5 \tag{3}$$

Here, $g(\alpha)$ represents the isotropic strain hardening function, and $\Gamma(\dot{\alpha})$ is rate sensitivity. In these mathematical models, σ_0 is the initial yield stress, and α_0 and $\dot{\alpha}_0$ are the reference strain and strain rate, respectively. $\Theta(T)$ in equation (3) predicts thermal

softening. $\alpha, \dot{\alpha}$ and T denote the equivalent plastic strain, plastic strain rate and temperature, respectively.

Adaptive remeshing capabilities in the software enable the model to account for the severe deformations intrinsic to the Lagrangian method. Deformations are being continuously monitored, and once a certain predefined tolerance is met, refinement/coarsening algorithms are applied to regenerate the mesh in the most effective way possible (Man, et al. 2012). In the current research, the cutting tool is modeled as a rigid body and Coulomb's friction law is applied to relevant zones. Some input parameters for the FEA study are listed in Table 2.3.

Table 2.3- Some of the parameters and methods used for the FEA studies

Total number of elements	24000
Minimum element size	0.02 mm
Maximum element size	0.1 mm
Element type	Four-node tetrahedral
Cutting geometry	Oblique
SiAlON thermal conductivity	10 W/m.K
IN718 thermal conductivity	11.5 W/m.K
Cutting edge prep	Negative land (0.1 m ×20°)

2.3 Results and Discussion

2.3.1 Tool Material Characterization

Selection of proper tool material is of prime importance for machining of heat resistant superalloys. The chosen workpiece for this study possesses a very high hardness around 45

HRC, which results in excessive machining forces. As discussed, IN718 also has a high tendency for work-hardening and producing extreme temperatures at the cutting zone, which make it categorized as one of the most difficult-to-cut alloys. Thus, any chosen tool material should have the capability to perform at extreme thermo-mechanical conditions.

There are various ceramic materials available as cutting tools; Black ceramic, oxide ceramic, whisker-reinforced ceramic, and SiAlON are the most widely used ceramic-based materials in cutting applications.

Since for the specific demands of the current study, the tools should overcome the high mechanical loads of intermittent cutting at high temperatures, high hardness and fracture toughness, together with an ability to maintain mechanical properties and microstructural integrity at temperatures above 1000 °C are considered as vital criteria for selecting a proper tool among other ceramic tools mentioned above.

The chosen KYS30 tool grade is categorized as a self-reinforced SiAlON ceramic (77% Si_3N_4 + 13% Al_2O_3) with the addition of Ytterbium (>5%) and Lanthanum (<1%). Adding rare earth elements is common in advanced ceramics as sintering aids and microstructure stabilizers (Santos, et al. 2005). The phase composition of SiAlON cutting inserts was determined with X-ray diffraction (XRD) phase identification. X-ray diffraction pattern and back-scattered SEM image of SiAlON are presented in Figure 2.3. The etchant solution used for the ceramics was 15 ml distilled water plus 85 ml Phosphoric acid boiled for 1 hour. In Figure 2.3(a), needle-shaped β-SiAlONs appear darker than α-SiAlONs; Unlike β-SiAlONs, α-SiAlON grains contain a small amount of rare earth elements and thus turn out brighter in the back-scattered SEM image.

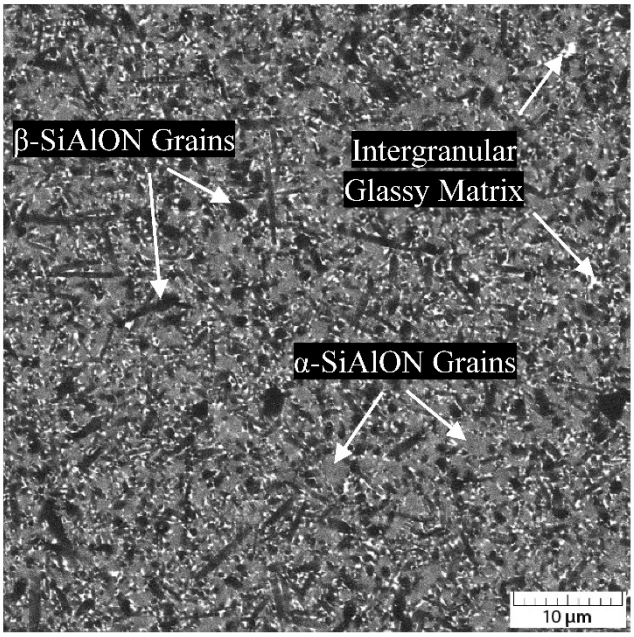

(a)

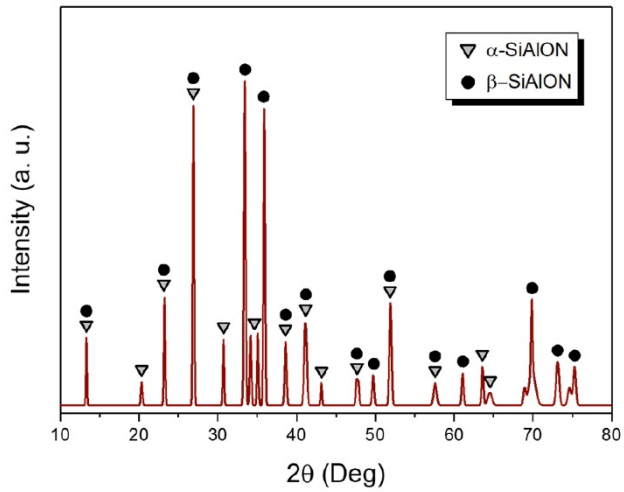

(b)

Figure 2.3- ***(a)*** *Back-scattered SEM image of the SiAlON microstructure;*
(b) *X-ray diffraction pattern of SiAlON*

The white phase is a glassy intergranular M-Si-Al-O-N matrix with a high rare earth element (M) content. This viscous phase penetrates and positions itself along the grain boundaries and triple junctions of the randomly intertwined β-SiAlON needles and hard

α-SiAlON grains, thus forming a strong structural bond with excellent fracture toughness and mechanical properties. This particular tool grade contains approximately 50% α-SiAlON, 40% β-SiAlON, and around 10% glass.

Table 2.4- Micro/nano-mechanical properties of advanced structural ceramics

Ceramic Material	**Microstructure**	**Mechanical Properties**		
		Microhardness	**Nano-impact Fatigue Fracture Resistance**	**Microfracture Toughness**
		Load: 1000 gf Dwell time: 10 s Pyramidal indenter	Load: 50 mN Pulse on duration: 2 s Pulse off duration: 2 s Total test time: 400 s Impact distance= 12 µm Cube corner indenter	Load: 50 N Loading speed: 5 (N/s) Lawn-Fuller equation Vickers Diamond indenter
		Vickers Hardness (HV)	Max Penetration Depth (nm)*	K_{Ic} ($MPa.m^{1/2}$)
SiAlON	$Si_3N_4 + Al_2O_3$	1882 ± 69	3831	5.9 ± 0.4
Black Ceramic	TiC + TiCN	2146 ± 23	4825	4.1 ± 0.5
Oxide Ceramic	$Al_2O_3 + ZrO_2$	1813 ± 28	4150	3.8 ± 0.5
Whisker-Reinforced	Al_2O_3 + SiC	2226 ± 92	4240	5.2 ± 0.2

* The lower, the better

A balanced combination of high hardness and impact toughness provides SiAlON with an advantage over the other examined ceramic tool materials, such as oxide ceramic and black ceramic, in the machining of high-temperature alloys. Table 2.4 presents a summary of SiAlON's micro/nano-mechanical properties, in comparison with other tested structural ceramics. To simulate the fatigue behavior of the material at high strain rates, in the nano-impact test, a sharp indenter with a cube corner geometry was dropped periodically from 12 microns above the polished ceramic surface, under a defined load. Figure 2.4(a) shows

variation in penetration depth over time and Figure 2.4(b) illustrates SEM images of the indent and debris after the 400-second fatigue fracture test for SiAlON and oxide ceramics.

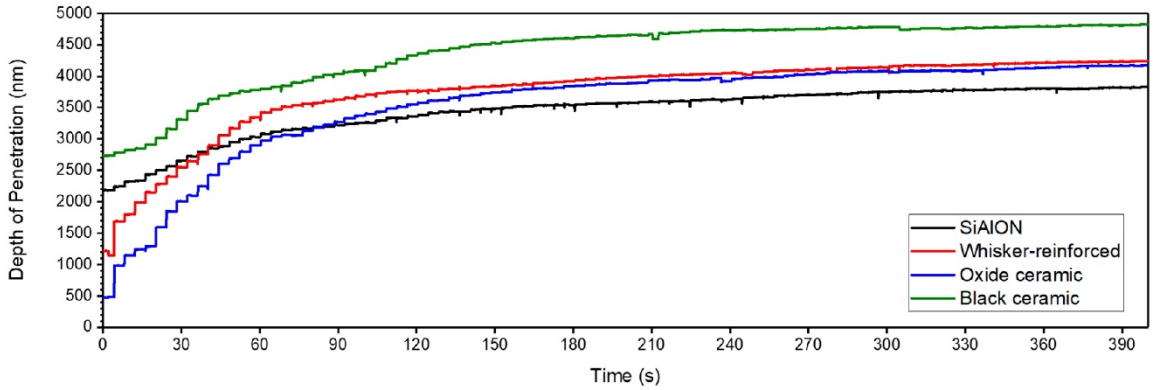

(a)

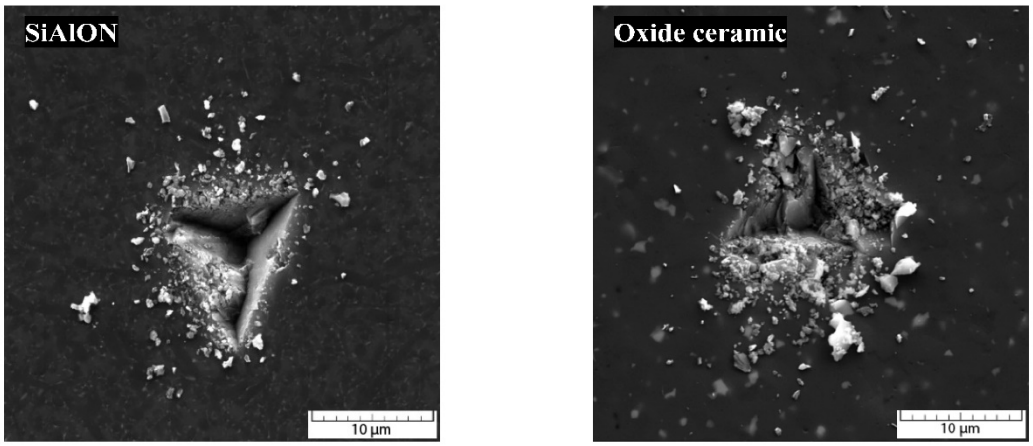

(b)

Figure 2.4- ***(a)*** *Depth-time graphs of Nano-impact indentation;*
(b) *SEM images of Nano-impact indentation*

Although the hardness value is similar to that of SiAlON, the oxide ceramic shows more indications of brittle fracture and production of larger debris. As can be seen in Figure 2.4(a), there are some sudden fluctuations in the depth versus time data for the oxide ceramic measurements, which imply the initiation and propagation of cracks. Similar trends

were also found in other tested ceramics. However, in SiAlON the depth grows much smoother and in a more predictable manner. The distinct microstructure of SiAlON exhibits a more stable crack propagation behavior compared to the other generations of fine ceramics. Figure 2.5 shows the propagated cracks on the SiAlON and black ceramic cutting tools after fracture toughness assessment via instrumented Vickers indentation method. Since brittle materials exhibit a median type crack in this test, the Lawn-Fuller equation was used to calculate the K_{Ic} value (Lawn and Fuller 1975).

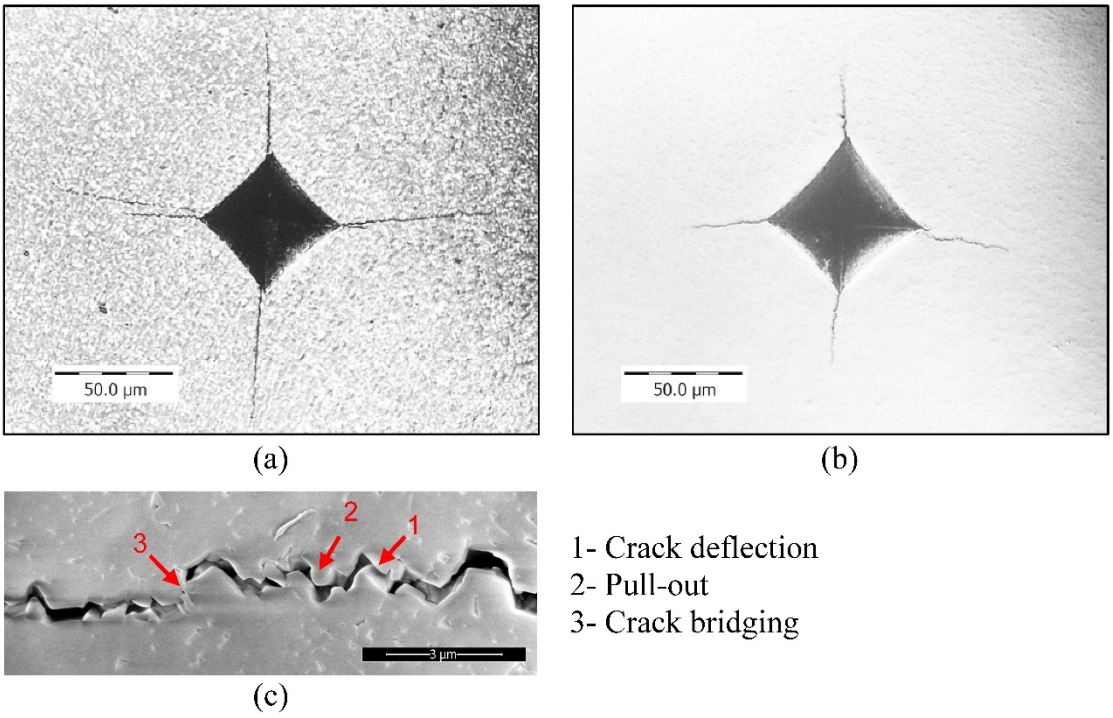

Figure 2.5- High-contrast optical microscope images of the imprints after instrumental microfracture toughness test: ***(a)*** *Black ceramic* ***(b)*** *SiAlON;* ***(c)*** *SEM image of SiAlON crack toughening mechanisms*

The smaller crack size compared to other ceramic tools indicates that the initiated crack in SiAlON requires more energy to grow, which results in higher toughness. In Figure

2.5(c) different toughening mechanisms could be detected right behind the crack tip on the SiAlON tool. These mechanisms are responsible for the relatively higher fracture resistance of SiAlON which is the most crucial mechanical property of the tool needed for efficient milling of hardened IN718.

2.3.2 Machinability Analysis

Optical microscope images of the worn flank surfaces during the initial stages of wear, after removing 21.75 cm^3 IN718 or 630 mm length of cut, are presented in Figure 2.6. At the lower range of cutting speeds around 500 to 700 m/min, significant chipping is observed (Figure 2.6(a)). As cutting speed is increased, the chipping intensity considerably reduces, especially within the range of 900 to 1100 m/min. However, chipping reappears at the speed of 1300 m/min, followed by a simultaneous growth in built-up edge formation (Figure 2.6(e)).

Tool life curves based on average volumetric and flank wear measurements are presented in Figure 2.7, at different cutting speeds. The wear values and their trends are in good agreement with the optical microscope observations illustrated in Figure 2.6. It should be noted that the cutting operation was stopped after the first wear measurement for 500 m/min and 1300 m/min due to severe premature chipping of the tool at these speeds. From the data presented in Figure 2.6 and Figure 2.7, it is concluded that there is an optimal range of cutting speed between 900 - 1100 m/min, where the chipping of the cutting edge is minimal, and tool life is the longest.

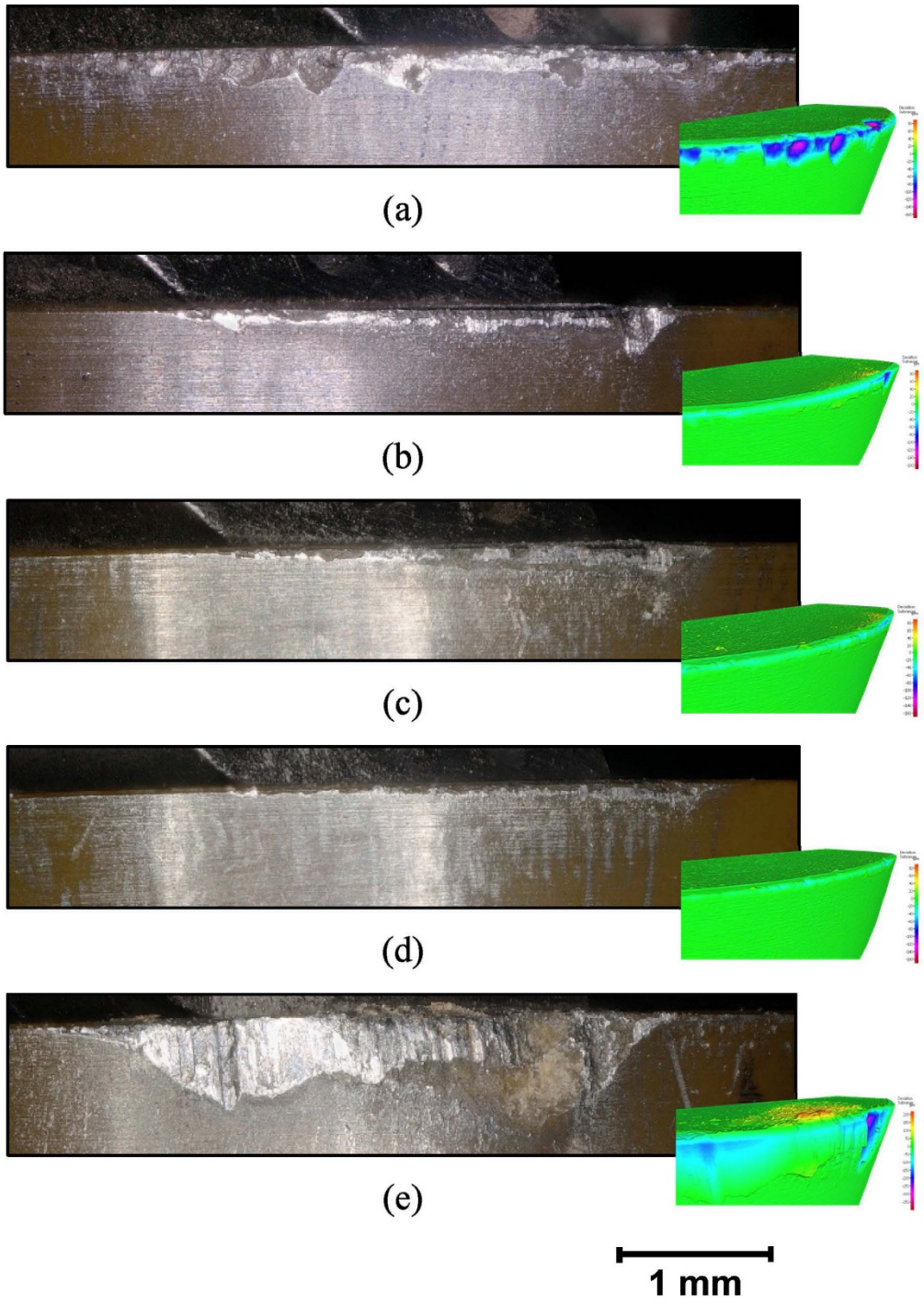

Figure 2.6- Optical microscope images and 3D wear scans of the flank surfaces of the inserts after cutting 21.75 cm^3 of IN718 (630 mm of workpiece length) with variation in the cutting speed: ***(a)*** *500 m/min;* ***(b)*** *700 m/min;* ***(c)*** *900 m/min;* ***(d)*** *1100 m/min;* ***(e)*** *1300 m/min*

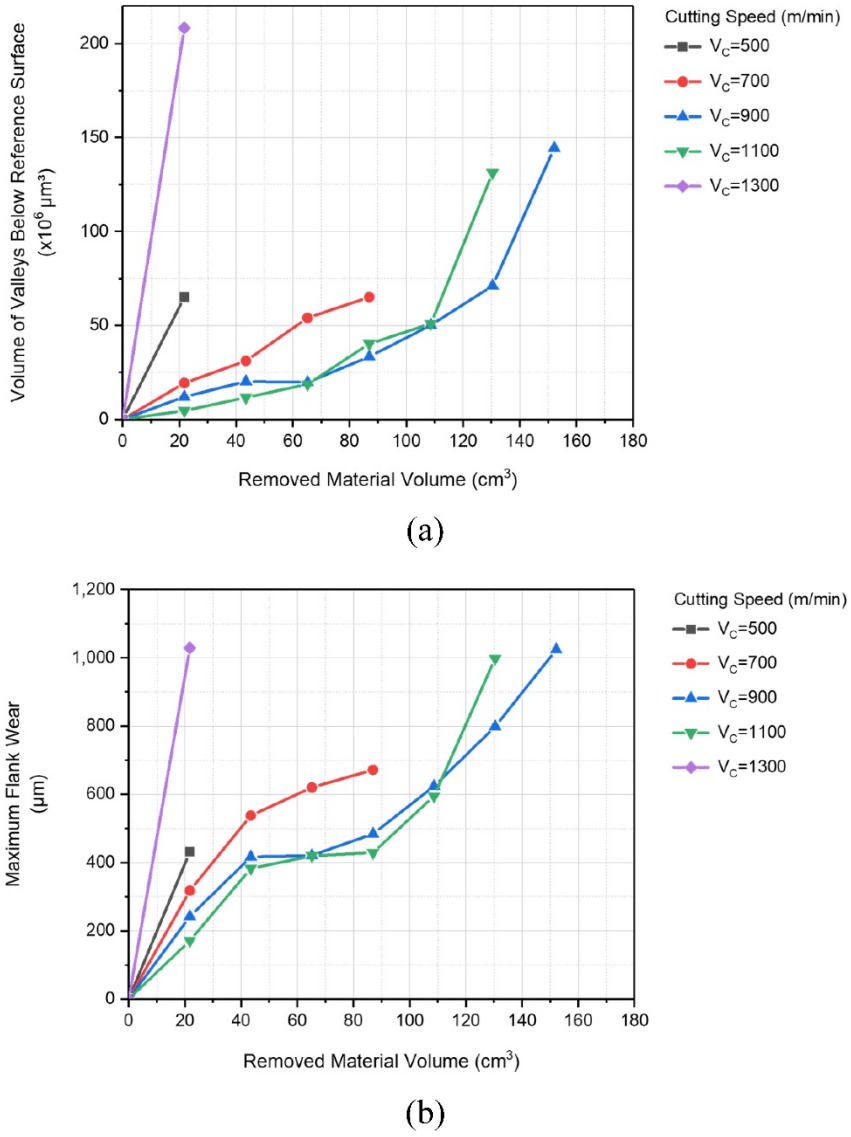

Figure 2.7- Tool life curves at different cutting speeds, based on ***(a)*** *Volumetric wear;* ***(b)*** *Flank wear*

The most important factors affecting the wear patterns are the resultant temperatures and mechanical stresses at the tool tip, which affect the tool's mechanical properties, tool oxidation rate, IN718 weldability and tendency to form BUE, and workpiece work-hardening rate. Thus, a finite element modeling was performed to assess the resultant

temperatures and stresses on the tool, and an attempt has been made to correlate the results with different phenomena observed in the experiments.

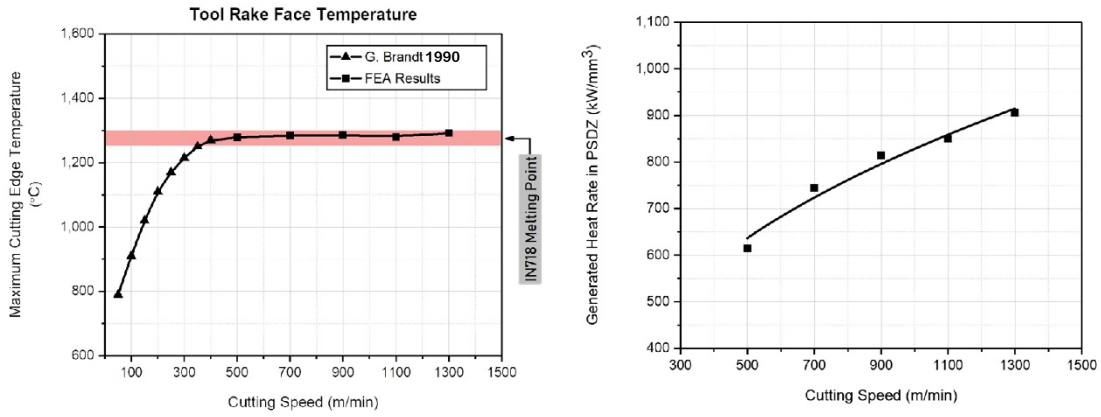

Figure 2.8- ***(a)*** *FEA: maximum temperature on the tool rake face at different cutting speeds;* ***(b)*** *FEA: heat generation rate in the primary shear deformation zone (PSDZ)*

Firstly, the numerical model was used to predict the maximum temperature generated on the rake surface of the tool (Figure 2.8(a)) and also the rate of heat generation at the primary shear deformation zone (Figure 2.8(b)). The FEA results agree with the experimental data published in previous studies, showing consistent temperature value (Brandt, et al. 1990). The results suggest that the maximum temperature on the tool rake face reaches a considerably high steady-state value with only a modest increase at higher cutting speeds. Meanwhile, when increasing the cutting speed, greater heat generation rate occurs, which cause more thermal softening of the workpiece material in the primary shear deformation zone. In order to confirm the validity of the results, cutting temperature was also measured with a thermal imaging camera in Figure 2.9. The temperature was found to be around 1250 - 1350 °C (more than 90% of the IN718 melting point), which is in a very

good agreement with the results obtained in the model. Emissivity coefficient of the pre-machined workpiece was set to be 0.27 for the expected temperature range. The effects of through-spindle and external cooling air were provisionally excluded in both FEA and thermal camera measurements.

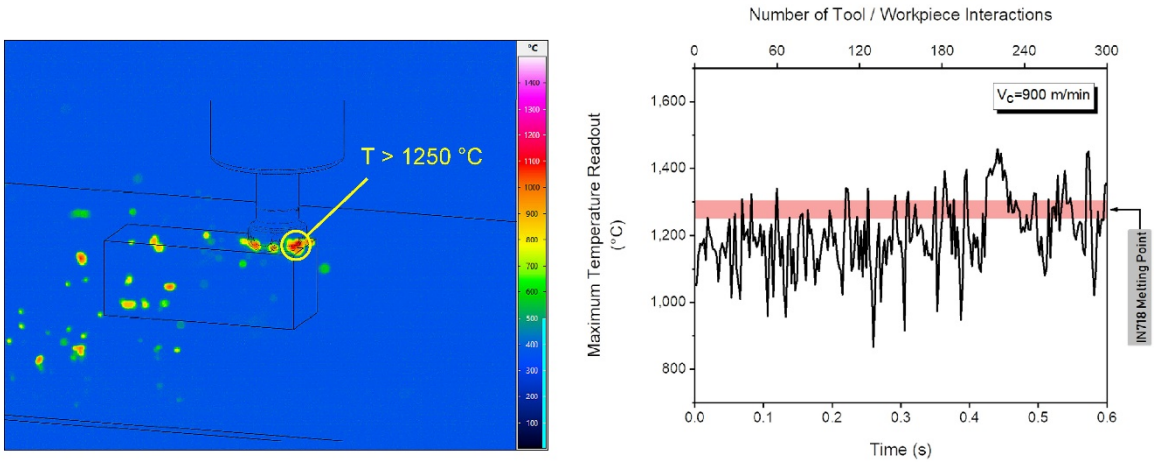

Figure 2.9- Infrared temperature measurement at 900 m/min

Figure 2.10(a) illustrates temperature gradient maps on the tool surface in various cutting speeds. Not only does the dry cutting process generate excessive heat at the tool-chip interface, but also the temperature distribution is highly concentrated in a narrow strip close to the secondary shear deformation zone. This is due to the extremely low thermal conductivity of SiAlON ceramic and also short cutting times for each insert at the selected RPM rates. It is shown that the depth of the effective heat penetration (above 1000 °C) is considerably reduced by increasing the cutting speed (Figure 2.10(b)).

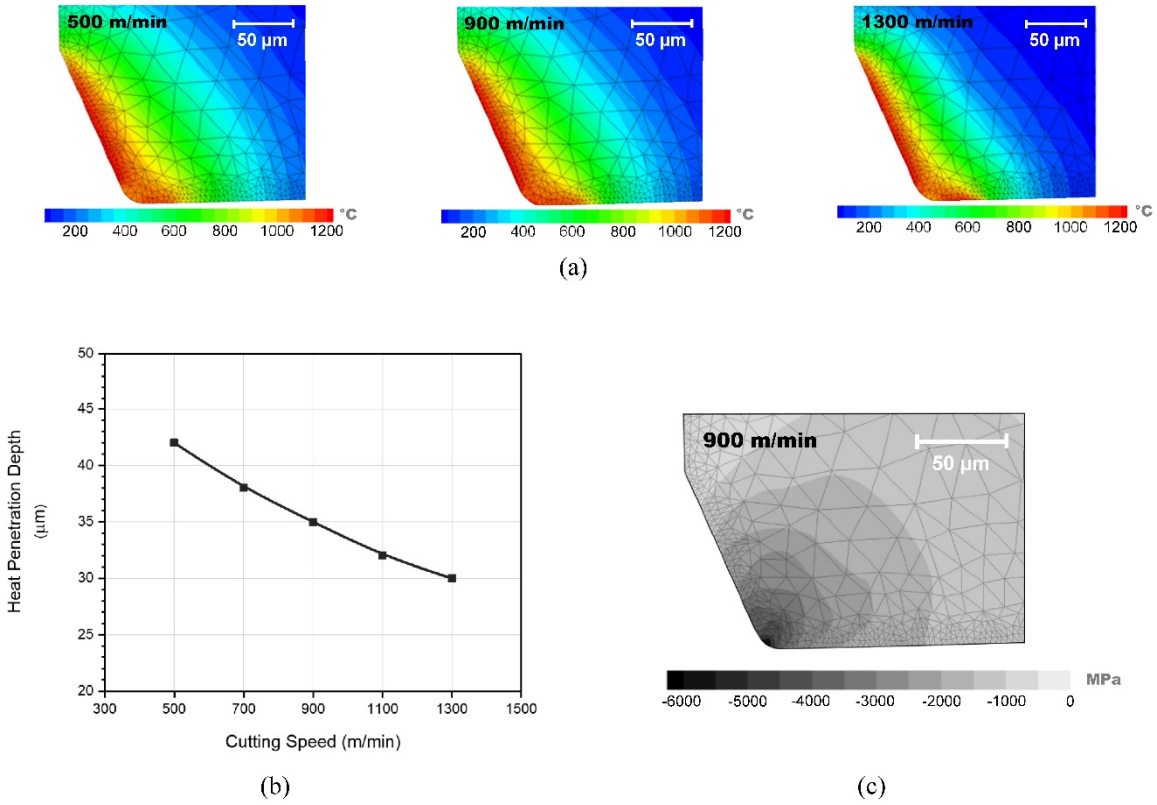

Figure 2.10- ***(a)*** *FEA: temperature profiles for different cutting speeds;*
(b) *Depth of thermally-affected zone on the tool rake face with variation in cutting speed;*
(c) *FEA: resultant stress profile on the tool at* V_C *= 900 m/min*

It should be noted that by increasing the cutting speed, the tool-workpiece engagement time reduces, which could affect the amount of heat transferred into the tool body. At V_C=1300 m/min each tool-workpiece engagement lasts for only 2.1 ms, while this value is three times higher at 5.8 ms, when cutting at V_C=500 m/min. Considering the results in Figure 2.8(b) and Figure 2.10(b) , it is concluded that by increasing the cutting speed, not only more heat is generated at the cutting zone, but also a bigger portion of generated heat is transferred to the chip, which would lead to longer tool life and also better workpiece surface integrity.

Meanwhile, in the FEA model, cutting speed does not significantly affect the intensity of the resultant stress on the tool. Nevertheless, maximum equivalent stress values are very high, e.g., around 5.8 GPa for V_C=900 m/min (Figure 2.10(c)). The geometry of the cutting inserts with negative axial and radial rake angles could be a contributing factor to such a high value.

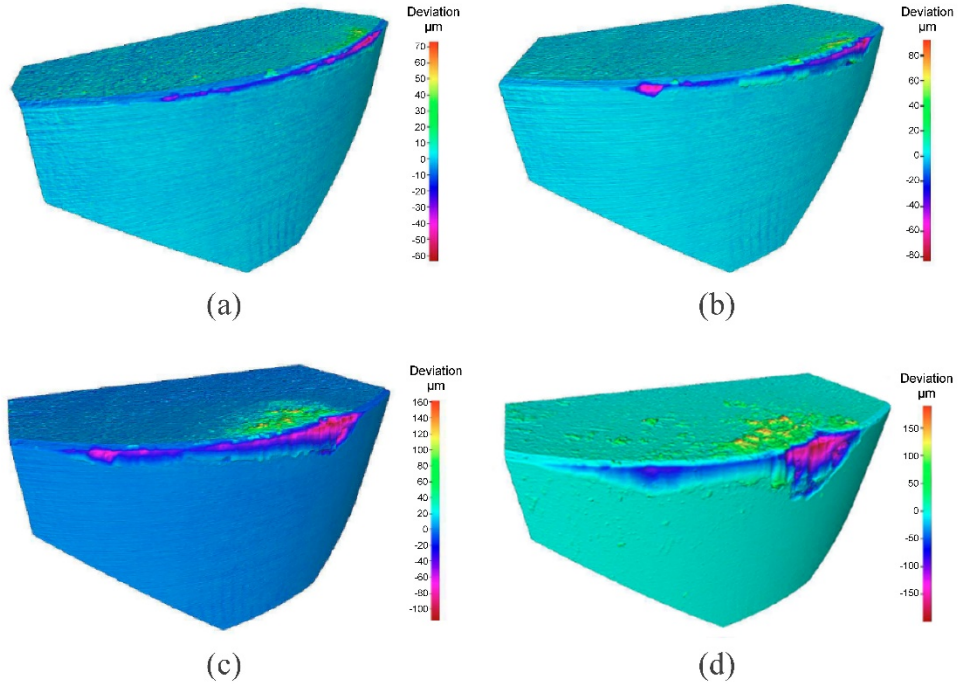

Figure 2.11- Progressive volumetric wear study for V_C = 900 m/min at different cutting lengths (volume removed from the workpiece): ***(a)*** *630 mm (21.75 cm³);* ***(b)*** *1890 mm (65.25 cm³);* ***(c)*** *3150 mm (108.75 cm³);* ***(d)*** *4410 mm (152.25 cm³)*

Figure 2.11 shows progressive volumetric wear study of the cutting edge at V_C=900 m/min during various stages of tool life. It is evident that the ceramic cutting edges deteriorate mostly due to micro-chipping combined with the adhesion of workpiece material to the tool; Severe formation of unstable built-up edges could lead to catastrophic

failure of the cutting edge. Figure 2.12 shows energy-dispersive spectroscopy (EDS) mapping of Ni on the worn surface of the ceramic inserts after cutting for 630 mm. Results show that at higher speeds, the adhesion of the workpiece material to the tool surface is largely promoted by the prevailing effect of thermal softening and temperature increase in the shear zone. Since BUE formation is an unstable process, the intermittent breaking of the excess material escalates the tool degradation (Fox-Rabinovich, et al. 2016). This phenomenon is relatively noticeable within the speed range of 1100 - 1300 m/min, which tends to promote chipping and accelerates the tool failure. Correspondingly, previous research confirms that machining at high cutting speeds increases the diffusion and oxidation wear rates due to the resultant high temperatures (Zhang, et al. 2009).

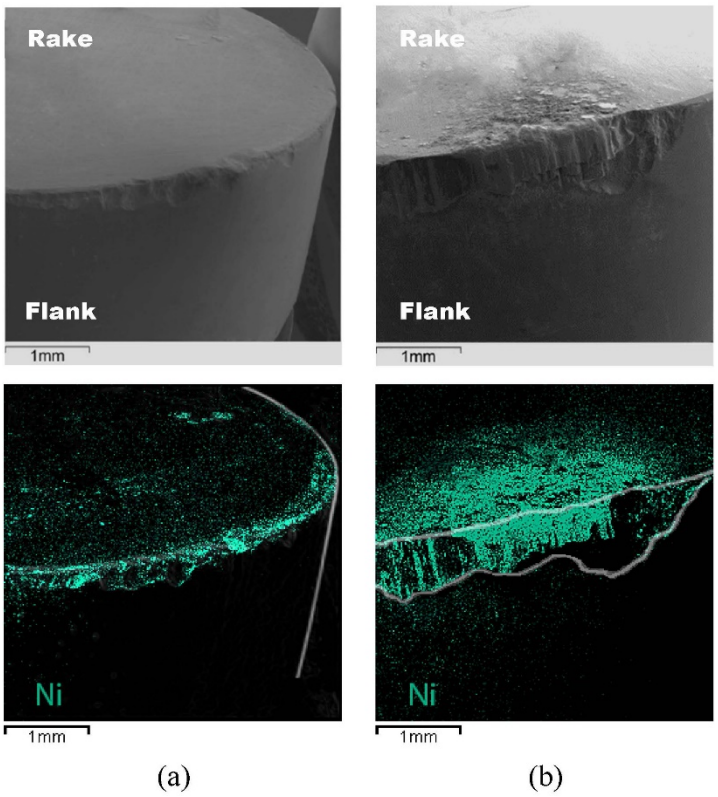

Figure 2.12- SEM/EDS image of worn tools at different cutting speeds: ***(a)*** *500 m/min;* ***(b)*** *1300 m/min*

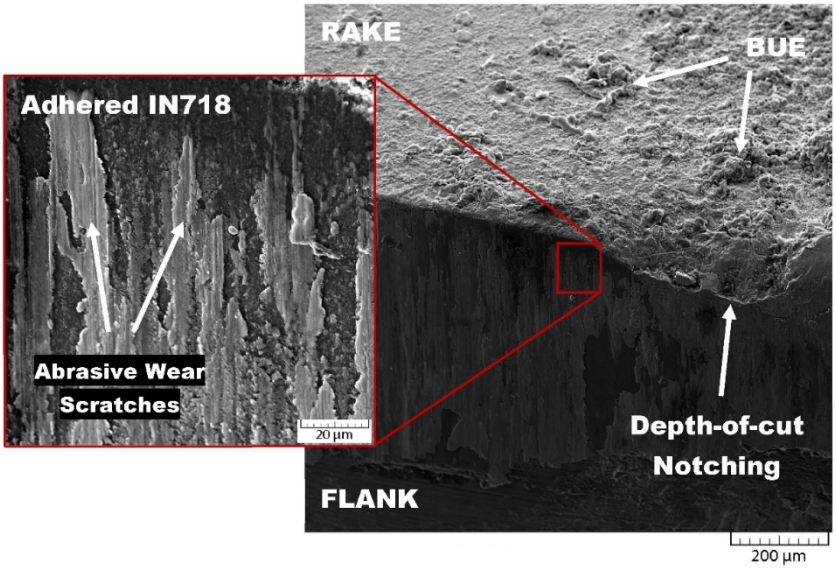

Figure 2.13- SEM image of the worn ceramic tool after cutting 152.25 cm^3 IN718 (4410 mm length of cut) at V_C = 900 m/min

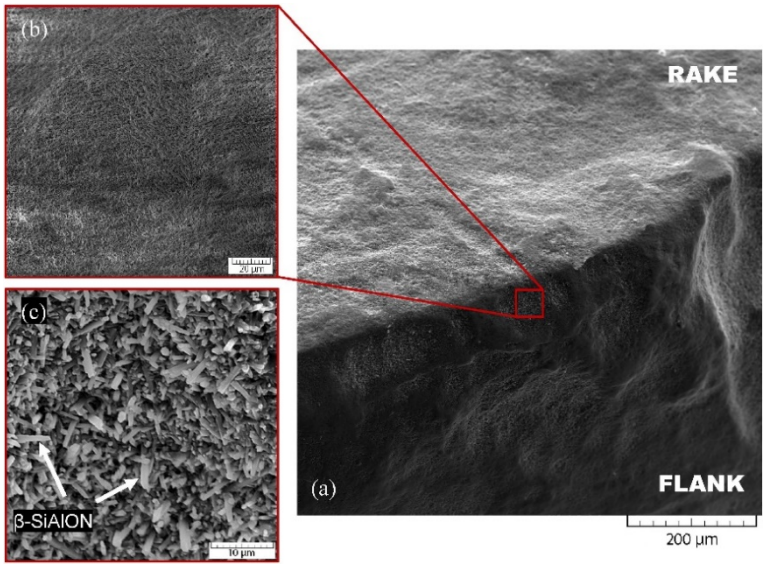

Figure 2.14- ***(a)*** *SEM image of the chipped tool after removing the BUE via thermochemical etching;*
(b) *fractured surface shows a shell-like pattern common in ceramics;*
(c) *Acicular β-SiAlON grains produce self-reinforcement microstructures*

SEM images of the worn ceramic tool at V_C=900 m/min, are presented in Figure 2.13. Abrasion wear, BUE formation, and depth-of-cut notch are present on the worn cutting

edge used for machining 152 cm^3 of hardened IN718 (4410 mm length of cut). Figure 2.14 shows high-magnification SEM micrograph of the same worn ceramic surface after removing the adhered workpiece material by thermo-chemical etching. The cutting tool's chipped surface shows a brittle shell-like structure, common in SiAlON ceramics. It is expected that elevated temperatures combined with an interrupted cutting process, lead to attrition wear and thermal fatigue cracks. However, the fractured surface shows no sign of thermal fatigue failure, which suggests the superiority of SiAlON to withstand alternating thermo-mechanical loads at extreme levels (Çelik, et al. 2017; Hao, et al. 2017).

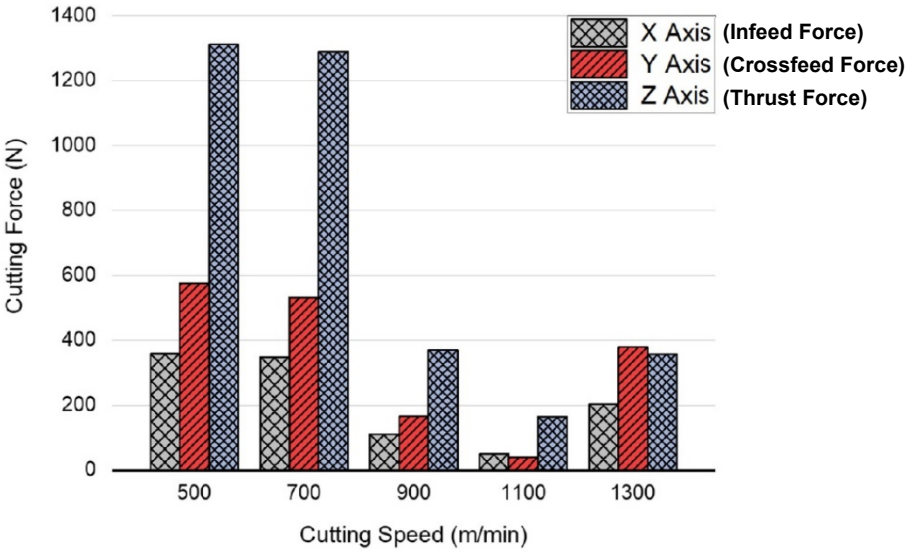

Figure 2.15- The maximum measured forces at different cutting speeds

Cutting forces measured with a high-frequency dynamometer, are presented in Figure 2.15. Increasing the cutting speed, it is expected that more thermal softening of IN718 reduces the cutting forces, a vital factor in efficient machining of hardened high-temperature alloys with ceramic tools. It is also worth noting that the thermal conductivity of IN718 increases significantly at elevated temperatures, reaching above 30 W/m.k at

1300 °C, while for SiAlON it remains effectively the same or even slightly lower than its value at 20 °C, around 9 W/m.k. Higher thermal conductivity besides extremely short cutting time leads to higher heat flux going through the workpiece material, which consequently makes the plastic deformation of IN718 easier.

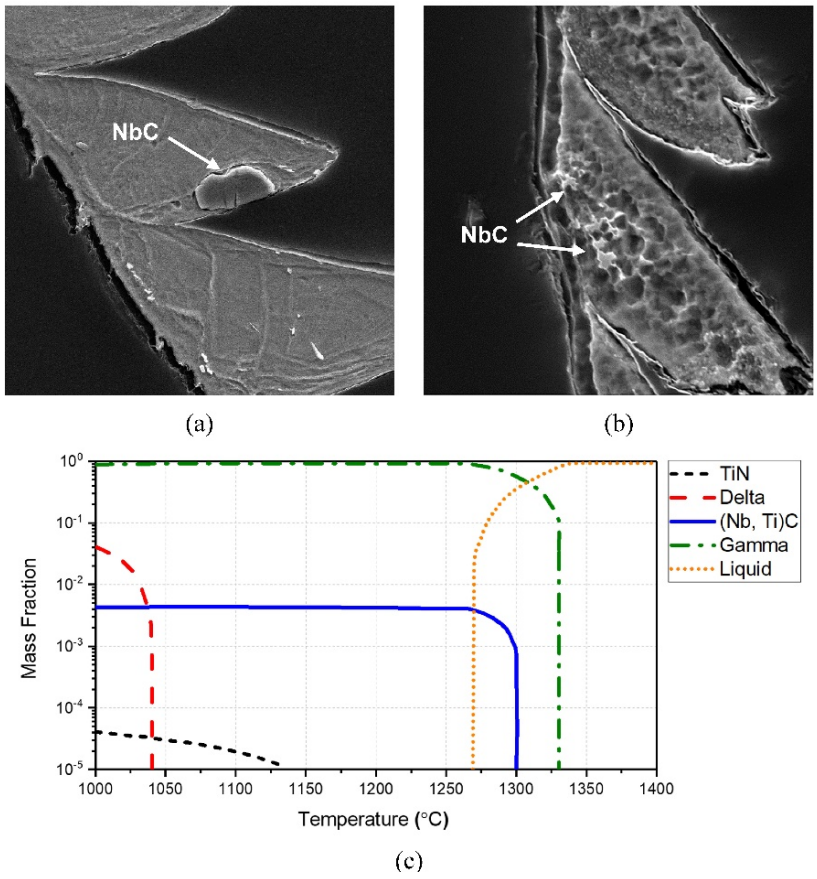

Figure 2.16- Cross section of chips at ***(a)*** *500 m/min;* ***(b)*** *1300 m/min;* ***(c)*** *Mass fraction of IN718 phases above 1000 °C*

However, the substantial drop in the cutting forces at V_C=900 m/min could not be solely related to thermal softening, as it only causes gradual changes. Further analysis of the chips' cross sections at different speeds shows that at higher cutting speeds the temperature in the IN718 reaches a critical microstructural value in which the Nb-rich carbides would be

entirely dissolved, and liquation of grain boundaries would occur (Araujo, et al. 2017). Evidence of such a phenomenon could be clearly observed in Figure 2.16. At the speed of 1300 m/min, the disintegrated NbC particles, produced by Nb segregation and boundary liquation at high enough speeds/temperatures, are solidified in Nb-rich Laves phase, while in 500 m/min the NbC particle still maintains its preferred cubic structure. Mass fraction of IN718 phases at temperatures above 1000 °C is illustrated in Fig. 16(c), showing rapid decline in the mass fraction of hard MC carbides starting from 1270 °C (Araujo, et al. 2017). The graph is drawn using TTN18 thermodynamic database in Thermo-Calc software package. It is known that under such microstructural alteration and also catastrophic oxidation at temperatures close to 1300 °C, the IN718 will collapse structurally (Araujo, et al. 2017). Thus, cutting forces at cutting speeds over 900 m/min would plummet drastically, as measured by dynamometer during the experiment.

Variation in feed rate per tooth was also investigated under the selected cutting speed of 900 m/min. Optical microscope images of the worn flank faces at the initial stages of the wear, combined with 3D wear scans and tool life curves at V_C=900 m/min (with various chip loads) are presented in Figure 2.17. The tool with 40 microns chip load exhibits the least amount of wear compared to other feed rates. FEA results in Figure 2.18 show that an increase in feed rate leads to a wider heat distribution but a lower maximum temperature near the secondary shear deformation zone. The maximum temperature at the cutting edge consistently reduces as feed rate is increased. Based on FEA results, at 0.06 mm/tooth the temperature at the cutting edge drops to 1187 °C, slightly less than the IN718 melting point. In contrast, stress values are very high and grow non-linearly upon increasing the feed from

0.02 mm/tooth to 0.06 mm/tooth (Figure 2.19). Thermal softening, disintegration of MC carbide particles, and local melting of IN718 largely govern the amount of mechanical stress induced into the tool body. Evidence of IN718 local melting at V_C = 1300 m/min is displayed in Figure 2.20. Given the above, the minimum intensity of chipping occurs at the feed rate of 0.04 mm/tooth.

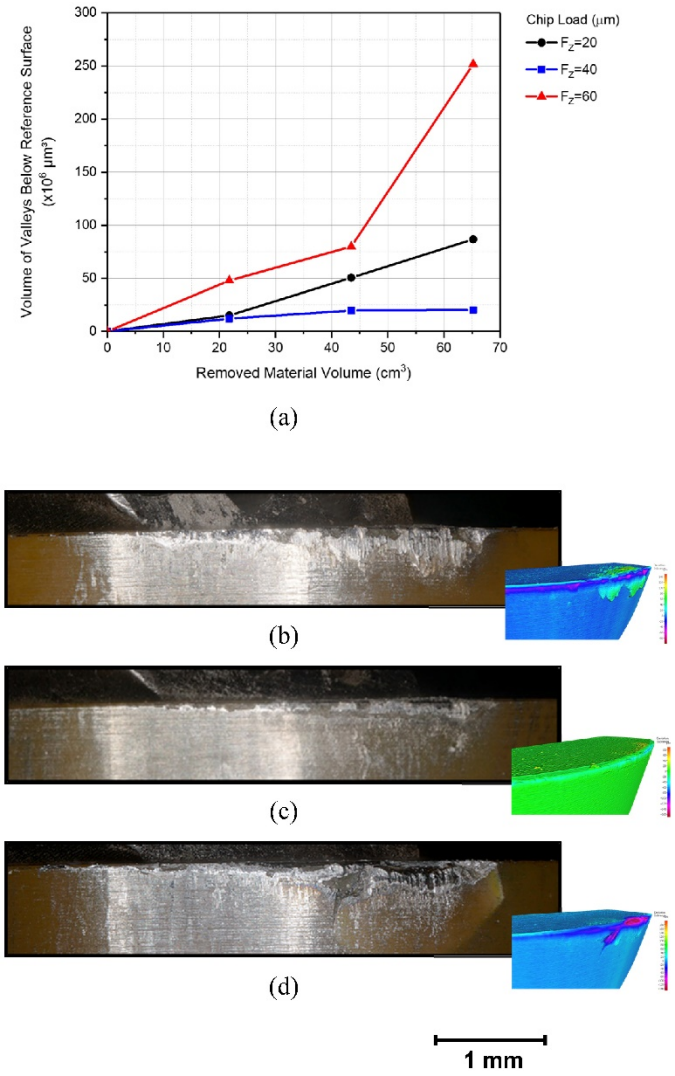

Figure 2.17- ***(a)*** *Tool life curves for different feed rates; Optical microscope images of the worn tools and volumetric wear scans after 630 mm of cut with variation in feed rate (V_C = 900 m/min):* ***(b)*** *0.02 mm/tooth;* ***(c)*** *0.04 mm/tooth;* ***(d)*** *0.06 mm/tooth*

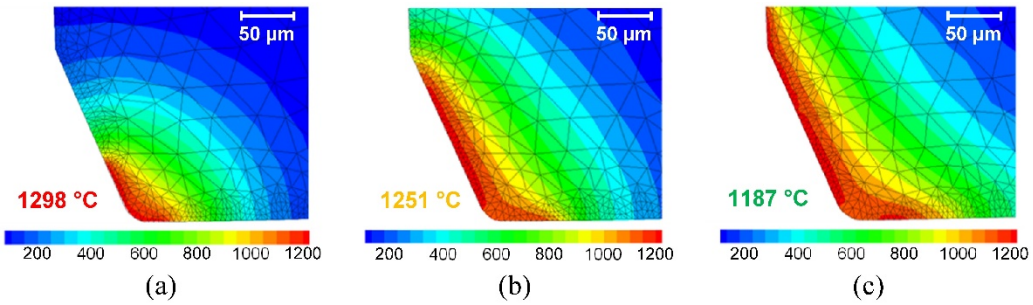

Figure 2.18- FEA: temperature profiles at different feed rates (V_C = 900 m/min): ***(a)*** *0.02 mm/tooth;* ***(b)*** *0.04 mm/tooth;* ***(c)*** *0.06 mm/tooth*

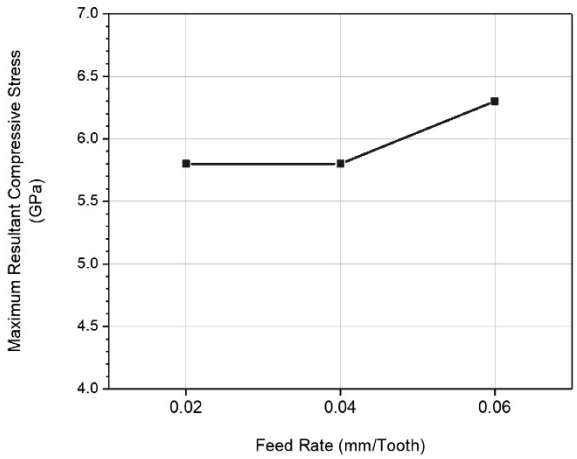

Figure 2.19- FEA: maximum equivalent mechanical stresses on the SiAlON

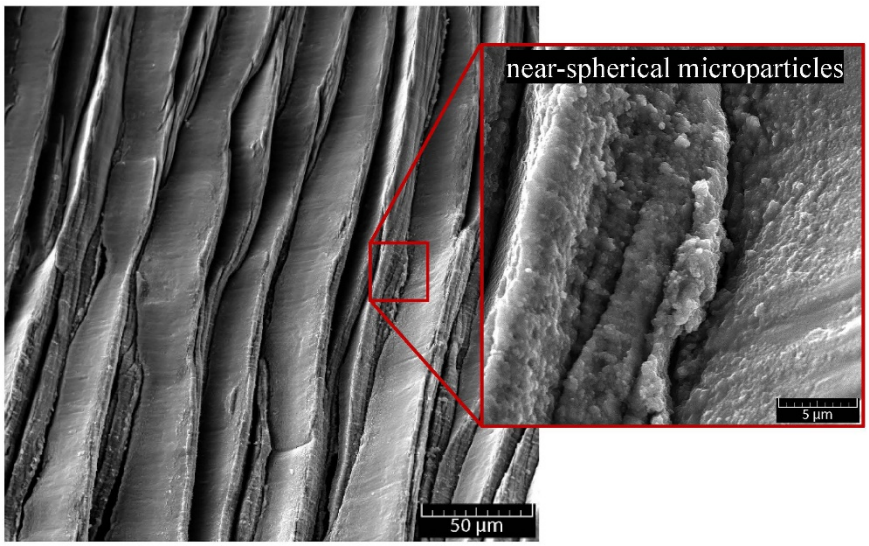

Figure 2.20- Evidence of local melting on IN718 chips machined at VC = 1300 m/min

A comparison between the machining productivity of SiAlON ceramic tools and that of cemented carbides is shown in Figure 2.21. By using SiAlON ceramic inserts at high cutting speeds, it is possible to achieve excellent productivity (MRR) enhancement of up to 4 to 5 times higher than PVD-coated cemented carbide tools commercially available in the manufacturing industry.

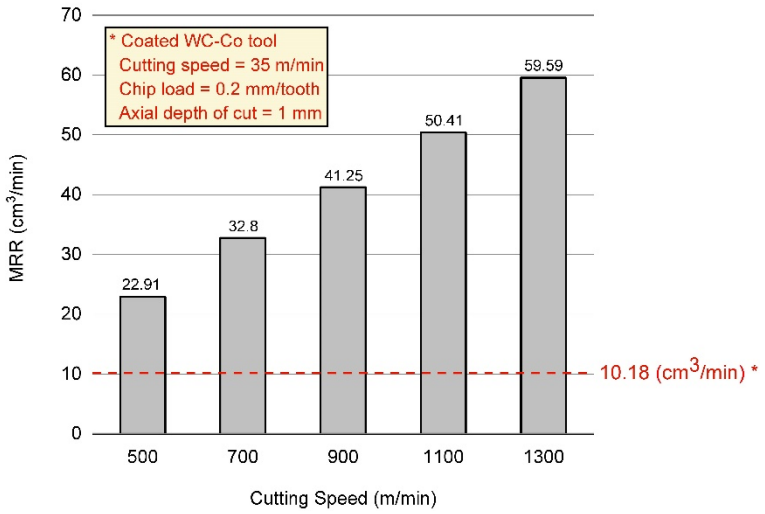

Figure 2.21- Process productivity comparison between SiAlON and WC-Co tools

2.4 Conclusion

The main purpose of this research was investigating the effect of different observed phenomena on the cutting performance of SiAlON ceramic inserts (grade KYS30 Kennametal). Experiments were carried out under extreme tribological conditions of dry high-speed rough face milling of hardened IN718 (45±2 HRC) aerospace superalloy. Tool life studies, optical 3D imaging, SEM/EDX investigation of wear patterns, and force measurements were performed. Then the ensuing results were related to the temperature and stress profiles obtained by finite element modeling.

FEA shows that the resultant mechanical stress and temperature values are incredibly high on the cutting edge of the SiAlON inserts. Such conditions mainly arise from the combination of high hot hardness and mechanical strength combined with the low heat dissipation properties of IN718. It was shown that several major phenomena control the tool life under the outlined cutting conditions, namely: (1) Very high cutting temperatures close to the melting point of Inconel 718. The heat is strongly localized around the cutting edge adjacent to the secondary shear deformation zone. (2) High levels of compressive mechanical stress (5.8 GPa) at the tool-chip interface. (3) Interrupted nature of the face milling operation along with thermal fatigue loading. (4) Intensive BUE formation due to high weldability of the soften (molten) workpiece material to the tool surface. And (5) Microstructural transformation of hard particles in the cutting zone. Combination of these factors causes micro-chipping wear to be the primary failure mechanism, which is predominant in the life of SiAlON ceramic tools. This is common during machining of materials with a high tendency of work hardening, as in the case of Inconel 718 milling. The study shows that there is an optimal range of cutting conditions (cutting speed of 900 m/min and a feedrate[1] of 40 μm) at which the tool performance is the best, and 3D wear intensity is minimal.

In summary, the cutting speed should be enough to generate required heat at the tool-chip interface to soften the workpiece and negate the damaging effect of carbide particles, but not so high as to deteriorate the cutting edge by excessive BUE formation and extreme temperature gradients. The feed rate should also be high enough to avoid work-hardening

[1] Modified from the journal text. At 1mm axial depth of cut, the maximum uncut chip thickness is 15μm.

and ploughing but not to the point of mechanically overloading the cutting edge. It is shown that reaching high temperatures in the cutting zone, around 1300 °C, is vital in this operation to dissolve the hard NbC particles and cause local grain boundary liquation, which in turn would lead to structural break down of IN718 in the primary shear deformation zone. The effect of this phenomenon is clearly exposed in the force measurement readings and chip cross section observations.

Implementing correct cutting parameters in milling with SiAlON tools would substantially increase the operation productivity compared to cemented carbide tools, in the form of 4 to 5 times higher material removal rates.

2.5 References

Araujo, Leonardo Sales, et al. 2017. "The Effect of a Very High Overheating on the Microstructural Degradation of Superalloy 718." *Journal of Materials Research and Technology*, no. x x: 4-10. https://dx.doi.org/10.1016/j.jmrt.2018.03.006.

Bitterlich, Bernd, et al. 2008. "Sialon Based Ceramic Cutting Tools." *Journal of the European Ceramic Society* 28, no. 5: 989-994. https://dx.doi.org/10.1016/j.jeurceramsoc.2007.09.003.

Brandt, G., et al. 1990. "Wear Mechanisms of Ceramic Cutting Tools When Machining Ferrous and Non-Ferrous Alloys." *Journal of the European Ceramic Society* 6, no. 5: 273-290. https://dx.doi.org/10.1016/0955-2219(90)90019-C.

Çelik, Ali, et al. 2017. "Wear Behavior of Solid Sialon Milling Tools During High Speed Milling of Inconel 718." *Wear* 378-379: 58-67. https://dx.doi.org/10.1016/j.wear.2017.02.025.

Devillez, A., et al. 2011. "Dry Machining of Inconel 718, Workpiece Surface Integrity." *Journal of Materials Processing Technology* 211, no. 10: 1590-1598. https://dx.doi.org/10.1016/j.jmatprotec.2011.04.011.

Ezugwu, E. O. 2005. "Key Improvements in the Machining of Difficult-to-Cut Aerospace Superalloys." *International Journal of Machine Tools and Manufacture* 45, no. 12-13: 1353-1367. https://dx.doi.org/10.1016/j.ijmachtools.2005.02.003.

Fox-Rabinovich, German, et al. 2016. "Control of Self-Organized Criticality through Adaptive Behavior of Nano-Structured Thin Film Coatings." *Entropy* 18, no. 8: 290-290. https://dx.doi.org/10.3390/e18080290.

Hao, Zhao Peng, et al. 2017. "New Observations on Wear Mechanism of Self-Reinforced Sialon Ceramic Tool in Milling of Inconel 718." *Archives of Civil and Mechanical Engineering* 17, no. 3: 467-474. https://dx.doi.org/10.1016/j.acme.2016.12.011.

Hoffmann, M. J., et al. 1994. "Tailored Microstructures of Silicon Nitride Ceramics." *Pure and Applied Chemistry* 66, no. 9: 1807-1814. https://dx.doi.org/10.1351/pac199466091807.

Izhevskiy, V. A., et al. 2000. "Progress in Sialon Ceramics." *Journal of the European Ceramic Society* 20, no. 13: 2275-2295. https://dx.doi.org/10.1016/S0955-2219(00)00039-X.

King, RI. 1985. *Handbook of High-Speed Machining Technology*. Boston, MA: Springer US. http://link.springer.com/10.1007/978-1-4684-6421-4.

Lawn, B. R., et al. 1975. "Equilibrium Penny-Like Cracks in Indentation Fracture." *Journal of Materials Science* 10: 2016-2024. https://dx.doi.org/10.1007/BF00557479.

Li, L., et al. 2002. "High Speed Cutting of Inconel 718 with Coated Carbide and Ceramic Inserts." *Journal of Materials Processing Technology* 129, no. 1-3: 127-130. https://dx.doi.org/10.1016/S0924-0136(02)00590-3.

Liu, Jia, et al. 2016. "Cutting Performance and Wear Mechanism of Sialon Ceramic Cutting Inserts with Ticn Coating." *Surface and Coatings Technology* 307: 146-150. https://dx.doi.org/10.1016/j.surfcoat.2016.08.069.

M'Saoubi, Rachid, et al. 2015. "High Performance Cutting of Advanced Aerospace Alloys and Composite Materials." *CIRP Annals - Manufacturing Technology* 64, no. 2: 557-580. https://dx.doi.org/10.1016/j.cirp.2015.05.002.

Man, Xialin, et al. 2012. "Validation of Finite Element Cutting Force Prediction for End Milling." *Procedia CIRP* 1, no. 1: 663-668. https://dx.doi.org/10.1016/j.procir.2012.04.119.

Marques, Armando, et al. 2016. "Surface Integrity Analysis of Inconel 718 after Turning with Different Solid Lubricants Dispersed in Neat Oil Delivered by Mql." *Procedia Manufacturing* 5: 609-620. https://dx.doi.org/10.1016/j.promfg.2016.08.050.

Metselaar, R. 1998. "Terminology for Compounds in the Si-Al-O-N System." *Journal of the European Ceramic Society* 18, no. 3: 183-184. https://dx.doi.org/10.1016/S0955-2219(97)00114-3.

Rahman, M., et al. 1997. "The Machinability of Inconel 718." *Journal of Materials Processing Technology* 63, no. 1-3: 199-204. https://dx.doi.org/10.1016/S0924-0136(96)02624-6.

Santos, C., et al. 2005. "Stabilization of A-Sialons Using a Rare-Earth Mixed Oxide (Re2o3) as Sintering Additive." *Materials Research Bulletin* 40, no. 7: 1094-1103. https://dx.doi.org/10.1016/j.materresbull.2005.03.017.

Schirra, J. J., et al. 1994. "Metallurgical Factors Affecting the Machinability of Inconel 718." *Superalloys 1994*: 827-838.

Schulz, Herbert, et al. 1992. "High-Speed Machining." *CIRP Annals - Manufacturing Technology* 41, no. 2: 637-643. https://dx.doi.org/10.1016/S0007-8506(07)63250-8.

Wacinski, Manuel. 2016. "Keramische Schaftfräswerkzeuge Für Die Hochgeschwindigkeitsbearbeitung Von Nickelbasis-Legierungen." *Fraunhofer Verlag*.

Zhang, S., et al. 2009. "Investigation on Diffusion Wear During High-Speed Machining Ti-6al-4v Alloy with Straight Tungsten Carbide Tools." *International Journal of Advanced Manufacturing Technology* 44, no. 1-2: 17-25. https://dx.doi.org/10.1007/s00170-008-1803-z.

Chapter 3. Chip Formation and Tribological Studies

F. Molaiekiya, M. Aramesh, and S. C. Veldhuis. "*Chip formation and tribological behavior in high-speed milling of IN718 with ceramic tools*" *Wear* 446 (2020): 203191.

Authors' Contributions

F. Molaiekiya	Conceptualized and performed the experiments Analyzed and interpret the results Wrote and prepared the manuscript
M. Aramesh	Assisted with writing, reviewing, and editing
S. C. Veldhuis	Supervised and administered the project

Abstract

Advanced ceramics exhibit excellent mechanical properties at elevated temperatures suggesting them as plausible cutting tool materials for machining of heat-resistant superalloys. However, despite numerous efforts to date, relative brittleness of ceramic tools can result in chipping or catastrophic failure, especially during an intermittent process where excessive thermo-mechanical alteration occurs, like high-speed face milling. Previous studies by the authors revealed that in high-speed milling of inconel with SiAlON tools, after surpassing a certain cutting speed where extreme levels of strain rates and temperatures exist, the IN718 machinability transforms drastically, showing a significant reduction in cutting force, chipping and tool wear. Following this observation, in the current paper, an attempt has been made to further investigate the phenomena acting at the shear deformation zones through analysis of chip formation mechanisms and tool-workpiece tribosystem. Numerous characterization techniques have been used in this research, such as cutting force measurements, chip cross-section studies, SEM/EDS, TEM, and nanoindentation. Results suggest that a reduction in material flow strength occurs at the extreme conditions of the cut, showing similarities to fluid flow in TEM images of the tool face. Increasing the cutting speed generally facilitates chip formation; However, a rise in cutting force by further increasing the speed, and excessive generation of unstable built-up layers practically limits the cutting speed. Additional XPS studies show that variation in cutting speed also changes the frictional response of the tool-workpiece tribosystem by forming lubricious and thermal-barrier tribofilms.

Keywords

High-speed machining; Chip formation; Tribology; SiAlON ceramic; Inconel 718; Material behavior at extreme conditions

3.1 Introduction

High-speed machining (HSM) has been a topic of interest among academic and industrial researchers during the past few decades. Considerable productivity improvement, cutting force reduction, mitigation of undesired thermal effects on the finished product, better surface integrity, and elimination of the cost and pollution of coolant and lubricants are some of the advantages of high-speed machining (Dudzinski, et al. 2004). However, successful implementation of a high-speed cutting process requires a comprehensive understanding of materials behavior at extreme conditions and calls for heavy investment in advanced and expensive cutting tools and machining centers (Schulz and Moriwaki 1992). Excessive tool wear has been reported as the main drawback in the machining of hard metals at high speeds, with chipping frequently identified as the main wear mechanism (Tonshoff, et al. 2000; Narutaki, et al. 1993). In effect, HSM strives to find a solution, which establishes a reasonable balance between cutting time and tool wear.

Advancements in cutting tool technologies have benefited the application of HSM to a great degree, notably by the introduction of diamond, CBN, and ceramic tools (Klocke and Eisenblatter 1997). In HSM, shearing hard-to-cut alloys at high strain rates without the presence of lubricants and coolants increases the thermo-mechanical demands on the cutting tools. In this regard, modern cutting tool materials such as advanced ceramics demonstrated promising mechanical and chemical stability at elevated temperatures compared to conventional carbide tools; And thus, provide a great opportunity to push the process parameters towards unprecedented cutting speeds (Klocke and Eisenblatter 1997; Sreejith and Ngoi 2000). High-temperature strength is particularly of prime importance

when cutting hard materials with low heat dissipation properties such as titanium or nickel alloys used in the aerospace industry (Kitagawa, et al. 1997). Nevertheless, relative brittleness of ceramics makes them susceptible to chipping and gross fracture when used for machining of difficult-to-cut materials.

Nickel-based superalloys and in particular, Inconel 718 are well known for being one of the most difficult-to-cut alloys. Excellent mechanical properties at high temperatures, low heat conductivity, and high work hardening rate are some of the main reasons behind Inconel's poor machinability (Arunachalam and Mannan 2000). In consideration of these characteristics, relatively tough and wear-resistant coated tungsten carbide inserts are currently the most common tools used for superalloy machining in the manufacturing industry. Nevertheless, cutting speed in IN718 milling is currently limited to less than 50 m/min using state-of-the-art coated carbide tools. Moreover, the process demands the application of high-flow coolant and lubricants at the cutting zone (Dudzinski, et al. 2004). Even at this relatively low speed, tool life is fairly limited, and finished products are prone to surface and subsurface damages due to high thermo-mechanical loads during the process (Roy, et al. 2018; Sharman, et al. 2008).

On the other hand, previous research by the authors showed that by switching to a carefully selected ceramic tool and by proper selection of cutting conditions, a significant improvement in Inconel's machinability is achievable, following a considerable reduction in cutting force and tool wear when face milling IN718 at around 1000 m/min. SiAlON tools used for the study showed excellent high-temperature stability, fracture toughness,

and fatigue impact resistance and achieved a remarkable material removal rate of 40-50 cm^3/min.

However, further understanding of the phenomena governing high-speed machinability of inconel using SiAlON tools requires more thorough investigations on the mechanism of chip formation, frictional interactions, and formation of built-up layers and tribofilms, which are covered in the current paper. Chip cross-section morphology can pose valuable information on the behavior of the material at extreme conditions and also on HSM frictional interactions (Wright and Chow 1982; Davies and Burns 2001). Tribology of the process can be further investigated by microscopic observations on the chip underside and by evaluating the formation of tribofilms and other transformed layers on the tool. Tribofilm is a self-organized thin layer that forms during friction and can act as a thermal barrier or lubricious layer to protect the surfaces during friction (Fox-Rabinovich, et al. 2014). Previous studies have shown that the generation of tribofilms has a noticeable effect on the tool's thermo-mechanical loads (Aramesh, et al. 2018; Aizawa, et al. 2005).

The purpose of the present paper is to study the material behavior at high cutting speeds and indicating the mechanisms responsible for the remarkable improvement in Inconel's machinability when milling with SiAlON cutting tools at extreme conditions. In-depth investigation has been performed on the deformation and tribological characteristics of the tool-chip-workpiece tribosystem through various characterization techniques, such as chip cross-section metallography, 3D tool wear measurements, SEM/EDS, TEM, XPS, nanoindentation, among others to develop an understanding of IN718 dry cutting at very high speeds close to 1000 m/min.

3.2 Materials and Methods

The workpiece material used for this study was a 45 HRC hardened IN718 block. The chemical composition and mechanical properties of the workpiece are shown in Table 3.1. Machining tests were performed on a high-speed Makino MC56-5XA CNC machine center with 30 kW spindle power and 15000 maximum RPM. Compressed air with three bar pressure was directed towards the cutting zone by means of through-spindle air channels, in parallel with external air nuzzles at seven bar pressure to provide an extra cooling and to facilitate the chip evacuation. SiAlON ceramic inserts were chosen from KYS30 grade by Kennametal (RNGN120400T01020 round milling inserts), clamped on an indexable face mill (Kennametal KCRA250RN4306S075L175). The clearance, axial rake, and radial rake angles were 10°, -10°, and -5°, respectively. Based on the results from previous research, cutting forces reaches a considerably different values at 500 and 900 m/min and an unpredicted rise happens at 1300 m/min; So, three cutting speeds of 500, 900, and 1300 m/min, and a fixed 40 µm chip load per tooth have been selected for the machinability studies.

Table 3.1- Chemical composition and mechanical properties of IN718

Chemical Composition							
Element	Ni	Cr	Fe	Nb	Al	Ti	Si
Weight (%)	53.70	18.43	18.30	6.37	1.20	1.03	0.97

Mechanical Properties (Room Temperature)				
Hardness (HRC)	Yield Strength $\sigma_{0.2}$ (MPa)	Tensile Strength σ_b (MPa)	Elongation δ_5 (%)	Toughness a_k (J/cm^2)
45	1230	1490	21	43

The chosen SiAlON grade contains approximately 77% silicon nitride (Si_3N_4) and 13% aluminum oxide (Al_2O_3), doped with an addition of some rare earth elements as sintering aids to improve the densification and stabilization of the ceramic microstructure during the insert production (Izhevskiy, et al. 2000). Formation of distinct phases of hard globular α-SiAlON and tough acicular β-SiAlON during the ceramic sintering process, provide a desirable combination of high hardness and fracture resistance compared to other available advanced ceramics.

Tool life studies were conducted using microscopic observations and 3D volumetric imaging. The volume of chipping was measured using a white light high-precision 3D measurement system (Alicona Infinite Focus XL200 G5) with two microns vertical, and five microns lateral scanning resolution. Flank wear measurements and other microscopic observations were done using Keyence VHX-5000 and Keyence VH-ZST optical microscopes.

Nanoindentation has been performed to assess the hardness distribution in the chip's cross-section using Anton Paar NHT^3 nanoindentation tester. The indentations have been made using a sharp Berkovich indenter with 10 mN maximum force, 5 s dwell time, and 20 mN/min loading/unloading rate. The results have been analyzed using the Oliver-Pharr method.

Cutting forces were measured by a Kistler 9255B piezoelectric dynamometer at a 10 kHz sampling rate. A Kistler type 5001 amplifier and a National Instruments USB-9162 DAQ system were used to transfer the force readings to a PC station with LabVIEW data acquisition software.

A Tescan Vega II LSU scanning electron microscope (SEM), equipped with an Oxford X-Max 80 Energy-Dispersive X-ray Spectroscopy (EDX) detector was used for high-resolution imaging of the worn tools, chip cross-section, and chip undersurface. A Philips CM12 transmission electron microscope (TEM) was used for higher magnification imaging of transferred layers (BUE/BUL). The instrument was operated at 120 keV using a LaB_6 filament. The thin-foil samples were sectioned and prepared using a focused gallium ion beam (FIB micro-milling).

The microstructural and phase transformations at the cutting tool-workpiece interface, as well as the chemical composition of the tribofilms formed on the tool cutting edge were studied with X-ray Photoelectron Spectroscopy (XPS) using a Physical Electronics (PHI) Quantera II spectrometer, equipped with a hemispherical energy analyzer and an Al anode source for X-ray generation and a quartz crystal monochromator for focusing the generated X-rays. The monochromatic Al K-α X-ray (1486.6 eV) source was operated at 50 W, 15 kV. The system base pressure was no higher than 1.0×10^{-9} Torr, with an operating pressure that did not exceed 2.0×10^{-8} Torr. Before any spectra were collected from the samples, they were sputter-cleaned for four minutes using a 4 kV Ar^+ beam. A 200 μm beam was used for all data collected on the samples. Pass energy of 280 eV was used to obtain the survey spectra, while the pass energy of 69 eV was selected to collect all high-resolution data. All spectra were obtained at a 45˚ takeoff angle, utilizing a dual-beam charge compensation system to ensure the neutralization of the samples. The instrument was calibrated using the C1s peak set at 284.8 eV. Data analysis was performed using the PHI Multipak software version 9.4.0.7.

3.3 Results and discussions

3.3.1 Shear deformation and chip morphology

Previous research revealed that cutting speed variation results in a considerable change in resultant cutting force and tool chipping during high-speed milling of IN718. shows that reduced force and tool wear occurs after increasing the cutting speed up to around 1000 m/min, while both lower and higher speeds create undesirable outcomes (Figure 3.1). Following this observation, 500, 900, and 1300 m/min have been chosen to represent different ranges of cutting speeds for further studies.

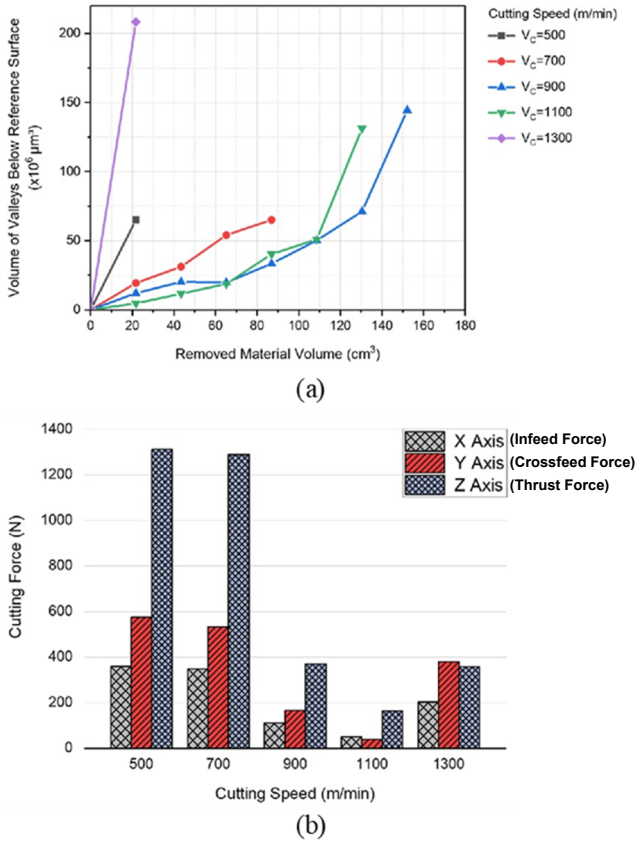

Figure 3.1- ***(a)*** *Tool life curves based on volumetric wear at different cutting speeds;* ***(b)*** *Maximum measured force at different cutting speeds*

The RNGN120400T01020 inserts used in this study have a round edge geometry with a 20° chamfer on the cutting edge. Considering the tool holder angles, the effective rake angle for 40 µm feedrate would be around -30°, approximately. The highly negative rake angle and high cutting speeds, alongside with low thermal conductivity and strain hardening sensitivity of IN718 cause shear instability in the workpiece material and generates segmented chips (Komanduri and Schroeder 1986), as shown in Figure 3.2. The generated chips are mostly discontinuous and needle-shaped; But, at the beginning of the cut, while the cutting edges are perfectly sharp, semi-continuous chips are generated that can be used for the process characterization. Since in milling, especially with round inserts, chip thickness is not constant, no precise quantification can be made over the chip morphology. Nevertheless, to qualitatively examine the cutting speed influence on IN718 deformation, multiple chips were collected from each range of speed and were carefully mounted perpendicularly on their leading edge. The chips were then lightly polished in order to minimize the dimensional error. Figure 3.2 shows the morphology of typical serrated chips at different cutting speeds at the point of maximum chip thickness (leading edge). As the tool wear evolves, the segments tend to get completely detached from each other and form thin needle-shaped chips, which eventually turn into tiny powder-like fragments towards the end of tool life. However, the cross-section of the needle-shaped chips still tends to keep geometrical similarities to the individual fragments in Figure 3.2. The change in the tool tip geometry is assessed by a white light 3D scanner (Alicona Infinite Focus XL200 G5), illustrated in Figure 3.3 for V_C=900 m/min at the point of maximum chip thickness. A considerable increase in the cutting edge radius and the effective rake

angle caused by the tool wear, combined with the chip thinning effect of milling especially at low feed rates, are the reasons behind the alteration in chip morphology during the life span of the cutting inserts. Moreover, as the edge becomes rounder, the material side flow occurs, and chips can get stuck at the trailing edge, which causes chipping.

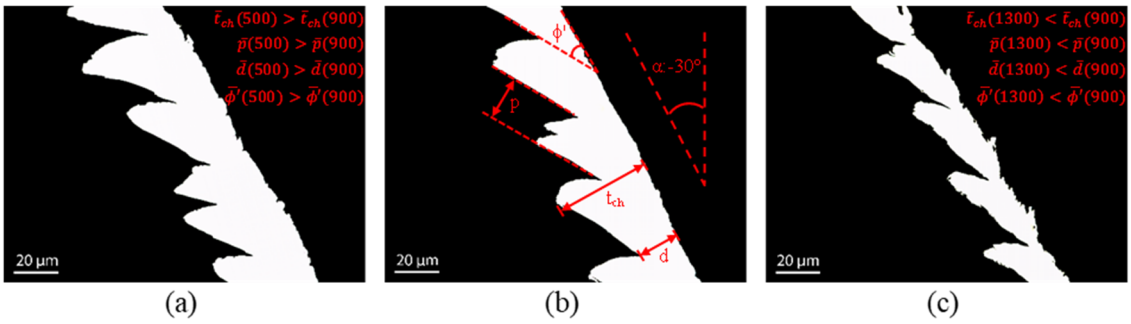

Figure 3.2- Morphology of the chip cross-section at different cutting speeds:
***(a)** 500 m/min; **(b)** 900 m/min; **(c)** 1300 m/min*

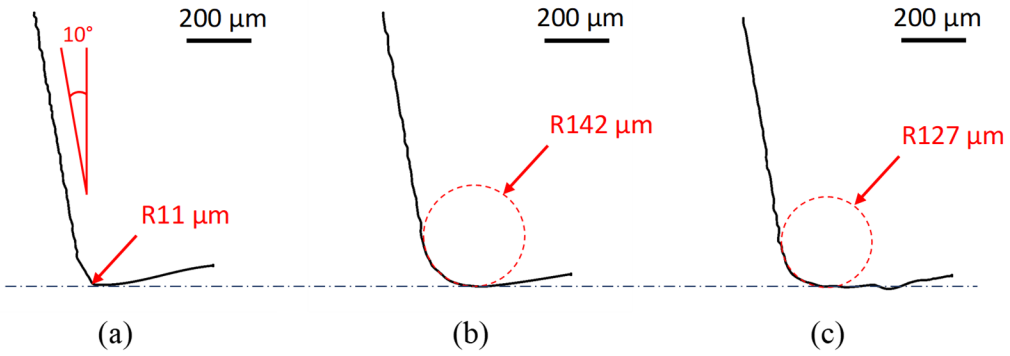

*Figure 3.3- Cutting edge geometry: **(a)** Fresh tool;*
***(b)** After removing 21.75 cm^3 of IN718 (20% of tool life);*
***(c)** After removing 87 cm^3 of IN718 (60% of tool life)*

As depicted in Figure 3.2, when cutting speed increases, the chips tend to get thinner, and the spacing between adjacent fragments (p) decreases. Also, by increasing the speed, the segments form more steadily. The degree of segmentation (Schulz, et al. 2001), would

also intensify by increasing the cutting speed, as well as the tendency to create discrete chip fragments. It should be noted that based on the geometry of the inserts, at 1 mm axial depth of cut, the maximum chip thickness does not exceed 15 μm. Although chips at 900 m/min are thinner than 500 m/min, change in the chip thickness is more pronounced after passing the VC=900 m/min mark, which is in agreement with the drastic reduction of cutting force and tool wear at this range of speed, reported previously.

Shear instability and formation of adiabatic shear bands collinear to the fractured surface of the segments can be seen in Figure 3.4(a). In HSM, higher cutting speeds cause larger strain and strain rates at the primary shear deformation zone, generating more heat inside the deforming segments. Besides, IN718's low thermal conductivity causes extreme heat concentration near the shear bands and increases the ductility via thermal softening mechanisms (Davies and Burns 2001). As the cutting edge advances through the workpiece, high compressive stresses are induced inside the material, which leads to the upsetting of wedge-shaped segments. Then, whenever the effect of thermally-induced deformation mechanisms overcomes the work hardening effect, sliding begins at the location of minimum normal stress, which is near the free surface of the deforming segment (Schulz, et al. 2001; Komanduri 1982), leading to the formation of individual fragments. In the examined chips, the separation of segments which is initiated at the free surface eventually comes to a halt before reaching the tool tip, which is an indication of very high normal stresses acting at the tool tip, responsible for the cessation of the ductile fracture. Meanwhile, there is not much deformation happening at the innermost of individual segments. Nevertheless, signs of plastically-deformed material can be detected in the form

of narrow shear bands and mechanical twinning at all cutting speeds (Figure 3.4(b)). Mechanical twinning seems to be more pronounced at low cutting speed, which suggests that the workpiece material exhibits more resistance to dislocation glide. In other words, deformation twinning is preferred over plastic slip at the lower cutting speeds/temperatures.

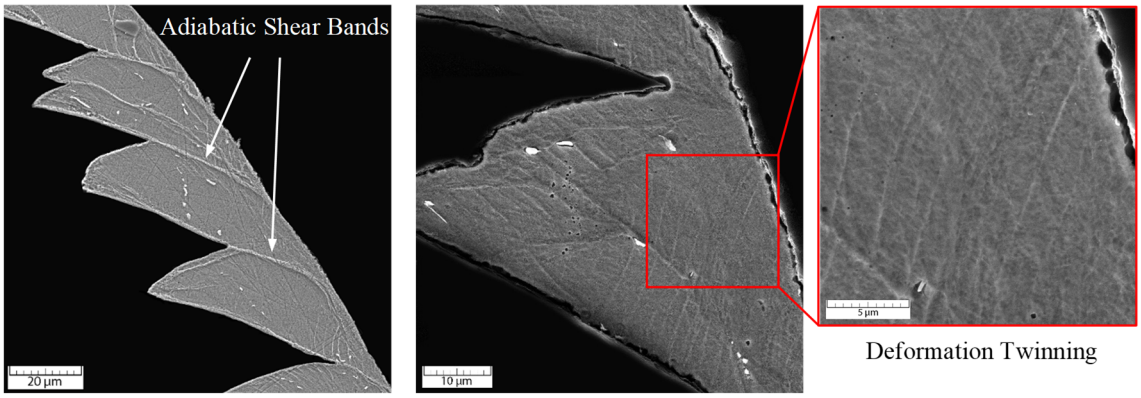

Figure 3.4- SE SEM images of the chip cross-section at:
(a) *V_C = 900 m/min;* ***(b)*** *V_C = 500 m/min*

The resultant force measurements at the cutting speed of 500 and 900 m/min in Figure 3.5 show a considerable decrease in the maximum axial cutting force at 900 m/min, which can explain the tool life increase at this speed as opposed to the lower cutting speed of 500 m/min. Nevertheless, the axial cutting force at 1300 m/min remains almost at the same level as 900 m/min, even with a slight increase. This increase can be partially related to the excessive amount of buildup edge forming on the cutting edge (due to extreme weldability of the softened workpiece to the tool) and also increase in IN718 flow stress following a higher strain rate deformation at 1300 m/min. One main consideration in high-speed machining of IN718 with ceramic tools is finding the right balance between the work

hardening, strain sensitivity, strain rate sensitivity, and thermal softening (Tonshoff, et al. 2000). It is known that the IN718 flow stress increases by increasing the strain rate/cutting speed, in a non-linear manner (Zhou and Baker 1994). However, considering the chip geometry depicted in Figure 3.2, by increasing the cutting speed a larger deformation strain also occurs, which can in turn decreases the flow stress of IN718 in a phenomenon known as strain softening (Hokka, et al. 2014). In this regard, cutting speeds at the range of 1000 m/min appears to provide the best balance between the aforementioned opposing phenomena, resulting in lower cutting forces and less tool wear.

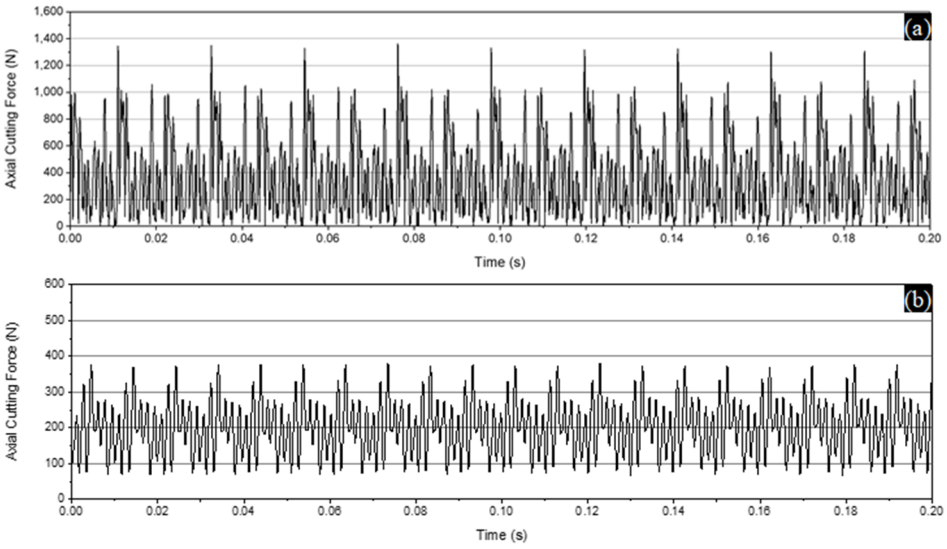

Figure 3.5- Axial cutting force measurement at: ***(a)*** V_C *= 500 m/min;* ***(b)*** V_C *= 900 m/min*

Another distinguished difference in the microstructure of the chip cross-section is the transformation in the morphology of NbC particles at different cutting speeds. At 500 m/min the micro-sized NbC particles remain intact or shattered as shown in Figure 3.6(a), but at higher cutting speeds, especially at 1300 m/min (Figure 3.6(c)), almost all visible NbC particles in the chips' cross-sections were dissolved during the deformation and

reappear in a Nb-rich Laves phase, typically seen in welded microstructures (DuPont Jn 1998; Janaki Ram, et al. 2004). This microstructural transformation can be an indication of IN718 abruptly losing its main strengthening mechanism as a precipitation hardened alloy when exposed to a certain high level of temperature and strain rate.

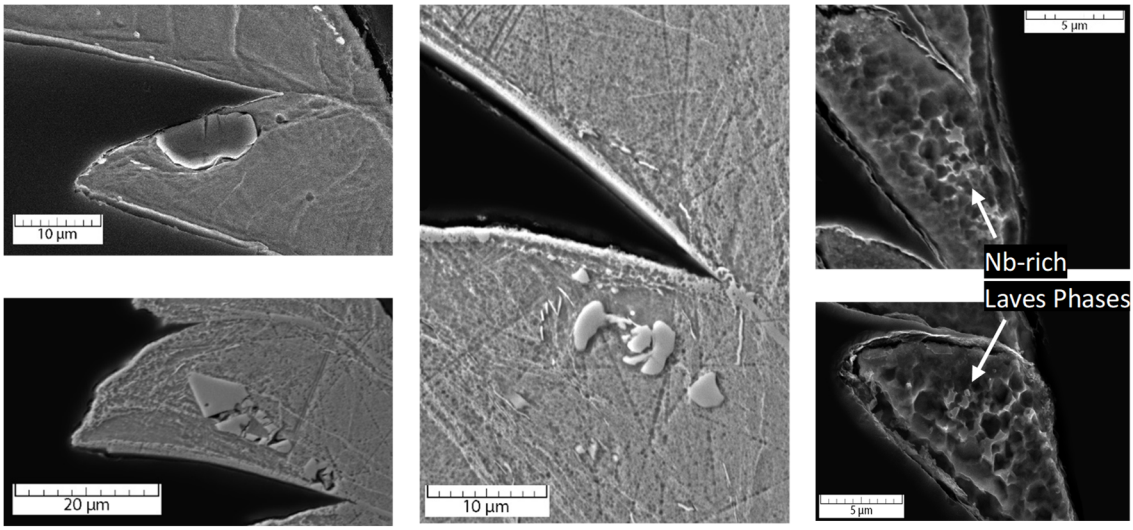

Figure 3.6- SEM images of NbC particles in the chip cross-section at ***(a)*** V_C *= 500 m/min;* ***(b)*** V_C *= 900 m/min;* ***(c)*** V_C *= 1300 m/min;*

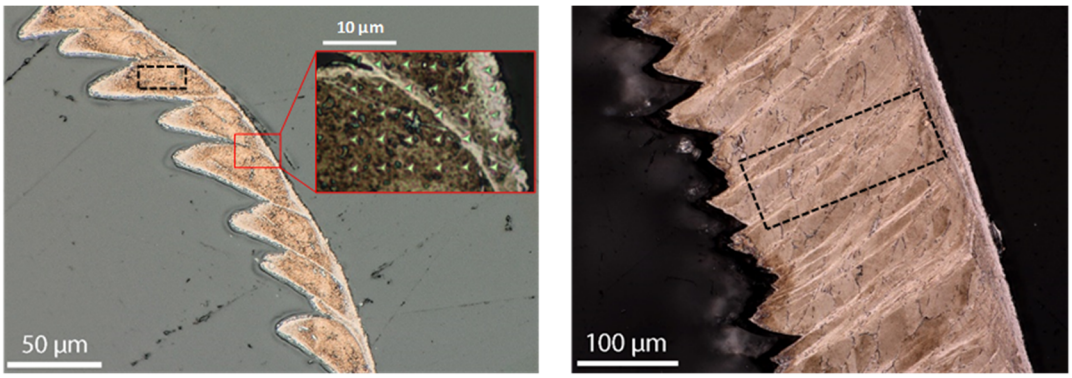

Figure 3.7- Optical images of the chip cross-section and location of nanohardness measurements at ***(a)*** *900 m/min (SiAlON tool);* ***(b)*** *35 m/min (WC-Co tool)*

For further examination of microstructural deformation at cutting zone, Figure 3.7 illustrates optical images of etched chip cross-section produced at 900 m/min and a cross-section from a chip produced at 35 m/min using a coated carbide tool for comparison. On the ceramic chip cross-section, two clear regions of shear concentration can be observed; Around and alongside the fracture in between adjacent segments and in the vicinity of the undersurface of the chip where it is in frictional contact with the tool's rake face. These are the regions where most of the mechanical work and heat is generated during the cutting process and thus experience the maximum microstructural transformation. The shear band remains unetched during the metallography and thus appears white under the microscope. In that region, the grains are extremely fine due to thermally-induced dynamic recrystallization after severe plastic deformation at high strain values (Wusatowska-Sarnek, et al. 2011; Österle and Li 1997).

Although high cutting temperatures close to the melting point of the workpiece can have drastic effects on the microstructure and mechanical properties of IN718, very short cutting times in the order of milliseconds mitigates the severity of thermally-induced microstructure alteration. To better investigate this, instrumented nanoindentation has been performed on the cross-section of the chips to measure the change in the nanohardness of the workpiece material. Numerous indentations have been made within the marked regions depicted in Figure 3.7, using a Berkovich indenter with 10 mN load and 5 s dwell time. The high-speed chips show around 30% higher hardness compared to the undeformed workpiece. i.e., using similar indentation parameters, the hardness of the IN718 bulk is 805±65 Vickers while the hardness of chips generated at 900 m/min with a ceramic cutter

is measured 1081±167 Vickers. The increase in the hardness value is attributed to the IN718 high sensitivity to strain hardening, which leads to the development of several dislocation barriers in the microstructure and diminishes the dislocations mobility (Hokka, et al. 2014). However, observation of shear localization at high-speed machining means that there is not much deformation happening in the chip's bulk, and thus, the amount of work-hardening in the center of chips is small (Komanduri 1982). To compare, the nanohardness of the chips generated at 35 m/min with a coated Tungsten carbide tool shows much higher hardness at 1240±188 Vickers. In the chips formed at 35 m/min, the gap between the shear bands is small, and the chip morphology is almost uniform; Hence, it is most likely that the indenter tip hits a shear band every time. As said, shear bands have extremely fine grains and are dense in dislocation quantity, which promotes higher hardness. A similar result is also observed on the ceramic tool's chips at all speeds, showing the maximum hardness value of 1249±57 Vickers when the indenter hits exactly on a shear band, around 15% more than the points away from the shear band (Figure 3.8).

Numerous indentations show that increasing the cutting speed from 500 to 1300 m/min seems to have no meaningful effect on the hardness distribution of the chip cross-section. Although it is true to say that the cutting temperature would increase by increasing the cutting speed, one should not lose sight of the fact that any increase in the cutting speed would decrease the cutting time in which the workpiece material is exposed to the heat. Nonetheless, from the nanohardness map shown in Figure 3.8, it can be seen that the hardness shows a slight decrease immediately adjacent to the shear band. This small change in hardness value can be related to the high temperatures generated during the process

which can affect the size and distribution of gamma prime, gamma double prime and MC carbides as they get unstable at high temperatures; This can increase the dislocation and grain boundary mobility and consequently reduces the hardness of IN718 (Zhou and Baker 1994). The relative hardness reduction is no more than 20% on the tested chips, and changing the cutting speed seems to have little to no effect on the severity of this observation.

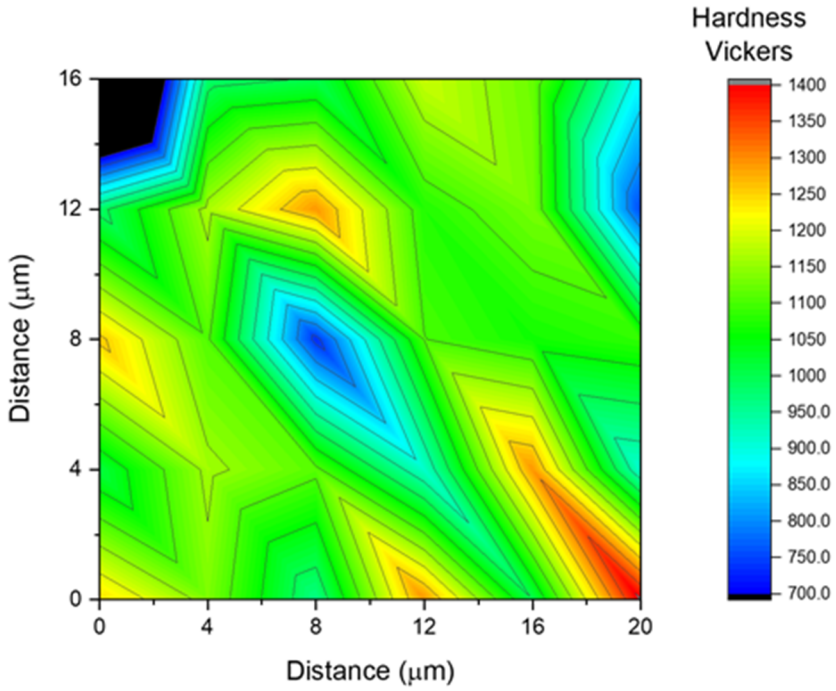

Figure 3.8- Nanohardness map of a chip produced at V_C = 900 m/min within the area shown in Figure 3.7(a)

3.3.2 Tribological studies

To investigate the secondary shear deformation zone, tribological aspects of the cutting process were evaluated using various characterization techniques. The maximum tool-chip contact length (TCCL) was measured by observing the wear trace on the rake face of the

ceramic tool, the result of which is shown in Figure 3.9. The maximum TCCL occurs at the leading edge of tool engagement with the workpiece, where the uncut chip thickness is approximately 15 µm. As the cutting speed increases the TCCL is also increased until it reaches a maximum value at the speeds around 900-1100 m/min and then drops as the cutting speed reaches 1300 m/min.

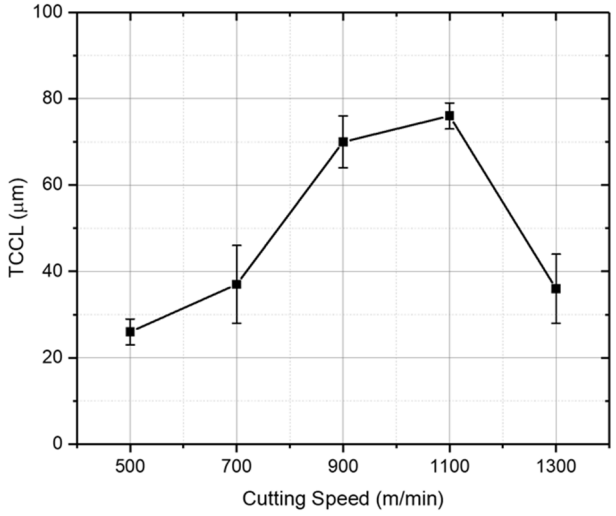

Figure 3.9- Maximum Tool-Chip Contact Length (TCCL)

The rise in the TCCL value by increasing the cutting speed from 500 to 900 m/min can be related to the difference in the temperature field at the tool-chip contact zone, reduction in the coefficient of friction in the contact zone, extensive softening of IN718, and generation of thinner chips at higher cutting speed. However, at 1300 m/min, the build-up edge and build-up layers start to develop intensively, which makes the tool to act as it has restricted contact length, and thus, the TCCL reduces (Friedman and Lenz 1970). The formation of the Nb-rich laves phase is also considered as another reason for the lower TCCL at 1300 m/min because of the embrittling effect of the high inclusion laves phase.

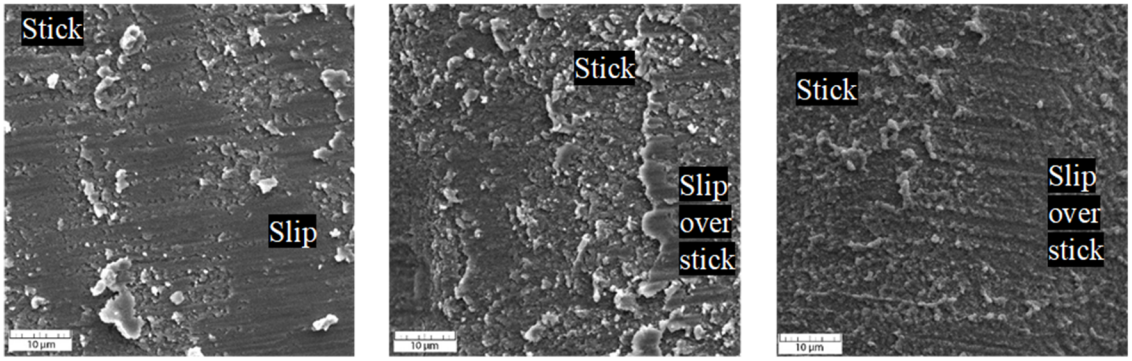

Figure 3.10- Chip undersurface at: ***(a)*** *500 m/min;* ***(b)*** *900 m/min;* ***(c)*** *1300 m/min*

Figure 3.10 shows SEM images of chip undersurfaces generated at various cutting speeds that can be used as an indicator of the frictional behavior of the process. At the speed of 500 m/min, "stick-slip" phenomena similar to avalanche friction behavior is observed, which indicates catastrophic wear mode (Markov and Kelly 2000) and reduces the tool life. At the speed of 900 m/min, the prevailing phenomenon is sticking with some areas of "slip over stick" which can be related to the significant thermal softening that happens at the vicinity of the chip undersurface. More pronounced sticking zones can be seen in Figure 3.10(c) at the cutting speed of 1300 m/min, as the temperature quickly rises very close to the melting point of IN718, which increases the weldability of the workpiece material to the rake face of the tool. Thus, as the cutting speed grows, chips become more prone to local melting and also sticking to the tool face in the form of built-up edges and built-up layers. High-resolution SEM images of the chips in Figure 3.11 show signs of local melting (semi-spherical micro-particles), which confirms the generation of extreme temperatures during high-speed milling of IN718 with SiAlON ceramic inserts. As EDS spectra show, the spherical particles contain elements from IN718 and trace of silicon from the SiAlON

tools, plus a considerable amount of oxygen, which is an indication of chemical reaction at high temperatures.

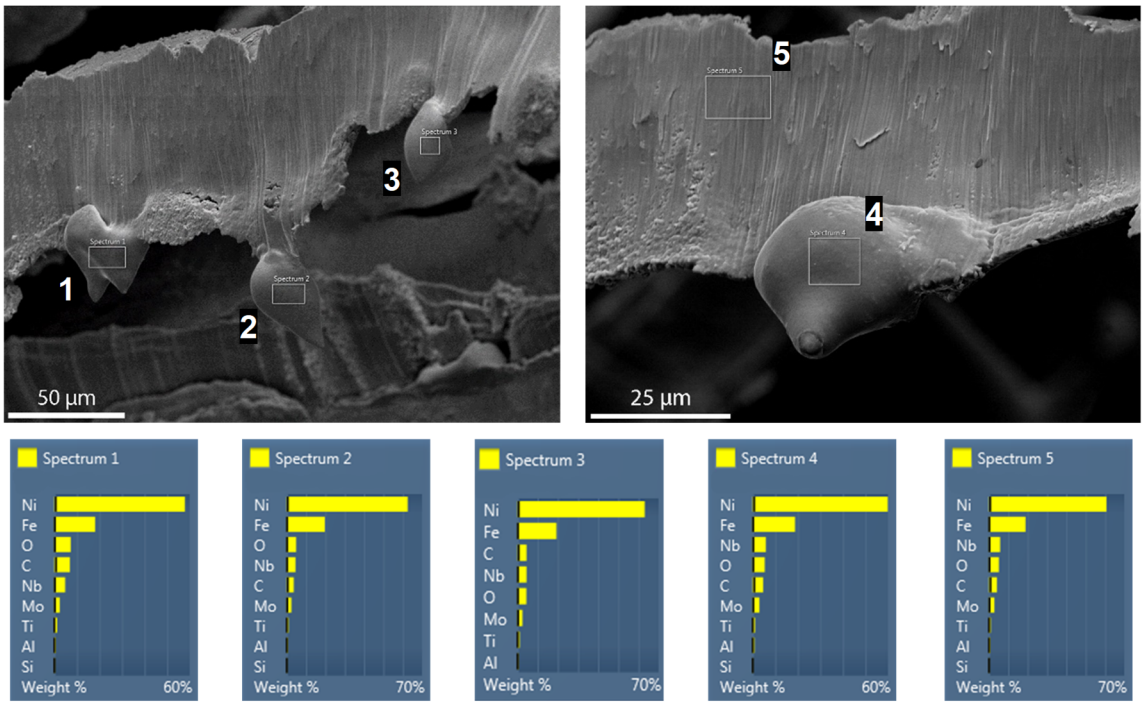

Figure 3.11- EDS spectra and HR-SEM images of chips at V_C = 1300 m/min showing signs of local melting

Detailed high-resolution SEM images of the needle-shaped chips at different speeds are shown in Figure 3.12. Signs of local melting in the form of smooth spherical micro-particles can be detected at all speeds, especially at 1300 m/min (Figure 3.12(b)). Once again, the change from more slipping behavior towards little/no slipping and more sticking and melting at higher speeds is visible. This can also explain the increase in TCCL by cutting speed (Figure 3.9), as local melting facilitates the metal flow of the thinner chips generated at higher cutting speeds.

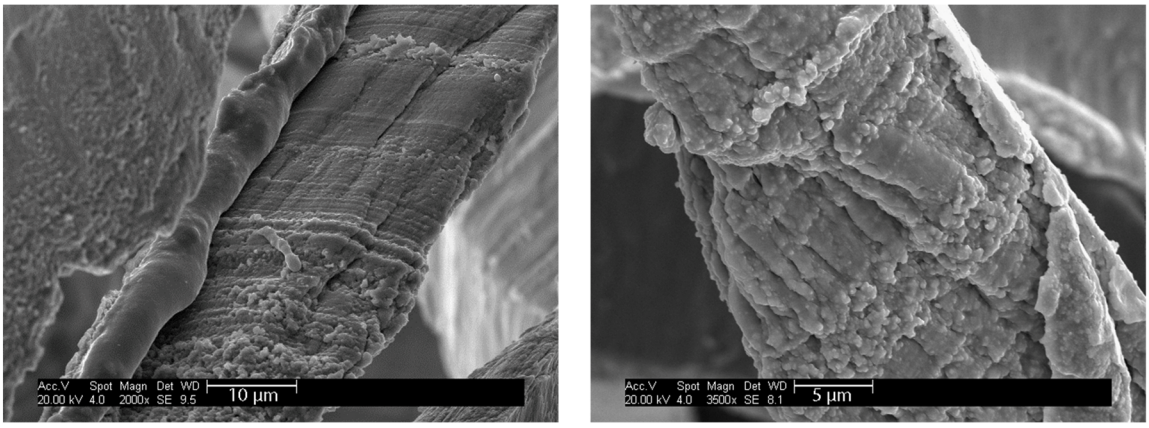

(a) (b)

Figure 3.12- Needle-shaped chip undersurface at: ***(a)*** *900 m/min;* ***(b)*** *1300 m/min*

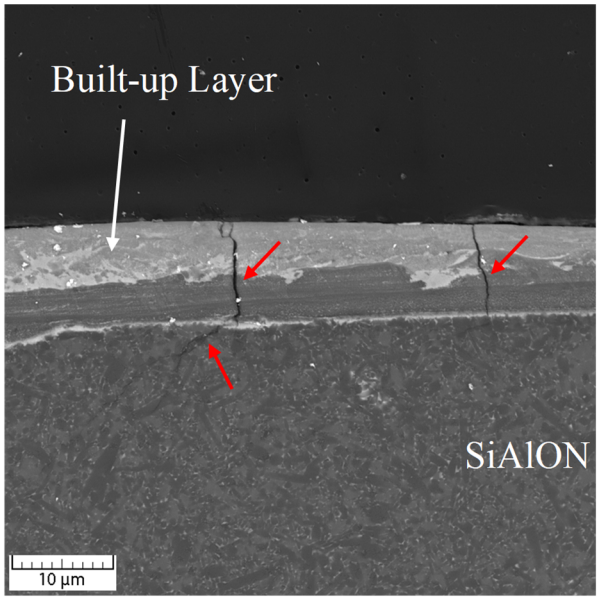

Figure 3.13- Cracks form on the BUL and propagates inside the tool as a result of tensile residual stress and thermal fatigue

Despite the positive influence that higher cutting speeds have in terms of chip morphology and chip flow, one of the reasons that restrict the tool life at 1300 m/min is the excessive formation of unstable built-up edge and built-up layer at 1300 m/min. It is known

that the generation of transferred workpiece material on the rake face of the tool in the form of built-up layers (BUL) can have protective properties. Also, BUL is considered being partially responsible for the cutting force reduction as it changes the tribological behavior of the tool at SSDZ (Hamann, et al. 1994; Desaigues, et al. 2016). But, in a heavily interrupted high-speed milling process, while the insert is cooling during its free rotation in air, the substantial mismatch in the coefficient of thermal expansion of IN718 and the ceramic tool leads to the initiation of small cracks that propagate through the tool-BUL interface and promote the attrition tool wear (Figure 3.13).

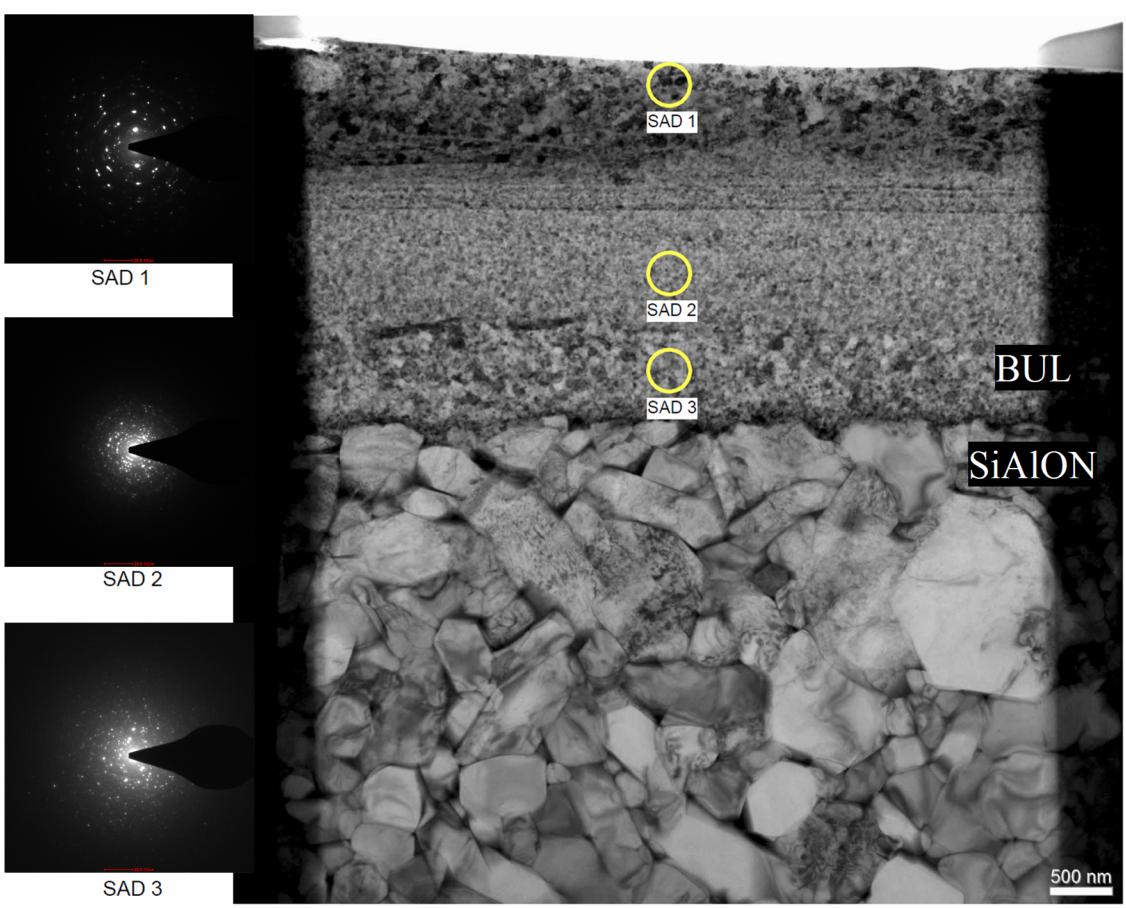

Figure 3.14- TEM image and selected area diffraction patterns of BUL at 1300 m/min

The transferred layer can react chemically with the tool material, especially at the extreme thermo-mechanical conditions present in the flow zone. Elevated temperatures combined with relatively slow chip velocity at the flow zone provoke diffusion and elements segregation within the transferred material thickness. Figure 3.14 shows a high magnification TEM image of the BUL formed at 1300 m/min on a thin section made via FIB. SAED patterns show that the grain size in the middle (zone 2) is smaller compared to the top layer. Also, grains at the middle layer have a wider range of orientation as opposed to the top layer, as there are more bright spots in the diffraction pattern of zone 2. In zone 3, close to the tool face, the grains seem to get larger again. The asymmetric diffraction pattern at zone 3 suggests that the microstructure is a composite polycrystal consist of multiple phases. This micron-sized amorphous layer can suggest that under the extreme conditions of temperature and mechanical stress, the transferred IN718 bears a liquid-type flow behavior as reported by some researchers when experimenting IN718 under similar temperature and strain rates (Ressa 2015). Further elemental analysis on the BUE shows a considerable amount of oxygen mixed with both tool and workpiece elements, which is an indication of the adaptive response of the tribosystem to the external environment (Fox-Rabinovich, et al. 2014). Electron energy loss spectrometry results also suggest that zone 1 is richer in Cr, Fe, and Ni, while zone 2 has considerably more Al, Ti, and O (Figure 3.15).

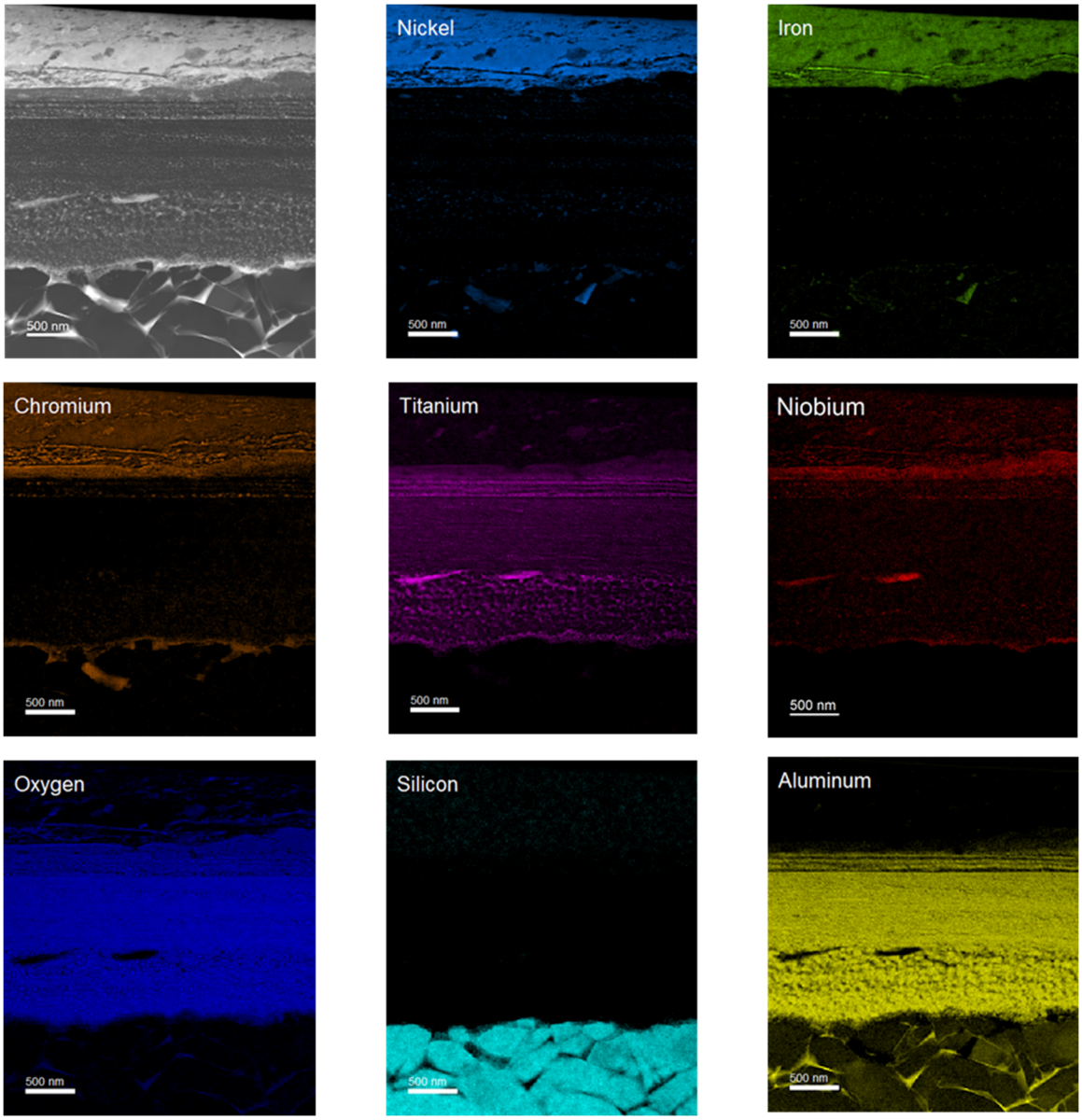

Figure 3.15- EELS elemental mapping of the BUL formed at V_C= 1300 m/min

The adaptive tribological response of the tool-chip interaction was further evaluated through XPS studies on the worn surface of the cutting tools. The initial phase composition of the tool's frictional surface is presented in Figure 3.16. HR XPS spectra indicate the presence of two phases on the surface before wear: Al_2O_3 (corundum, Figure 3.16(a)) and

Si_3N_4 (Figure 3.16(b)). XPS study of the worn tools in Figure 16 shows that during the friction, tribofilms are forming on the cutting edge.

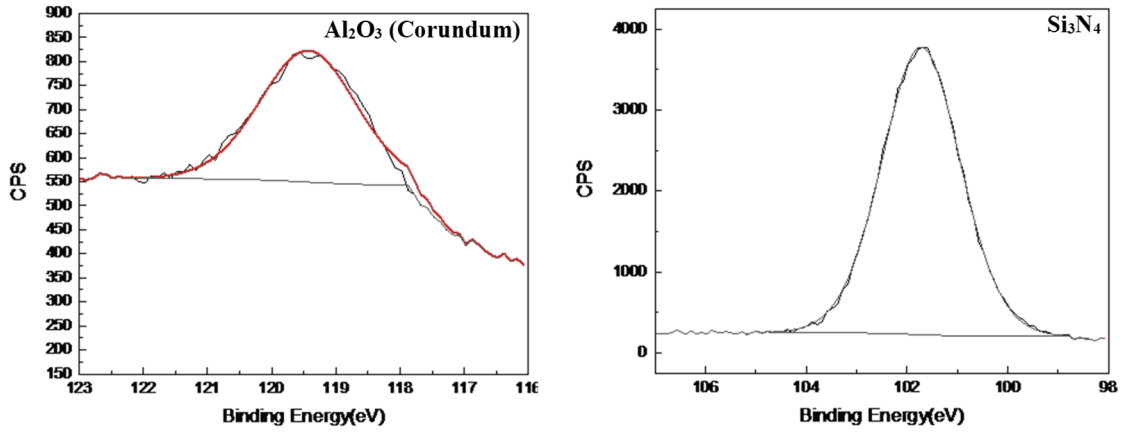

(a) (b)

Figure 3.16- HR spectra of the ceramic tool surface in the initial state (fresh tool): (a) Al2s; (b) Si2p

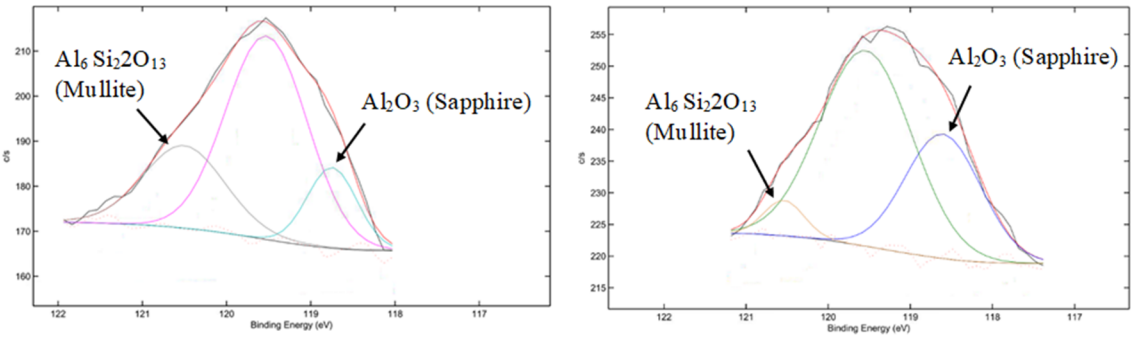

(a) (b)

Figure 3.17- HR XPS spectra of the worn tool surface at the optimal cutting speed of 900 m/min: ***(a)*** *rake surface;* ***(b)*** *flank surface*

It can be seen that the rake surface (due to its higher resultant temperature) has a bit higher amount of protective tribofilms, and therefore, it is better protected (Figure 3.17(a)) than the flank face (Figure 3.17(b)). The overall amount of protective tribofilms was

measured 41% for the rake face and 37% for the flank face. Also, the adaptive response of the entire tribosystem is stronger with increasing the cutting speed (Figure 3.18). At higher cutting speeds, the tool surface is better protected/lubricated through tribo-oxidation via the formation of thermal barrier (sapphire Al_2O_3 and mullite $Al_6Si_2O_{13}$) and lubricating (SiO_x) tribofilms.

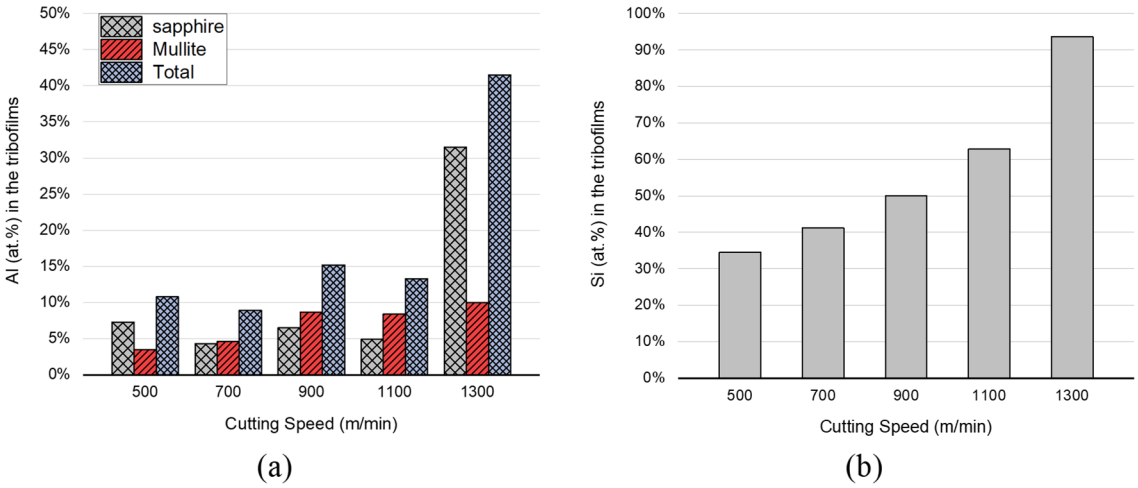

Figure 3.18- Analysis of tribofilm formation on the rake face of the tool
***(a)** thermal barrier tribofilms; **(b)** lubricating tribofilms*

3.4 Conclusion

Phenomena-based studies of chip formation and tribological behavior in high-speed milling of hardened IN718 using SiAlON ceramic tools have been performed. Evaluations of wear and deformation zones have been made using various characterization techniques such as chip's cross-section metallographic studies, 3D tool wear measurements, SEM/EDS, TEM, XPS, nanoindentation, among others. Studies reveal that:

1- High-speed cutting of IN718 with ceramic tools produces highly-segmented chips. As the cutting speed increase, chip cross-section becomes thinner and more uniform, and the angle in which the segments form becomes larger. These phenomena show a positive effect on machinability and tool wear.

2- In the chip microstructure, the morphology of MC carbide particles, in special NbC, changes by variation of cutting speed. At lower speeds, the NbCs remain almost intact, but at higher temperatures, as a consequence of high thermo-mechanical loads, the NbC particles dissolve during the deformation and reappear in a Nb-rich Laves phase which is typically seen in welded microstructures. Results show that this abrupt loss of Inconel's main strengthening mechanism as a precipitation hardened alloy influences the resultant cutting force and tool-chip frictional interaction.

3- Chip thinning, combined with the microstructural transformation of the workpiece material, affects the tribology of the process. By increasing the cutting speed, thinner chips flow easier with signs of local melting and fluid-type flow, which results in the TCCL growth. TCCL eventually drops at V_C=1300 m/min, mainly due to the excessive formation of BUE.

4- Experimental results and microscopic observations suggest that a dramatic change related to the material structure happens during the high-speed machining that improves the IN718 machinability. The TEM result specifically helped to show this microstructure change. Investigation of diffraction patterns in TEM shows that a micron-sized layer of IN718 at the tool-workpiece interface can bear a liquid type behavior under the extreme conditions of elevated temperature and mechanical stress.

5- Instrumented nanohardness measurements show that the cutting speed has no meaningful effect on the hardness of the generated chip. Nevertheless, nanohardness values on the chip cross-section are 30% higher than the workpiece, with a further 15% increase on the shear bands.

6- By increasing the cutting speed, local melting is intensified, and the chip undersurface shows signs of sticking as a result of the high weldability of IN718 at elevated temperatures. Nonetheless, the undersurface of chips produced at lower cutting speeds shows “stick-slip” phenomena similar to avalanche friction behavior, which indicates catastrophic wear mode and reduced tool life.

7- At higher speeds, the tool surface is better protected by thermal-barrier and lubricous tribofilms. In XPS studies, more than 40% of the tool face is covered by different products of Al and Si, such as Mullite and sapphire.

3.5 References

Aizawa, T., et al. 2005. "Self-Lubrication Mechanism Via the in Situ Formed Lubricious Oxide Tribofilm." *Wear* 259, no. 1-6: 708-718. https://dx.doi.org/10.1016/j.wear.2005.02.025.

Aramesh, Maryam, et al. 2018. "A Novel Treatment for Cutting Tools for Reducing the Chipping and Improving Tool Life During Machining of Inconel 718." *Wear* 414-415, no. May: 79-88. https://dx.doi.org/10.1016/j.wear.2018.08.002.

Arunachalam, R., et al. 2000. "Machinability of Nickel-Based High Temperature Alloys." *Machining Science and Technology* 4, no. 1: 127-168. https://dx.doi.org/10.1080/10940340008945703.

Davies, M. A., et al. 2001. "Thermomechanical Oscillations in Material Flow During High-Speed Machining." *Philosophical Transactions of the Royal Society A: Mathematical, Physical and Engineering Sciences* 359, no. 1781: 821-846. https://dx.doi.org/10.1098/rsta.2000.0756.

Desaigues, Jean Edouard, et al. 2016. "Experimental Study of Built-up Layer Formation During Machining of High Strength Free-Cutting Steel." *Journal of Materials Processing Technology* 236: 204-215. https://dx.doi.org/10.1016/j.jmatprotec.2016.05.016.

Dudzinski, D., et al. 2004. "A Review of Developments Towards Dry and High Speed Machining of Inconel 718 Alloy." *International Journal of Machine Tools and Manufacture* 44, no. 4: 439-456. https://dx.doi.org/10.1016/S0890-6955(03)00159-7.

DuPont Jn, Robino C. V. Marder A. R. 1998. "Solidification and Weldability of Nb-Bearing Superalloys." *Welding Journal* 77, no. 10: 417-431. https://dx.doi.org/10.4319/lo.2013.58.2.0489.

Fox-Rabinovich, German, et al. 2014. "Tribofilm Formation as a Result of Complex Interaction at the Tool/Chip Interface During Cutting." *Lubricants* 2, no. 3: 113-123. https://dx.doi.org/10.3390/lubricants2030113.

Friedman, M. Y., et al. 1970. "Investigation of the Tool-Chip Contact Length in Metal Cutting." *International Journal of Machine Tool Design and Research* 10, no. 4: 401-416. https://dx.doi.org/10.1016/0020-7357(70)90001-6.

Hamann, J. C., et al. 1994. "Selective Transfer Built-up Layer Displacement in High-Speed Machining - Consequences on Tool Wear and Cutting Forces." *CIRP Annals - Manufacturing Technology* 43, no. 1: 69-72. https://dx.doi.org/10.1016/S0007-8506(07)62166-0.

Hokka, M., et al. 2014. "Dynamic Behavior and High Speed Machining of Ti-6246 and Alloy 625 Superalloys: Experimental and Modeling Approaches." *Experimental Mechanics* 54, no. 2: 199-210. https://dx.doi.org/10.1007/s11340-013-9793-7.

Izhevskiy, V. A., et al. 2000. "Progress in Sialon Ceramics." *Journal of the European Ceramic Society* 20, no. 13: 2275-2295. https://dx.doi.org/10.1016/S0955-2219(00)00039-X.

Janaki Ram, G. D., et al. 2004. "Control of Laves Phase in Inconel 718 Gta Welds with Current Pulsing." *Science and Technology of Welding and Joining* 9, no. 5: 390-398. https://dx.doi.org/10.1179/136217104225021788.

Kitagawa, T., et al. 1997. "Temperature and Wear of Cutting Tools in High-Speed Machining of Incone1718 and Ti-6a1-6v-2sn." *Wear* 202, no. 2: 142-148. https://dx.doi.org/10.1016/S0043-1648(96)07255-9.

Klocke, F., et al. 1997. "Dry Cutting." *CIRP annals* 46, no. 2: 519-526.

Komanduri, R. 1982. "Some Clarifications on the Mechanics of Chip Formation." *Wear* 76: 15-34.

Komanduri, R., et al. 1986. "On Shear Instability in Machining a Nickel-Iron Base Superalloy." *Journal of Engineering for Industry* 108, no. 2: 93-100. https://dx.doi.org/10.1115/1.3187056.

Markov, D., et al. 2000. "Mechanisms of Adhesion-Initiated Catastrophic Wear: Pure Sliding." *Wear* 239, no. 2: 189-210. https://dx.doi.org/10.1016/S0043-1648(99)00373-7.

Narutaki, N., et al. 1993. "High Speed Machining of Inconel 718 with Ceramic Tools." *CIRP annals* 42, no. 1: 103-106. https://dx.doi.org/10.2493/jjspe.61.1463.

Österle, W., et al. 1997. "Mechanical and Thermal Response of a Nickel-Base Superalloy Upon Grinding with High Removal Rates." *Materials Science and Engineering A* 238, no. 2: 357-366. https://dx.doi.org/10.1016/S0921-5093(97)00457-7.

Ressa, Aaron. 2015. "Plastic Deformation and Ductile Fracture Behavior of Inconel 718."

Roy, Soumikh, et al. 2018. "A Brief Review on Machining of Inconel 718." *Materials Today: Proceedings* 5, no. 9: 18664-18673. https://dx.doi.org/10.1016/j.matpr.2018.06.212.

Schulz, H., et al. 2001. "Material Aspects of Chip Formation in Hsc Machining." *CIRP Annals - Manufacturing Technology* 50, no. 1: 45-48. https://dx.doi.org/10.1016/S0007-8506(07)62067-8.

Schulz, Herbert, et al. 1992. "High-Speed Machining." *CIRP Annals - Manufacturing Technology* 41, no. 2: 637-643. https://dx.doi.org/10.1016/S0007-8506(07)63250-8.

Sharman, A. R. C., et al. 2008. "Surface Integrity and Tool Life When Turning Inconel 718 Using Ultra-High Pressure and Flood Coolant Systems." *Proceedings of the Institution of Mechanical Engineers, Part B: Journal of Engineering Manufacture* 222, no. 6: 653-664. https://dx.doi.org/10.1243/09544054JEM936.

Sreejith, P. S., et al. 2000. "Dry Machining: Machining of the Future." *Journal of Materials Processing Technology* 101, no. 1-3: 287-291. https://dx.doi.org/10.1016/S0924-0136(00)00445-3.

Tonshoff, H. K., et al. 2000. "Cutting of Hardened Steel." *CIRP Annals - Manufacturing Technology* 49, no. 2: 547-566. https://dx.doi.org/10.1016/S0007-8506(07)63455-6.

Wright, P. K., et al. 1982. "Deformation Characteristics of Nickel Alloys During Machining." *Journal of Engineering Materials and Technology* 104, no. 2: 85-93. https://dx.doi.org/10.1115/1.3225057.

Wusatowska-Sarnek, A. M., et al. 2011. "Microstructural Characterization of the White Etching Layer in Nickel-Based Superalloy." *Metallurgical and Materials Transactions A: Physical Metallurgy and Materials Science* 42, no. 12: 3813-3825. https://dx.doi.org/10.1007/s11661-011-0779-8.

Zhou, L. X., et al. 1994. "Effects of Strain Rate and Temperature on Deformation Behaviour of in 718 During High Temperature Deformation." *Materials Science and Engineering A* 177, no. 1-2: 1-9. https://dx.doi.org/10.1016/0921-5093(94)90472-3.

Chapter 4. Surface Integrity

F. Molaiekiya, A. Khoei, M. Aramesh, and S. C. Veldhuis. " *Surface integrity of inconel 718 in high-speed dry milling using SiAlON*" Submitted to *The International Journal of Advanced Manufacturing Technology,* currently under peer review.

Authors' Contributions

F. Molaiekiya	Conceptualized and performed the experiments Analyzed and interpret the results Wrote and prepared the manuscript
A. Khoei	Assisted with XRD experiments
M. Aramesh	Assisted with writing, reviewing, and editing
S. C. Veldhuis	Supervised and administered the project

Abstract

The surface integrity of complex engineering components has a major effect on their mechanical properties, especially fatigue resistance. Recently, modern ceramic tools have demonstrated themselves as potential candidates for high-speed machining of heat resistant superalloys, delivering a substantial increase in productivity. The results of previous studies showed that after surpassing a cutting speed of 800m/min the cutting forces experienced a sharp, significant decrease accompanied by a reduction in tool wear and cutting edge chipping. However, in such applications, extreme temperature and mechanical loads are generated at the cutting zone, implying a possible negative influence on the surface integrity of the workpiece. To investigate this, in this study, numerous characterizations have been performed to evaluate the different aspects of inconel 718 (IN718) machined surface integrity after face milling with SiAlON cutting tools at the range of 900 m/min. Surface roughness, nanohardness and residual stress of the surfaces were measured alongside with near-surface metallography and SEM/EDS microscopy observations. Since the resultant thermomechanical conditions are remarkably far from those experienced during conventional cutting, the results are also compared to those obtained during conventional milling of inconel with a commonly used commercial coated carbide tool. Results show that the machining process induces high tensile residual stresses on the surface while generating an unwanted white layer and a rougher surface as compared to surfaces machined with conventional carbide tools. Nevertheless, defects and imperfections were contained within a thin sublayer of the workpiece, suggesting the ceramic tools can be used for roughing or semi-finishing processes provided further finishing operations are used to remove the damaged layer.

Keywords

High-speed machining; Cutting parameters; Surface integrity; SiAlON ceramic; Inconel 718

4.1 Introduction

Inconel 718 (IN718) is a heat-resistant superalloy that is widely employed when making engineering components that are subjected to high thermo-mechanical loads, especially in the aerospace industry. However, because of its high-temperature shear strength, low thermal conductivity, and extensive tendency to work hardening, IN718 is considered as one of the most difficult-to-cut alloys. Low machinability of this material can lead to rapid tool wear, limited material removal rate, excessive use of coolant, or poor surface integrity (Rahman, et al. 1997; Li, et al. 2002; Ezugwu 2005; Thakur and Gangopadhyay 2016).

Recent studies by the authors show that using a SiAlON ceramic tool under extreme conditions associated with high cutting speeds for the milling of hardened IN718 provides a significant improvement in the machinability of this material. Studies showed that even at 500 m/min, the cutting forces were so high that the ceramic inserts were completely shattered after a few seconds of machining. However, surprisingly by increasing the speeds to 900 m/min the forces were abruptly reduced by 70%, leading to a considerable increase in the tool life. This behaviour under extreme conditions was attributed to the noticeable change in localized microstructure of inconel related to some of its unique strengthening mechanisms and fluid-like flow of deformed material at high temperature and high strain rates.

Implementing the concepts of high-speed machining for IN718 has proven to be a cost-effective solution that can eliminate the use of coolant while achieving unprecedented material removal rate with an acceptable tool life (Tonshoff, et al. 2000; Sreejith and Ngoi 2000). But, since most of the industrial inconel components are used in demanding

applications such as rotating parts, operating at high-temperature corrosive conditions in a gas turbine, surface integrity and microstructural reliability of manufactured parts are of prime importance preventing catastrophic premature failure of the components under service, especially following a high-speed intermittent cut at dry conditions (Matsumoto, et al. 1999; Akhtar, et al. 2016).

In high-speed machining of nickel-based superalloys, the low thermal conductivity of the workpiece generates very high temperatures, which leads to undesired thermal effects resulting in poor surface integrity of the machined surface (Brandt, et al. 1990; Arunachalam, et al. 2004). Also, high shear strength and high strain hardening rate of inconel under extreme deformation mean there is a possibility of mechanically-induce imperfections during machining. Previous studies also report the formation of excessive built-up edge and transferred layers during the milling process (Hamann, et al. 1994; Desaigues, et al. 2016). The unstable nature of this phenomenon can lead to the development of attrition wear patterns on the tool and poor surface quality of the finished product. These are critical issues as the roughness of the surface plays a prominent role in the resistance to creep and fatigue of the component (Suraratchai, et al. 2008; Xun, et al. 2018). Since in high-speed machining with ceramic inserts, the tool life flank wear based criterion is defined to be more than a conventional flank wear criteria for tungsten carbide tools, the roughness of the final machined surface can be compromised but needs to be monitored carefully. Therefore, comprehensive investigations need to be performed on the surface and sub-surface of a machined IN718 component to understand the impact on surface roughness and surface texture, sublayer plastic deformation and work-hardening,

near-surface microstructural defects and inclusions, and residual stress after high-speed dry milling with SiAlON ceramic tools.

Evaluation of machinability and surface integrity of IN718 parts has been a topic of interest during the past few decades (Arunachalam, et al. 2004; Pawade, et al. 2008; M'saoubi, et al. 2008; Devillez, et al. 2011; Jawahir, et al. 2011). Many researchers attempted to characterize the properties of the inconel machined surface and subsurface, however, most of the studies are focused around turning with common carbides tools at conventional conditions, with a few using ceramic tooling. High tensile residual stress is considered the most common phenomenon observed during machining of heat resistant alloys (Akhtar, et al. 2016; Devillez, et al. 2011). Also, an increase in sub-surface hardness is reported by some researchers that is attributed to strain hardening sensitivity of the material in plastic deformations (Jawahir, et al. 2011).

Considering the lack of significant data on high-performance dry milling of hardened IN718 with SiAlON ceramic tools and the possible damaging effects that extreme heat and deformations of such a process can induce on the life expectancy of a sensitive product, a comprehensive study is presented in this paper aiming to investigate the major aspects of surface integrity. Furthermore, wherever possible, the results of the experiments and characterizations are compared to the outcome of a conventional cutting process using a common coated WC-Co tool.

Various machinability experiments and characterization techniques have been used in this research such as 3D surface scanning, XRD measurements, cross-section metallography, nanoindentation and SEM/EDS to study and control the surface roughness,

residual stress, work-hardening, microstructural alterations, surface inclusion and contamination, grain distortion, cracks, and heat-affected zones and other imperfections on the machined workpiece.

4.2 Materials and Methods

Machining experiments were performed on a block of 45 HRC age-hardened IN718 using a robust high-speed CNC machine center (Makino MC56-5XA) with 30 kW spindle power and 15000 maximum RPM. The chemical composition of the workpiece consists approximately of 53.7% Ni, 18.4% Cr, 18.3% Fe, 6.4% Nb and Al, Ti and Si (1% of each) in weight percentage. The yield strength and tensile strength of the workpiece are 1230 and 1490 MPa, respectively. IN718 has an extremely low thermal conductivity of around 12 W/m.K, and its melting point is between 1250-1300 °C.

The cutting tool was a Kennametal KCRA250RN4306S075L175 indexable face mill with 10° clearance, -10° axial rake, and -5° radial rake angle. SiAlON ceramic grade KYS30 was used for the cutting tool material (Kennametal RNGN120400T01020 round milling inserts). For the sake of comparison, a similar tool geometry was also tested using a state-of-the-art coated tungsten carbide inserts. The inserts were chosen from Kennametal KC725M grade TiAlN PVD-coated carbide inserts clamped on a KDR250R1207S075L200 shell mill. Flank and volumetric tool wear were measured using a Keyence VHX-5000 and Alicona focus variation microscope. Flank wear of 300 and 1000 microns were selected as the end of tool life criterion for cemented carbide and ceramic inserts, respectively.

Based on the result of the previous studies, the cutting speed of 900 m/min was selected for the SiAlON ceramics as the cutting forces were found to be minimum at this speed, and the tool life longest. V_C= 35 m/min was selected for the carbide insert with flood coolant turned on. Various axial depths of cut (1-3 mm) were selected to investigate the effect of increasing productivity (material removal rate), by increasing the depth of cut, on the characteristics of the workpiece surface.

Optical microscopic observations were done using a Keyence VHX-5000 and Keyence VH-ZST. To reveal the microstructure, the material was etched by swabbing a cotton ball rinsed in a solution consisting of 15 ml Hydrochloric acid, 10 ml Nitric acid, 10 ml Acetic acid, and less than a drop of Glycerin for 10 seconds.

High-precision 3D optical microscope (Alicona Infinite Focus XL200 G5) with 2 µm vertical, and 5 µm lateral scanning resolution was used to scan and measure the roughness of the surfaces based on the ISO 4288 standard. Further microscopic observations were done using a Tescan Vega II LSU scanning electron microscope (SEM), equipped with an Oxford X-Max 80 energy-dispersive X-ray spectroscopy (EDX) detector and Inca software version 4.14. The spatial resolution of the EDS data was set to 1-5 μm^3 for low and 0.2-1 μm^3 for high atomic numbers using a 10 kV accelerating voltage.

Sub-surface nano hardness was measured using an Anton Paar NHT^3 nanoindentation tester. The indentations were done using a sharp Berkovich indenter with 35mN maximum force, 5s dwell time, and 10mN/min loading/unloading rate. The results were analyzed using the Oliver-Pharr nonlinear curve fit method. The indentations were extended up to 100 microns in depth from the machined surface at a one-micron resolution.

For residual stress measurement, sectioned samples were mounted on the Bruker D8 Discover with Davinci design diffractometer. The instrument is equipped with a cobalt sealed tube source (λ_{avg}= 1.79026Å) and the power settings of 35kV, 45mA. The Phi angles of 0°, 72°, 144°, 216° and 288° were selected. For each phi angle, the Chi angle is changed to 10°, 30° and 50°. The frame exposure time was 420s/frame, and the data were collected in the range of 104-126°. 2D frames were processed with DIFFRAC measurement suite version 6.5 and analyzed in Leptos V7.

4.3 Results and Discussion

Tool wear curves obtained for both ceramic and cemented carbide tools are depicted in Figure 4.1. The criteria for the end of tool life was selected based on common industrial practices. The SiAlON ceramic tool machined IN718 for a total of 4410 mm in feed length until the end of life, while the coated carbide tool travelled for 3360 mm, 25% less. Furthermore, in terms of productivity of the process, the SiAlON tool also delivered four times higher material removal rate compared with the carbide tool. During the machinability experiments, SiAlON ceramics showed steady and repeatable 3D wear volume and flank wear rate in various experiments and is believed to be able to perform similarly until 2mm flank wear if the right cutting conditions are implemented. The cutting speed of 900 m/min was selected based on the outcome of previous research aimed at the highest tool life and the lowest cutting force and tool chipping. The selection of cutting parameters was performed within a range of speeds between 500 to 1,300 m/min while

investigating various aspects of the cutting process such as tool wear mechanism, cutting forces, chip formation, built-up layers, and tribology at high speeds.

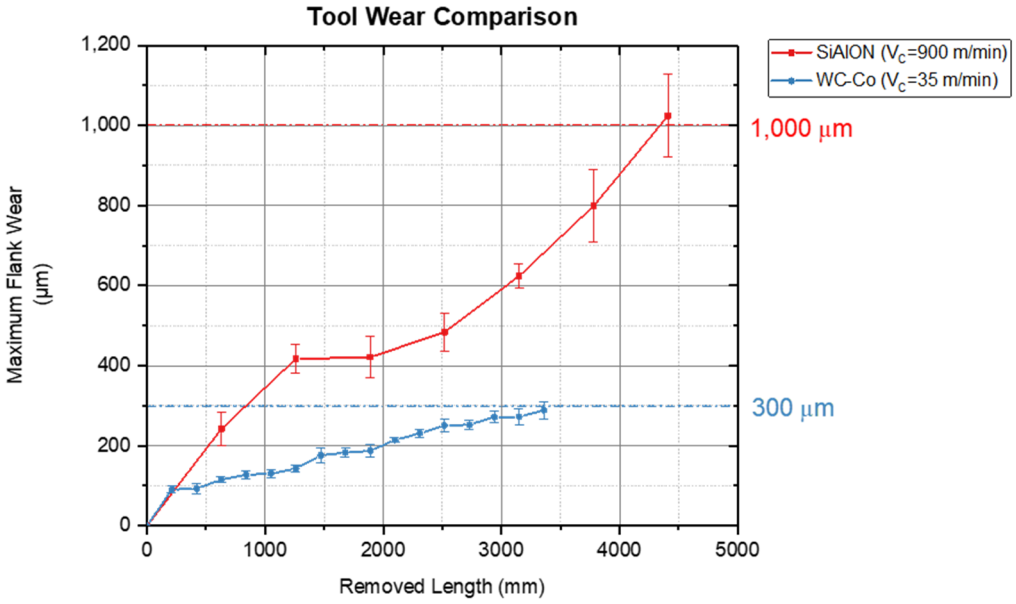

Figure 4.1- Tool life curves obtained for WC-Co (35 m/min) and SiAlON ceramic (900 m/min)

The roughness and texture of the machined surfaces were examined for different tools. Figure 4.2 illustrates the topography of surfaces captured by the Alicona focus variation microscope. For the SiAlON ceramic tool cutting at V_C=900 m/min and F_Z=40 µm/tooth, the roughness of the surface produced by a fresh tool was 0.52±0.11 µm while the roughness of the fresh carbide tools was measured to be 0.82±0.07 µm at V_C=35 m/min and F_Z=200 µm/tooth. The surface texture (S_a) values were 0.66±0.1 µm and 1.10±0.1 µm, respectively. The roughness of the workpiece surface generated by the worn tools was also evaluated, and the results can be seen in Table 4.1. There are many factors affecting the surface roughness, the most reported is the cutting parameters, especially the feedrate.

Despite the lower feed rate and higher cutting speed of the SiAlON tool, the surface roughness at the end of tool life is worse than the roughness generated by the carbide tool, which is a result of higher tool wear and change in the geometry of the cutting edge. Meanwhile, the surface that is machined using worn ceramic tools shows much higher Rz value representing more random grooves which can be the result of external particles getting stuck between the tool and workpiece abrading the machined surface at the tertiary shear deformation zone.

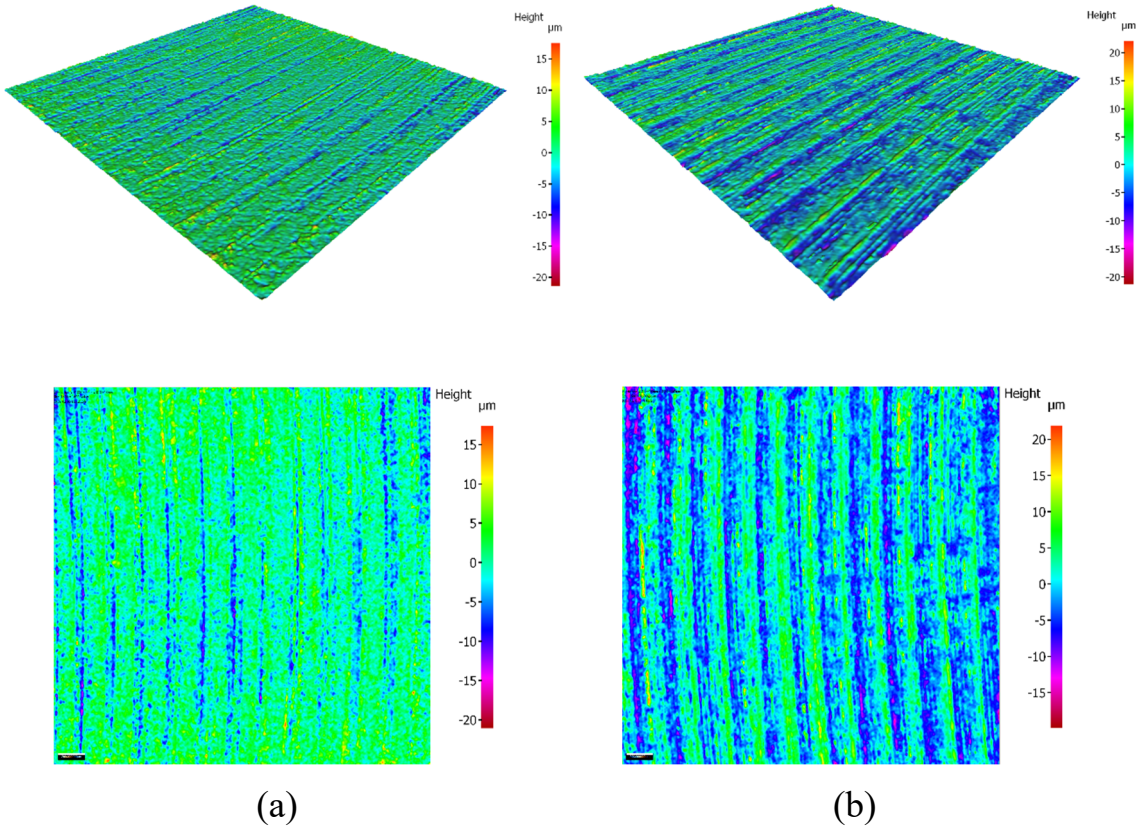

Figure 4.2- Surface topography of the machined IN718 with sharp tools:
***(a)** SiAlON Ceramic tool; **(b)** PVD-coated WC-Co tool*

Table 4.1- Surface roughness and texture measurements for the worn tools

Tool	Worn SiAlON	Worn WC-Co
Cutting parameters	V_C=900 m/min F_Z=40 µm/tooth Axial DOC=1 mm	V_C=35 m/min F_Z=200 µm/tooth Axial DOC=1 mm
R_a	4.50±0.64 µm	2.19±0.22 µm
R_z	16.61±1.7 µm	4.90±0.39 µm
S_a	4.42±0.89 µm	2.38±0.34 µm

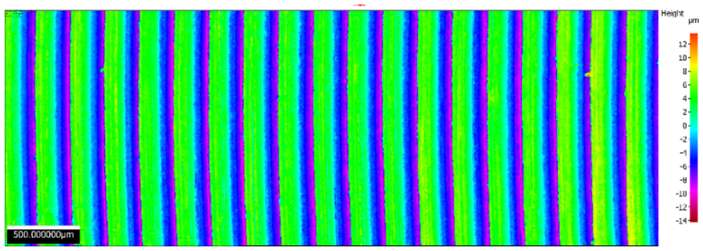

(a)

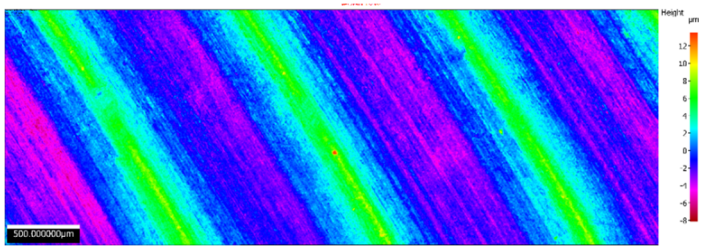

(b)

Figure 4.3- Texture illustration of the machined surfaces at the end of tool life by:
***(a)** Worn SiAlON ceramic; **(b)** Worn PVD-coated WC-Co*

High-speed milling of IN718 with SiAlON ceramics produced an extensive amount of built-up layers on the cutting edges. As the tool wear evolved, the unstable built-up layer can detach from the tool and stick on the workpiece surface. Not only does this phenomenon

cause dimensional inaccuracy and an increase in surface roughness, but also can transfer unwanted elements from the tool material to the machined surface. SiAlON or silicon aluminum oxynitride contains a high percentage of Si. Silicon and other non-metallic contaminations such as silica and alumina are known to be a source of reduction in fatigue life in aerospace components by creating inclusion initiated cracks (Chan 2010; Wang, et al. 2002).

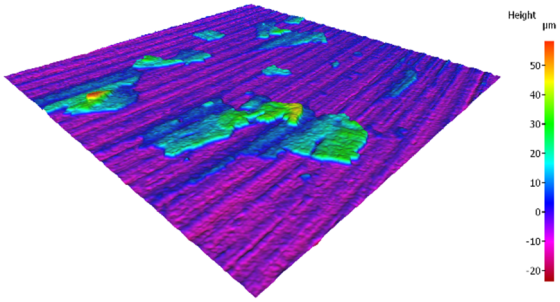

(a)

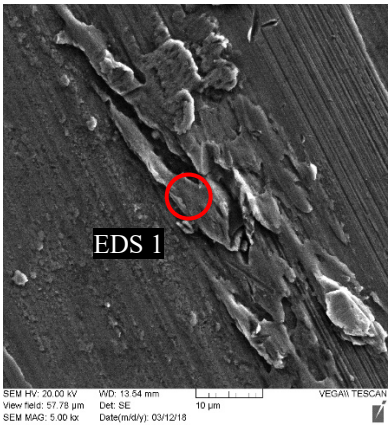

(b)

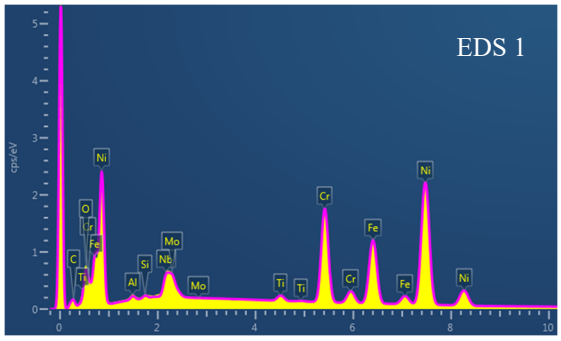

(wt%)

Ni	50.14	**Nb**	4.22	**Si**	0.26
Fe	16.82	**Ti**	0.74		
Cr	17.06	**Al**	0.41		

(C)

Figure 4.4- detached build-up layers stick on the machined surface:
***(a)** Alicona microscope scans showing irregularity on the surface;*
***(b)** SEM graph of the built-up transferred layer;*
***(c)** EDS elemental studies of the adhered BUE to the workpiece*

Figure 4.4 shows the contamination of the workpiece surface after high-speed milling with ceramic tools at V_C=900 m/min. Thus, a final finishing pass is still required if a SiAlON tool is used for roughing of high-temperature aerospace engine parts. This phenomenon intensified as the tool wear further evolves and, in some cases, can generate signs of material pull-out on the workpiece surface as can be seen in microscopic images of the machined surface in Figure 4.5 and the cross-section in Figure 4.6(d). In Figure 4.6(a)(b) the generated surface after a few passes of high-speed milling with sharp ceramic tools shows no sign of major sub-surface damages, cracks, grain distortions or excessive plastic deformations. However, the sub-surface cross-section of the workpieces after machining with a worn tool, especially at the location of built-up edge irregularities, shows cracks and pits which have a negative influence on the tensile and fatigue strength of the part.

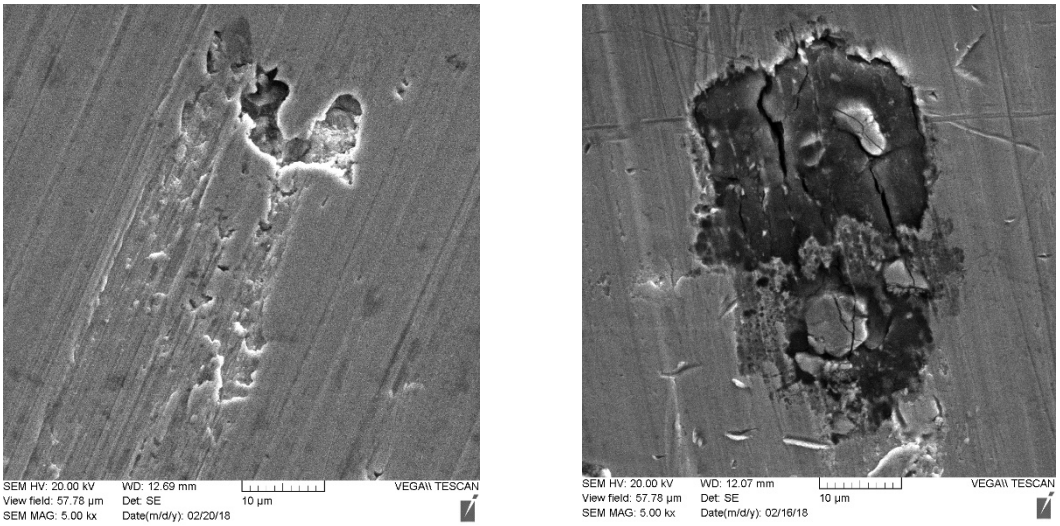

Figure 4.5- Surface damage and wear signs on the machined inconel surface in the forms of pits and cracks

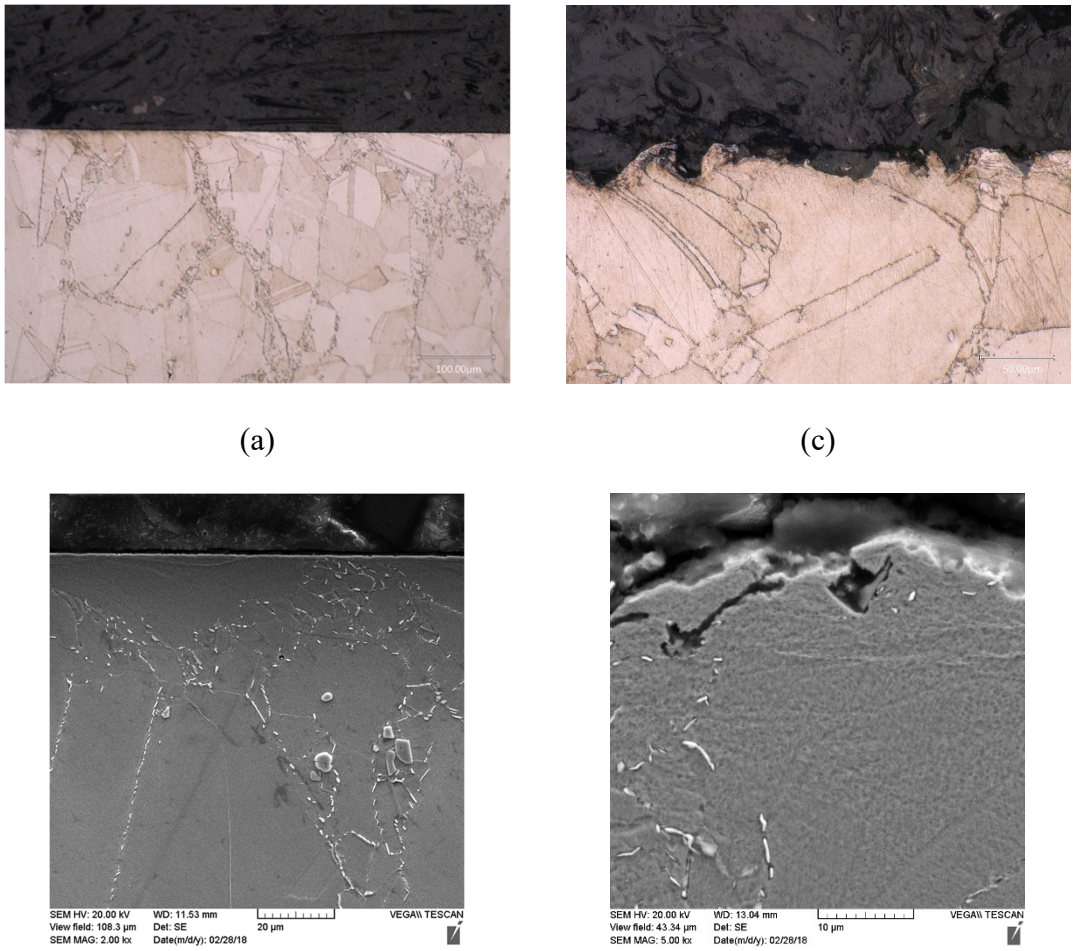

*Figure 4.6- Optical and electron microscope images of the cross-sections of the machined surfaces after high-speed milling with **(a)(b)** Sharp SiAlON tools **(c)(d)** Worn ceramic tools*

A 1-2 µm hardened layer known as a white layer is observed to be formed on the machined surface after high-speed machining (Figure 4.7). This layer is usually seen during processes involving rapid heating and cooling cycles or on surfaces that experienced extreme frictional conditions (Wusatowska-Sarnek, et al. 2011; Chen, et al. 2017; Bushlya, et al. 2011). Extreme thermomechanical loads result in microstructure refinement and dynamic recrystallization that are believed to be mechanisms behind the formation of white

layers after machining. The nano-hardness of this layer was measured to be close to 21 GPa using a sharp Berkovich indenter under a 10 mN load.

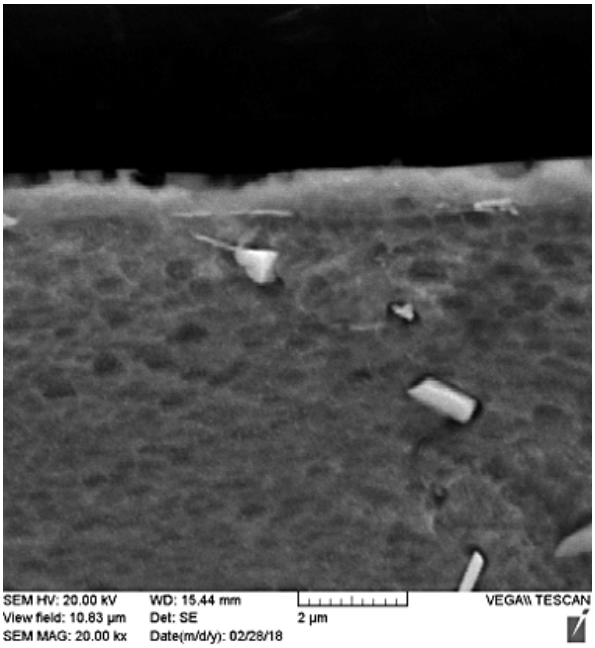

Figure 4.7- Formation of a white layer on the surface machined with ceramic tools at high speed

Nano-hardness of the machined cross-sections was measured using 35 mN load indentations with a sharp Berkovich diamond indenter. As illustrated in Figure 4.8, no major sub-surface hardening is observed after high-speed machining with SiAlON tools. The hardness of the bulk of the material was measured to be 7.1±0.65 GPa. The effect of the axial depth of cut was also investigated in this experiment and showed no major influence on the work-hardening level of the sub-layer. Increasing the axial depth of cut is the easiest way to increase the material removal rate of the machining process. The same measurement for WC-Co tools under wet conditions shows approximately a 10% higher

hardness value as compared to samples produced at high cutting speeds using SiAlON tooling.

Round geometry of the inserts and subsequent chip thinning effect at the trailing edge of the cutting tool lead to minimum plastic deformation at the tertiary shear deformation zone and consequently, a negligible alteration in the nano-hardness of the near-surface.

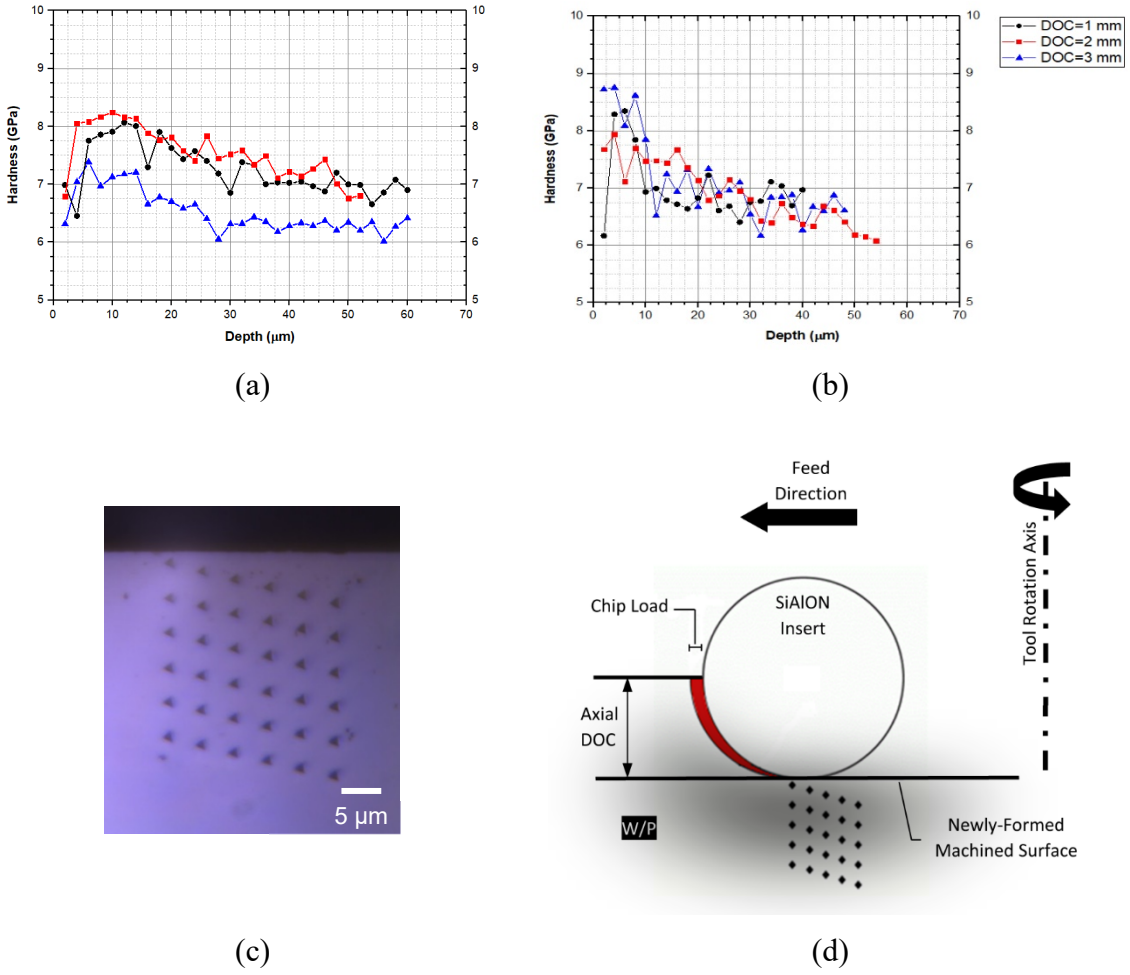

Figure 4.8- ***(a)*** *nano-hardness of the machined surface after machining with SiAlON at 900 m/min with varying axial DOC;* ***(b)*** *nano-hardness of the machined surface after machining with WC-Co at 35 m/min with varying axial DOC;* ***(c)*** *Typical indentation matrix on one of the samples at one-micron mapping resolution;* ***(d)*** *Chip thinning effect in face milling with round cutting inserts*

Residual stress levels on the surfaces were also measured using an x-ray diffraction (XRD) instrument, the result of which is listed in Table 4.2 for both ceramic and carbide tools at their respective cutting parameters.

Table 4.2- Residual stress measurements on the workpiece surface after machining with ceramic at dry high-speed and WC-Co at wet conditions using sharp and worn tools

Tool	Wear Condition	Normal Residual Stress (MPa)
SiAlON Ceramic	Sharp	1635.2±30.2
	Worn	2016.6±17.9
PVD-coated WC-Co	Sharp	226.9±34.3
	Worn	804.1±42.6

Results show that the high-speed milling operation with SiAlON ceramic tools generates very high levels of tensile residual stress on the machined product which is the result of high-temperature gradients generated during plastic deformations at high strain rates alongside with friction between the worn cutting edge and the newly-formed machined surface at the tertiary shear deformation zone. Low thermal conductivity of both tool and workpiece also plays a prominent role in the cutting temperature rise as it impairs the proper dissipation of heat from the cutting zone. On the other hand, IN718's resistance to heat and fast-moving heat source at high speeds means the damaging effect of the machining process will be contained within a narrow band underneath the machined surface and will not penetrate deep into the bulk of the material. In most cases, a finishing pass can be used to remove the damaged layer.

High tensile residual stress on the machined surface suggests that the high-speed milling process of hardened IN718 has a stronger thermal effect on the surface rather than mechanically induced stresses. The negative rake angle of the inserts can create a considerable axial mechanical load during the process; Nevertheless, reduction in the cutting force at V_C=900 m/min eliminates the mechanically-induced compressive residual stresses. Higher cutting forces at a lower speed of 500 m/min and shorter cutting (heating) time at a higher speed of 1,300 m/min suggest the generation of lower residual stresses compared to optimal V_C=900 m/min. This is confirmed by XRD measurement as the residual stress levels for sharp tools at 500, and 1,300 m/min were 1,013.1±19.5 and 1,419.0±48.8 MPa, respectively.

4.4 Conclusion

The integrity of IN718 machined surface generated by high-speed dry milling using SiAlON ceramic tools and wet conventional milling using coated cemented carbide tools with similar geometries were examined in a set of machinability investigations, tool wear studies, near-surface metallography methods, optical and electron microscopy imaging, EDS, roughness measurements, nanoindentation, and XRD. It is shown that SiAlON ceramic cutting tools can significantly increase the productivity of the manufacturing process when used at optimal cutting speeds around 1,000 m/min. However, reaching such cutting speeds generates extreme localized heat and mechanical loads that can potentially deteriorate the integrity of the machined surface. Following the observations discussed in this study, it is recommended that the ceramic tools should be used only for semi-finishing

or roughing applications with a few tens of microns stock left for removing the surface imperfections generated using the SiAlON tool by performing a subsequent finish machining operation with a sharp coated cemented carbide tool.

1- The roughness of the surface produced by fresh tools is better when cutting at high-speeds with ceramics in comparison with conventional tools. Worn ceramic tools generate a rougher surface at the end of the tool life of R_a=4.5 µm compared to R_a=2.19 µm obtained from the cemented carbide tools at the end of life.

2- Cutting with ceramic tools at high speeds generates an excessive amount of built-up edge, which intensifies with the evolution of tool wear. Unstable BUE and transferred layers can detach from the tool and stick to the workpiece and cause cracks, pits, smearing and material pull-out signs on the surface. Traces of silicon contamination was found on the workpiece surface after machining with SiAlON tools. This is deemed to be a concern as the presence of Si on a surface is known to impact the fatigue life of sensitive engineering components, particularly high-temperature aero-engine components.

3- High-speed machining with ceramic tools generates a 1-2 µm white layer on the surface. This layer is very hard and fine-grained and remains unetched in metallography and thus appears white under the microscope. This layer is believed to be formed following the effect of rapid cooling from high temperatures. For the machining tests performed in this study, the surface approached the melting point of IN718 while also experiencing high mechanical and tribological loads in the tool-workpiece friction zone.

4- The round geometry of the inserts, selected for their structural strength, had a chip thinning effect when used in the face milling process. The use of round inserts in this application was found to cause minimum work-hardening on the immediate sub-layer of the machined surface, thus ensuring acceptable final part quality in this aspect.

5- Dry high-performance milling of inconel generates extreme tensile residual stress on the IN718 machined surface, up to 2.5 times higher than when WC-Co inserts with similar geometry are used in wet milling at lower cutting speeds. The residual stress of the surface was measured to be more than two gigapascals on the final machined surface. However, the low thermal conductivity of the workpiece material leads to a narrow heat-affected zone, thus allowing a final finishing pass using a WC-Co insert to remove the high residual stress area.

4.5 References

Akhtar, Waseem, et al. 2016. "Effect of Machining Parameters on Surface Integrity in High Speed Milling of Super Alloy Gh4169/Inconel 718." *Materials and Manufacturing Processes* 31, no. 5: 620-627. https://dx.doi.org/10.1080/10426914.2014.994769.

Arunachalam, RM, et al. 2004. "Surface Integrity When Machining Age Hardened Inconel 718 with Coated Carbide Cutting Tools." *International Journal of Machine Tools and Manufacture* 44, no. 14: 1481-1491.

Brandt, G., et al. 1990. "Wear Mechanisms of Ceramic Cutting Tools When Machining Ferrous and Non-Ferrous Alloys." *Journal of the European Ceramic Society* 6, no. 5: 273-290. https://dx.doi.org/10.1016/0955-2219(90)90019-C.

Bushlya, V., et al. 2011. "Characterization of White Layer Generated When Turning Aged Inconel 718." *Procedia Engineering* 19: 60-66. https://dx.doi.org/10.1016/j.proeng.2011.11.080.

Chan, Kwai S. 2010. "Roles of Microstructure in Fatigue Crack Initiation." *International Journal of Fatigue* 32, no. 9: 1428-1447.

Chen, Zhe, et al. 2017. "Nano-Scale Characterization of White Layer in Broached Inconel 718." *Materials Science and Engineering A* 684: 373-384. https://dx.doi.org/10.1016/j.msea.2016.12.045.

Desaigues, Jean Edouard, et al. 2016. "Experimental Study of Built-up Layer Formation During Machining of High Strength Free-Cutting Steel." *Journal of Materials Processing Technology* 236: 204-215. https://dx.doi.org/10.1016/j.jmatprotec.2016.05.016.

Devillez, A., et al. 2011. "Dry Machining of Inconel 718, Workpiece Surface Integrity." *Journal of Materials Processing Technology* 211, no. 10: 1590-1598. https://dx.doi.org/10.1016/j.jmatprotec.2011.04.011.

Ezugwu, E. O. 2005. "Key Improvements in the Machining of Difficult-to-Cut Aerospace Superalloys." *International Journal of Machine Tools and Manufacture* 45, no. 12-13: 1353-1367. https://dx.doi.org/10.1016/j.ijmachtools.2005.02.003.

Hamann, J. C., et al. 1994. "Selective Transfer Built-up Layer Displacement in High-Speed Machining - Consequences on Tool Wear and Cutting Forces." *CIRP Annals - Manufacturing Technology* 43, no. 1: 69-72. https://dx.doi.org/10.1016/S0007-8506(07)62166-0.

Jawahir, IS, et al. 2011. "Surface Integrity in Material Removal Processes: Recent Advances." *CIRP annals* 60, no. 2: 603-626.

Li, L., et al. 2002. "High Speed Cutting of Inconel 718 with Coated Carbide and Ceramic Inserts." *Journal of Materials Processing Technology* 129, no. 1-3: 127-130. https://dx.doi.org/10.1016/S0924-0136(02)00590-3.

M'saoubi, R, et al. 2008. "A Review of Surface Integrity in Machining and Its Impact on Functional Performance and Life of Machined Products." *International Journal of Sustainable Manufacturing* 1, no. 1-2: 203-236.

Matsumoto, Y, et al. 1999. "Surface Integrity Generated by Precision Hard Turning." *CIRP Annals* 48, no. 1: 59-62.

Pawade, RS, et al. 2008. "Effect of Machining Parameters and Cutting Edge Geometry on Surface Integrity of High-Speed Turned Inconel 718." *International Journal of Machine Tools and Manufacture* 48, no. 1: 15-28.

Rahman, M., et al. 1997. "The Machinability of Inconel 718." *Journal of Materials Processing Technology* 63, no. 1-3: 199-204. https://dx.doi.org/10.1016/S0924-0136(96)02624-6.

Sreejith, P. S., et al. 2000. "Dry Machining: Machining of the Future." *Journal of Materials Processing Technology* 101, no. 1-3: 287-291. https://dx.doi.org/10.1016/S0924-0136(00)00445-3.

Suraratchai, Monchai, et al. 2008. "Modelling the Influence of Machined Surface Roughness on the Fatigue Life of Aluminium Alloy." *International Journal of fatigue* 30, no. 12: 2119-2126.

Thakur, A., et al. 2016. "Dry Machining of Nickel-Based Super Alloy as a Sustainable Alternative Using Tin/Tialn Coated Tool." *Journal of Cleaner Production* 129: 256-268. https://dx.doi.org/10.1016/j.jclepro.2016.04.074.

Tonshoff, H. K., et al. 2000. "Cutting of Hardened Steel." *CIRP Annals - Manufacturing Technology* 49, no. 2: 547-566. https://dx.doi.org/10.1016/S0007-8506(07)63455-6.

Wang, QY, et al. 2002. "Effect of Inclusion on Subsurface Crack Initiation and Gigacycle Fatigue Strength." *International Journal of Fatigue* 24, no. 12: 1269-1274.

Wusatowska-Sarnek, A. M., et al. 2011. "Microstructural Characterization of the White Etching Layer in Nickel-Based Superalloy." *Metallurgical and Materials Transactions A: Physical Metallurgy and Materials Science* 42, no. 12: 3813-3825. https://dx.doi.org/10.1007/s11661-011-0779-8.

Xun, LI, et al. 2018. "Influences of Milling and Grinding on Machined Surface Roughness and Fatigue Behavior of Gh4169 Superalloy Workpieces." *Chinese Journal of Aeronautics* 31, no. 6: 1399-1405.

Chapter 5. Conclusions and Future Work

In this research, the high-speed machinability of heat-resistant superalloys was investigated using material characterization methods and face milling experiments. It was shown that the machinability of hardened IN718 could be significantly improved in a dry face milling setup using SiAlON ceramic tools. By choosing the right cutting conditions, including a cutting speed as high as 1,000 m/min, SiAlON cutting inserts can deliver four times better productivity by substantially increasing the material removal rate of the machining process.

IN718 is known as one of the hardest metallic alloys to machine. Using conventional practices in the manufacturing industry, superior high-temperature mechanical properties of IN718 dictates that very low cutting speed should be selected to prevent overheating and overloading the cutting edge. However, in this study, the range of cutting speed has been increased to around 30 times higher, by using advanced ceramic tools. This research investigated machinability under these extreme conditions. In the initial stages of the study, comprehensive characterization has been done on several structural ceramics to select the proper ceramic compound for reaching the desired extreme conditions. Then, by studying the cutting parameters a sweet spot at around 900 to 1,100 m/min was observed that showed a dramatic improvement in the machinability of IN718 following a significant drop in the cutting forces and tool wear. This favourable operational window is overlooked in the

literature and can initiate many discussions on the unique deformation behavior of hard-to-cut materials under extreme thermomechanical conditions.

Different aspects of a machinability study such as tool material selection, tool life studies, wear mechanisms, cutting parameter optimization, chip formation mechanisms, chip cross-section morphology, tool-workpiece tribology, the formation of transferred layers, surface integrity of the workpiece were covered in this thesis. Various characterization methods such as optical microscopy, nano-indentation, IR thermal camera measurements, optical microscopy, SEM/EDS observations, XRD, XPS, cutting force measurement, roughness measurements, near-surface metallography, finite element modelling and FIB/TEM were used for the investigations performed in this study.

The aim of this study was to develop a comprehensive understanding around realizing the benefits of high-speed machining benefits for IN718, a difficult-to-cut heat resistant alloy. The extreme local machining conditions associated with high-speed machining of IN718 are very difficult to achieve with WC-Co tooling due to the temperature limitations of WC-Co. The higher temperature properties of SiAlON allow for a significant boost in the achievable productivity of the cutting process. This research is supported by a phenomena-based machinability investigation; an area around which there is currently a significant lack of data in the literature.

The following section outlines the general conclusions made from this investigation.

5.1 General Conclusions

Major conclusions of this research can be summarized as follows:

1. SiAlON ceramic has the best fracture toughness and impact fatigue resistance among commercially available structural ceramics and thus was well suited to survive the extreme periodic thermo-mechanical loads experienced in a face milling application.

2. Finite element modelling and IR thermal camera results showed that the maximum temperature on the ceramic tool face can reach values over 90% of the melting point of the workpiece material. In addition, the compressive mechanical loads on the tooltip can reach values over 5 GPa.

3. Machinability experiments and investigation of tool wear patterns showed that the best cutting condition in terms of maximum tool life happened at V_C=900 m/min and F_Z=40 μm. Micro-chipping of the cutting edge and built-up edge formation were identified as the main tool wear mechanisms in IN718 high-speed milling using ceramics, with chipping observed to be more pronounced at lower speeds and built-up edge formation more dominant at higher cutting speeds.

4. Cutting force drops dramatically at around V_C=1,000 m/min to 30% of the force measured at lower cutting speeds. The axial cutting force starts to rise again after the best observed cutting speed. This is attributed to excessive formation of a

built-up edge which impacts chip formation and an increase in the material flow stress during deformation at high strain and strain rates.

5. High-speed face milling of hardened IN718 generates highly segmented chips as a result of low thermal conductivity of the workpiece material and high strain rate deformations in a phenomenon known as catastrophic thermoplastic shear. Higher speeds produced thinner chips due to a high shear angle, which results in a measured cutting force reduction for a range of cutting speeds.

6. Evidence of local melting was detected in high-resolution electron microscopy images on the high-speed chips. Also, a transformation in the morphology of NbC was detected at higher cutting speeds. Grain boundary liquidation and microstructural breakdown happen at higher cutting speeds following the dissolution of strengthening niobium carbides back into the gamma matrix. This can significantly reduce the material strength in the primary shear deformation zone and consequently reduce the resultant cutting forces.

7. At higher cutting speeds both flank and rake face of the SiAlON tools were covered and protected by thermal barrier tribofilms (Al products) and lubricating tribofilms (Si products) which make a significant contribution to facilitating the frictional interactions at the tool-chip interface thus reducing tool wear.

8. Built-up edge studies performed using transmission electron microscopy depicted a considerable difference in the structure of the transferred layer on the

rake face of the ceramics, showing liquid-type flow patterns at the extreme conditions associated with machining IN718 at speeds of over 1,000 m/min.

9. High-speed machining with ceramic tools produced a relatively rough surface in comparison with a conventional coated WC-Co tool used at lower speeds. However, the roughness of the surface was within limits accepted for rough or semi-finish machining.

10. Constant formation and removal of unstable BUE result in deep random grooves on the IN718 when cutting with ceramic tools. BUE leads to the formation of pits and cracks on the workpiece surface. Also, it was observed to transfer unwanted elements, such as silicon, from the tool on to the workpiece surface, which considerably reduces the fatigue life of a component. This is important as fatigue life is a critical performance parameter for aerospace engine components, for example.

11. High-speed milling with ceramic tools resulted in the generation of a thin white layer on the workpiece surface with a hardness three times higher than the bulk material. This white layer was attributed to the high surface temperatures generated when cutting at high speeds and results in a high tensile residual stress on the machined surface. This layer will need to be removed in subsequent finishing operations for most applications which experience fatigue.

12. Although high-speed milling with SiAlON ceramic tools produced cracks and imperfection on the workpiece surface and subsurface, experimental results and

observations suggest that the defects were confined within a narrow band in the sublayer of the machined surface and can be removed in a subsequent finishing process.

In summary, using SiAlON tooling has been shown to be a high productivity solution for rough machining IN718. Surface and subsurface defects have been observed but are contained within the near-surface and can be removed with subsequent finishing operations using WC-Co tooling operating under traditional conditions.

5.2 Research Contributions

The key contributions of this research can be summarized as:

1. This research work demonstrated that implementation of high-speed machining concepts for a difficult-to-cut superalloy like inconel 718 is possible if the correct cutting condition for a SiAlON ceramic tool is selected for a rough face milling operation. Various machinability investigations were performed to contribute to the present research gap in this area and to support scientific discussions regarding the achievement of the process. The incorporation of such a concept can provide a significant boost in the productivity of the manufacturing application with significant economic impacts in the superalloy machining industry.
2. This research presents a detailed understanding of the wear mechanisms and micro/nano-mechanical properties of SiAlON ceramic tools relevant to high-

performance machining conditions associated with milling nickel-based superalloys and compares the results with other ceramic tools available in the market.

3. The study finds the carefully selected combination of cutting parameters in high-speed face milling of IN718 in which maximum tool life with unprecedented process productivity is achieved. A significant increase in the machinability of IN718 was observed when favourable cutting conditions were identified and implemented.

4. This dissertation provides detailed knowledge and reasoning around tool-chip-workpiece interactions and tribological behaviors in high-speed machining of IN718 with ceramic tools. The research presents new observations on the phase transformations of IN718 built-up layers and also in the morphology of carbide precipitations, as well as the adaptive formation of beneficial tribofilms and also material behavior under extreme thermomechanical conditions.

5. This research strives to understand the effect of process parameters and tooling selection on the surface integrity of the workpiece after high-speed dry machining with ceramic tools in comparison with a conventional wet milling process with currently-used PVD-coated tungsten carbide tools.

5.3 Recommendations for future work

This study showed that SiAlON ceramics could improve the poor machinability of IN718. However, studies show that the chipping of the cutting edge is still a major wear mechanism for the current grade of SiAlON ceramics. Improvements in fracture toughness of SiAlONs are being made over time as new ceramic grades are emerging as the results of academic and industrial research and developments. With tool wear better understood, additional machinability experiments can be designed and performed to assess different tool geometries' ability to further improve machining performance and final part quality.

More comprehensive finite element modelling is needed to better understand local conditions in the cutting zone and understand the behavior of the tool and workpiece material under extreme conditions. In addition, more detailed modelling and validation are required to simulate and understand the high strain rate thermo-plastic deformation mechanisms that happen in this application and drive machinability. Following the observations in the machinability studies, it may be useful to replicate the IN718 behavior at extreme conditions in a separate experiment other than high-speed machining using a simple geometry that can be easily modelled. Considering the high mechanical and thermal stresses at the cutting zone, a Split-Hopkinson pressure bar test with a proper micro-shear specimen geometry can induce similar conditions on an IN718 sample. Characterization techniques such as high-speed imaging, flow stress measurements, metallographic studies, and microscopic imaging could be used to investigate the results.

Furthermore, following the developments in the SiAlON toughness and fracture resistance in the future, the surface of the tool can be protected against built-up edge

formation and oxidation by introducing nano multilayered PVD coatings such as TiAlCrSiYN/TiAlCrN which is known for its superior tribological properties. However, both the substrate and the coating must have an appropriate combination of properties such as hot hardness, elasticity, shear strength, fracture toughness, thermal expansion, and adhesion. Control of the tool chipping is of prime importance as the substrate is the carrier for the coating layer and thus needs to be addressed before a coating can be successfully applied.

5.4 Publications

1. F.Molaiekiya, P. Stolf, J. M. Paiva, B. Bose, G. Fox-Rabinovich, S. C. Veldhuis "Influence of process parameters on the cutting performance of SiAlON ceramic tools during high-speed dry face milling of hardened Inconel 718." The International Journal of Advanced Manufacturing Technology 105.1-4 (2019): 1083-1098.

2. F. Molaiekiya, M. Aramesh, and S. C. Veldhuis. "Chip formation and tribological behavior in high-speed milling of IN718 with ceramic tools." Wear 446 (2020): 203191.

3. F. Molaiekiya, A. Khoei, M. Aramesh, and S. C. Veldhuis. " Surface integrity of inconel 718 in high-speed dry milling using SiAlON" Submitted to The International Journal of Advanced Manufacturing Technology, currently under peer review.

Table 5.1- Research outcome mapping

Research objective vs. Research outcome mapping					
Journal Paper	Research Objective (please refer to section 1.3)				
	OBJ 1	OBJ 2	OBJ 3	OBJ 4	OBJ 5
Paper 1	✕	✕			
Paper 2			✕	✕	
Paper 3					✕